ROLE OF PLATELET CLEC-2 AND PODOPLANIN IN INFLAMMATION AND VASCULAR INTEGRITY.

By

Stephanie Eileen Lombard

A thesis submitted to the University of Birmingham for the degree of

DOCTOR OF PHILOSOPHY

Institute of Cardiovascular Sciences

College of Medical and Dental Sciences

University of Birmingham

November 2016

UNIVERSITY OF
BIRMINGHAM

University of Birmingham Research Archive

e-theses repository

This unpublished thesis/dissertation is copyright of the author and/or third parties. The intellectual property rights of the author or third parties in respect of this work are as defined by The Copyright Designs and Patents Act 1988 or as modified by any successor legislation.

Any use made of information contained in this thesis/dissertation must be in accordance with that legislation and must be properly acknowledged. Further distribution or reproduction in any format is prohibited without the permission of the copyright holder.

Abstract

Introduction: The platelet receptor CLEC-2 is believed to play a key role in many of the newly emerging roles of platelets, such as development and inflammation. The aim of this thesis was to look further into the interaction of CLEC-2 and podoplanin and to investigate the role these proteins play in inflammation.

Methods: In-vitro flow experiments using recombinant podoplanin and whole blood were used to investigate the interaction of CLEC-2 and podoplanin under shear stress. The role of CLEC-2 in inflammation was investigated using a range of mouse models such as LPS induced peritonitis model, DSS induced colitis and a mouse model of atherosclerosis.

Results: Mouse podoplanin induces platelet aggregation under arterial rates of shear through the receptor CLEC-2. The aggregation is likely due to the high affinity interaction between mouse CLEC-2 and podoplanin. The results of role of CLEC-2 in inflammation revealed a lack of CLEC-2 from inception causes a more acute inflammatory reaction to LPS. CLEC-2 (removed post development) also plays a protective role in an acute model of ulcerative colitis. Mice lacking CLEC-2 do not upregulate podoplanin on lymphatic endothelial cells and epithelial cells in the colon to the same degree as their wildtype counterparts following induction of colitis. CLEC-2 is also protective against atherosclerosis however there was a greater upregulation of podoplanin in the plaques of atheroprone platelet CLEC-2 deficient mice. The results of this thesis highlight the complicated role of CLEC-2 in inflammatory disorders. There is also a clear difference in the

affinity of mouse and human forms of CLEC-2 and podoplanin which has important consequences for the interpretation of mouse models examining the role of these proteins in human diseases.

In Loving memory of

Linda Kelly

Acknowledgements

I would like to thank my supervisor Prof. Steve Watson for the support during my PhD and the Wellcome Trust for providing funding. I would also like to thank Sian Lax and Alice Pollitt for teaching me a range of laboratory techniques, and for their guidance in experimental design and general scientific discussion.

I am also very grateful to all members of the wider Birmingham Platelet group, for all their help and laughs over the last three years. I would to thank Kate and Sam for the chats and much needed food and wine evenings, Julie for being fabulous, Craig for his general pranks and mischievousness and Beata and Stef for keeping everything afloat, always with a smile! And to everyone else, students and post-docs alike, for being great people to work with.

Thank you also to my Mum and Dad for their support and believing I could do it. Thank you to Tom for being there for me during the crazy write-up period, and making it all feel worth it. I would like to thank all the occupants of 25 Eastern for the fun times! Lastly, I am eternally grateful for the love and support I received during my PhD from my sister Frances, brother-in-law Michael, and gorgeous niece and nephew Fiona and George, could not have done it without you!

Table of Contents

List of Figures

Chapter 1

List of Tables

List of Abbreviations

ADP	Adenosine diphosphate
APC	Antigen Presenting Cell
ATP	Adenosine triphosphate
BSA	Bovine Serum Albumin
CD	Crohn's Disease
CHO	Chinese Hamster Ovary cells
CLEC-2	C-type lectin-like receptor
DAMPs	Danger Associated
DC	Dendritic Cell
DIC	Disseminated Intravascular Coagulopathy
DMSO	Dimethyl sulfoxide
DSS	Dextran Sodium Sulphate
E	Embryonic Day
EDTA	Ethylenediaminetetraacetic acid
FAE	Follicular-Associated Epithelium
FBS	Fetal Bovine Serum
FRC	Fibroblastic Reticular Cell
GALT	Gut-Associated Lymphoid Tissue
GBM	Glioblastoma Multiforme
GI	Gastrointestinal
GPVI	Glycoprotein VI
GTP	Guanine triphosphate
Grb2	Growth factor receptor-bound protein 2
HEV	High Endothelial Venule
HIV	Human Immunodeficiency virus
IBD	Inflammatory Bowel Disease
Ig	Immunoglobulin
ICAM-2	Intercellular adhesion molecule 2
IFN	Interferon

IL	Interleukin
ILCs	Innate lymphoid cells
ITAM	Immunoreceptor tyrosine based activation motif
IVH	Intraventricular haemorrhage
kDa	Kilodalton
LAT	Linker for activation of T-cells
LDL	Low-density lipoprotein
LEC	Lymphatic endothelial cell
LPS	Lipopolysaccharide
mAb	Monoclonal antibody
MAdCAM-1	Mucosal Vascular Addressin Cell Adhesion Molecule 1
MCP-1	Monocyte Chemoattractant Protein 1
MHC	Major Histocompatibility Complex
MDP	Muramyl dipeptide
MLNs	Mesenteric Lymph Nodes
MS	Multiple Sclerosis
NET	Neutrophil Extracellular Trap
PAMPs P	athogen Associated Molecular patterns
PBS	Phosphate-buffered Saline
PBST	Phosphate-buffered Saline/0.1% Tween
PF4	Platelet-factor 4
PLAG	Platelet Aggregation Stimulation Domain
PLC	Phospholipase C
PLNs	Peripheral Lymph Nodes
PP	Peyer's Patches
PRP	Platelet rich plasma
PRR	Pattern Recognition Receptors
S1-P	Sphingosine-1-phosphate
SFK	Src family kinase
SH2	Src homology 2
SLP76	SH2 containing leukocyte protein of 76 kDa

TGF	Transforming growth factor
TH17	T-helper 17
TLR	Toll-like receptor
TM	Transmembrane domain
TNF	Tumor Necrosis Factor
TPO	Thrombopoietin
TxA2	Thromboxane A2
UC	Ulcerative Colitis
VEGF	Vascular endothelial growth factor
VWF	Von Willebrand Factor
WT	Wild-type

Chapter 1

1.1 Platelet anatomy and function

1.1.1 What are platelets?

Platelets are small cell fragments derived from megakaryocytes in the bone marrow. They circulate in the blood in high numbers of between 150,000 – 350,000/μl, and are crucially important in haemostasis as well as in maintaining vascular integrity. These anucleated cell fragments are 2-3μm in diameter and remain alive for between 5-9 days. Platelets are composed of three types of secretory organelles, dense granules, α-granules and lysosomes. Dense granules contain molecules such as serotonin, ADP, ATP, and polyphosphate, α-granules containing over 100 bioactive proteins including clotting factors (e.g. fibrinogen and von Willebrand Factor (VWF) and growth factors (e.g. vascular endothelial growth factor (VEGF)), and lysosomes contain enzymes such as hydrolases. Platelets have an open canicular system which allows for efficient transport of substances into and out of the platelets which is especially important during release of granule contents.

1.1.2 Platelet production

Megakaryocytes, the producers of platelets, derive from multipotent haematopoietic stem cells which give rise to all circulating blood cells (Kondo et al., 2003) (Figure 1.1). Platelets are released through megakaryocyte cytoplasmic processes known as pro-platelets which extend through bone marrow sinusoid epithelial cells to reach the blood system. The cytokine thrombopoietin

(TPO) is a critical regulator of megakaryocyte number and maturation (Machlus and Italiano, 2013).

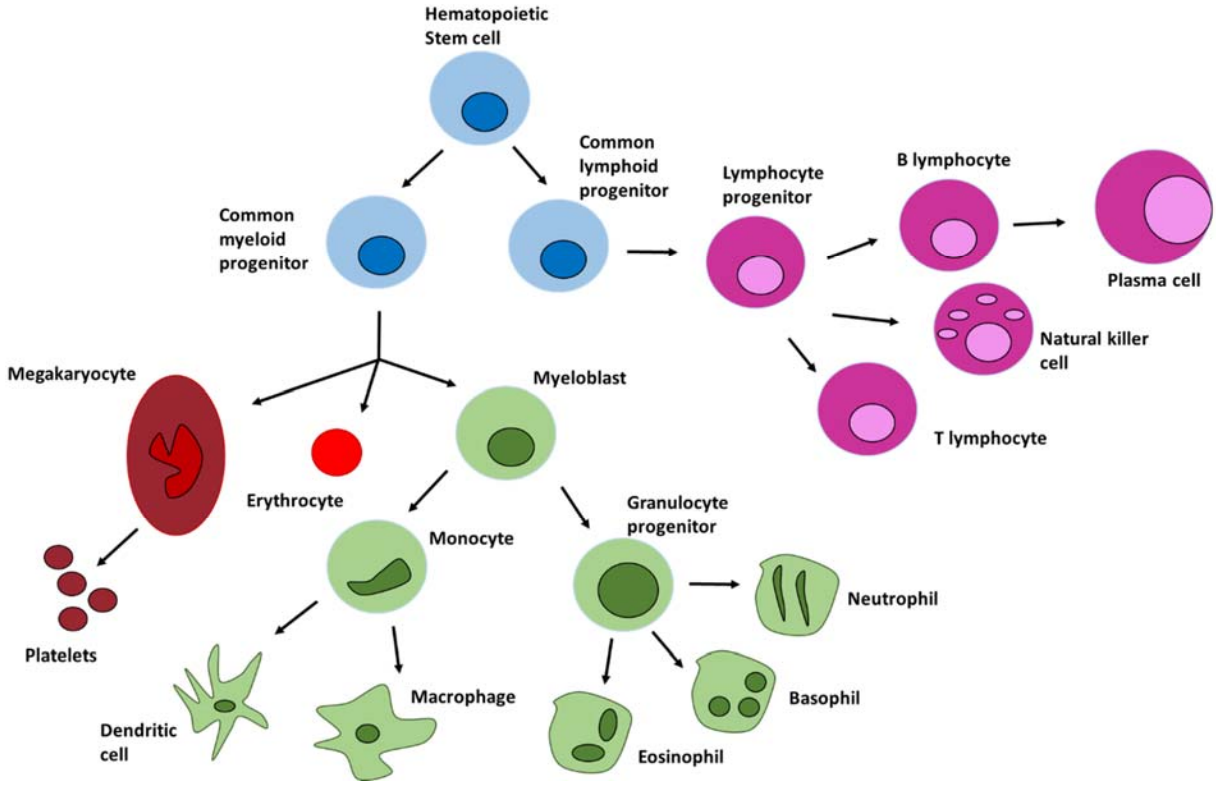

Figure 1.1: Haematopoietic stem cell lineages.

Hematopoietic stem cells (HSCs) are multi-potent cells whose self-renewal is critical to the maintenance of numbers of all cells in the blood system. Within the bone marrow these cells are directed to either a myeloid or lymphoid lineage, which differentiate to further cell type lineages. Image modified from (Kondo et al., 2003).

1.1.3 Platelet function in haemostasis

Haemostasis involves several different physiological processes working together in order to arrest bleeding. It is generally described to happen in three stages: firstly primary haemostasis or platelet plug formation, followed by coagulation where stable clots are formed from the conversion of fibrinogen to fibrin and lastly clot dissolution by the process of fibrinolysis. Platelets play an integral role in the initial stages of haemostasis by adhering firmly to a damaged vessel wall. In resting conditions, nitric oxide and prostacyclin released by the endothelium of blood vessels and the expression of ectonucleotidase CD39 on platelets maintains these cells inactive while marginalized to the endothelial surface in flowing blood. However, upon vascular injury subendothelial collagen is exposed which captures plasma VWF and in turn tethers platelets through the GPIb-V-IX complex (Savage et al., 1998). This enables clustering of the low affinity immunoglobulin receptor, GPVI, by collagen and activation of platelet integrins including α2β1 (also known as GPIa-IIa) and αIIbβ3 (also known as GPIIb-IIIa), which bind to collagen and VWF respectively, strengthening adhesion (Ni and Freedman, 2003). The adherence of platelets to the damaged vessels causes "platelet spreading" namely formation of filopodia and lamellipodia which are triggered by mobilisation of intracellular Ca^{2+} and activation of small G proteins. The release of ADP from dense granules acts alongside the formation and release of thromboxane A_2 (TxA_2) to reinforce platelet activation. Further recruitment of platelets happens through tethering of non-activated platelets captured by VWF and further release of ADP and TxA_2 from α-granules. The formation of thrombin via the coagulation cascade mediates the conversion of fibrinogen to fibrin and leads to the formation a platelet-rich clot. The haemostatic plug which subsequently

develops is vital to the wound healing process (Figure 1.2) (Sachs and Nieswandt, 2007, Varga-Szabo et al., 2008). The pathological counterpart of haemostasis is the formation of occlusive thrombi which obstruct the flow of blood in the circulatory system and thereby deprive a tissue of oxygen (hypoxia). For example, the formation of a thrombus in cerebral arteries causing stroke while in coronary arteries it causes myocardial infarction. Platelet aggregation is therefore one of the leading causes of mortality, and is estimated to account for 25% of deaths globally (Ho-Tin-Noe et al., 2011).

The importance of platelets is not limited to their role in haemostasis. A growing body of research has identified biological roles of platelets in development, vascular integrity, innate immunity and in cancer metastasis (Ware et al., 2013). Some of these roles appear to require only a fraction of circulating platelet numbers (e.g. vascular integrity) which may explain why they have been missed in the past (Ghoshal and Bhattacharyya, 2014).

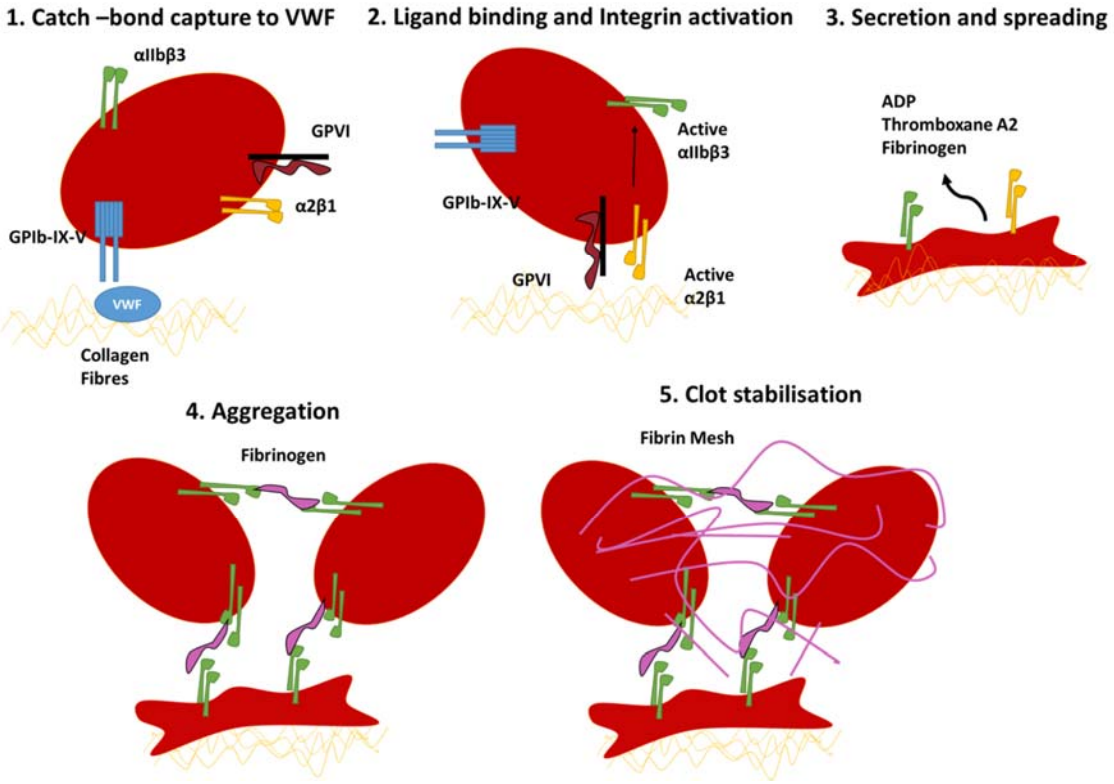

Figure 1.2: Platelet aggregation and thrombus formation

Stages involved in platelet capture, aggregation and thrombus formation in haemostasis. Initial platelet tethering under high shear stress via the VWF receptor GPIb-IX-V, leads to engagement of the collagen receptor GPVI. Inside-out signalling triggers an active confirmation change in αIIbβ3 and α2β1 and release of platelet mediators which trigger the activation of other further platelets. Fibrinogen is converted to fibrin, leading to formation of stable clot. Image modified from (Varga-Szabo et al., 2008) and (Sachs and Nieswandt, 2007).

1.1.4 Roles of platelets outside of haemostasis and thrombosis

The role of platelets stretches beyond their well-studied haemostatic role. Platelets have been shown to be key players in the immune system and inflammation, as well as in development and in the maintenance of vascular integrity. Data supports the idea that platelets can play both a supporting and detrimental role in the immune system. Platelets express many different types of receptors which are common on immune cells such as Toll-like receptors, CD40 and CD40L and intercellular adhesion molecule 2 (ICAM-2). They also have the ability to release various chemokines and cytokines, which are critical to the recruitment of immune cells to a site of injury (Ware et al., 2013).

Platelets have been shown to be important in the initiation and development of a number of thrombo-inflammatory disorders such as atherosclerosis, ischaemic stroke and inflammatory bowel disease (McNicol and Israels, 2008). Platelets also play a critical role in immune defence by trapping bacteria within thrombi thereby preventing their dissemination throughout the body and facilitating immune cell targeting. However, in the case of secondary metastasis it is thought that platelets aid the extravasation of tumour cells into the blood stream while protecting these cells from immune cell capture (Ghoshal and Bhattacharyya, 2014, Lowe et al., 2012).

Platelet immunoreceptor tyrosine-based activation motif (ITAM) receptors such as GPVI and the C-type lectin-like receptor CLEC-2 are believed to be involved in many of the newly emerging non-haemostatic roles of platelets. For example, CLEC-2 has been shown to play a critical role in the

separation of blood and lymphatic vasculatures during development (Finney et al., 2012). CLEC-2 has also been shown to be a key player in the maintaining the structural integrity of blood vessels (vascular integrity) particularly during an inflammatory reaction (Boulaftali et al., 2013).

1.2 CLEC-2

Determining the role that CLEC-2 plays in platelet physiology, and how it contributes to the role of platelets in immunity and infection is a major focus of this thesis. The following section focuses on the discovery of CLEC-2 and how it mediates platelet activation.

1.2.1 Discovery of CLEC-2

Rhodocytin (also termed aggretin) is a powerful human and mouse platelet agonist that was isolated from the venom of the Malayan pit viper, *Calloselasma rhodostoma* (Huang et al., 1995).In the original studies, Rhodocytin was proposed to activate platelets through the collagen integrin receptor α2β1 due the inhibitory effect of a monoclonal antibody (Huang et al., 1995, Inoue et al., 1999). Rhodocytin induced platelet aggregation was later suggested to involve GPIbα (Navdaev et al., 2001). This hypothesis was later proved incorrect when Rhodocytin was shown to activate platelets deficient in either of these receptors and failed to bind to recombinant α2β1 (Bergmeier et al., 2001). CLEC-2 was originally discovered in a transcriptomics study on chromosome 12 of the human genome alongside six other C-type lectin-like receptors (Colonna et al., 2000). Thereafter it was identified by mass spectrometry following affinity purification using rhodocytin (Suzuki-Inoue et al., 2006). The presence of CLEC-2 mRNA was shown to be restricted with the highest expression in the megakaryocyte/platelet lineage of the mouse genome (Suzuki-

Inoue et al., 2006, Senis et al., 2007). CLEC-2 was also believed to be expressed by neutrophils when tested using an antibody to CLEC-2 but has since been confirmed to be only expressed on megakaryocytes, platelets and subsets of myeloid suppressor cells and activated dendritic cells when using tissues from CLEC-2 deficient mice as a control (Kerrigan et al., 2009, Lowe et al., 2015b).

1.2.2 CLEC-2 Signalling

CLEC-2 is a type II transmembrane glycoprotein with a single YxxL motif (single animo acid code) downstream of a conserved triacidic amino acid sequence in a short cytoplasmic tail. The extracellular portion of the protein lacks the residues needed for binding to carbohydrate moieties suggesting that it binds to a protein ligand and is hence classed as a C-type lectin-like receptor (Watson et al., 2007). The single YxxL sequence in CLEC-2 is termed a hemITAM because it differs to the dual YxxL sequence in immunoglobulin (ITAM) receptors, such as the collagen receptor GPVI-Fc receptor γ-chain complex (Hughes et al., 2010). Upon ligand engagement, it is thought that the tyrosine kinase Syk is phosphorylated by Src family kinases (SFKs) (Hughes et al., 2010, Severin et al., 2011). Activated Syk then phosphorylates the YxxL motifs of dimerised CLEC-2 and binds to these via its tandem SH2 domains (Severin et al., 2011). The events that follow mirror the signalling cascade of a typical ITAM receptor and involve further phosphorylation of adaptor proteins such as LAT and SLP-76 and activation of PLCγ2 which allows for an increase in intracellular Ca^{2+} and platelet activation (Figure 1.3).

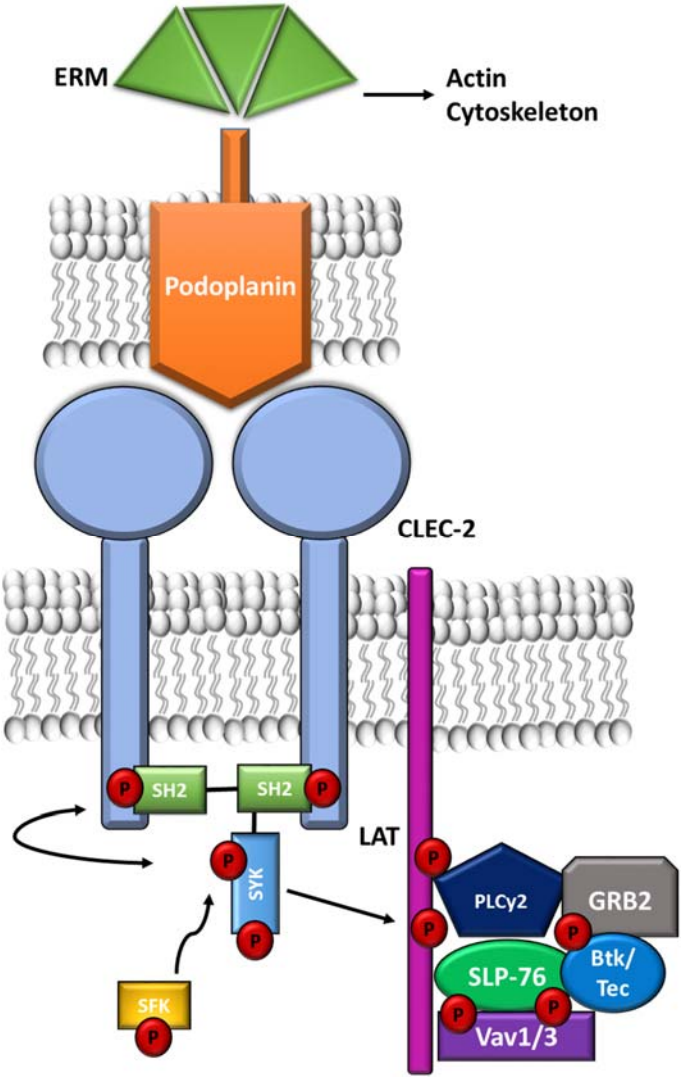

Figure 1.3 CLEC-2 –Podoplanin signalling axis.

CLEC-2 interacts with podoplanin resulting in its phosphorylation by Syk and Src family kinases. Phosphorylation initiates a signalling cascade involving the adaptor proteins LAT, SLP-76, Grb2, Tec family kinases and the Vav family of guanine exchange factors which support activation of the effector enzyme PLCγ2 and Ca^{2+} release, culminating in platelet activation. Podoplanin signals through ERM proteins and influences actin cytoskeletal rearrangements.

1.3 Podoplanin

1.3.1 Podoplanin – Discovery of a CLEC-2 ligand

Podoplanin was first identified on osteoblasts and named as OTS-8 (Nose et al., 1990). It was later identified on lymphatic endothelial cells (LECs), fibroblastic reticular cells (FRCs), and on alveolar type 1 epithelial cells under a range of different names based on its location or function (Astarita et al., 2012) (Table 1.1). The final decided name of podoplanin was given due to its expression on kidney podocytes and its' in involvement in maintaining kidney structure (Breiteneder-Geleff et al., 1997). Notably podoplanin has not been found to be expressed by blood vascular endothelial cells. Both colorectal tumour cells and lung squamous carcinoma cells expressing podoplanin have been shown to be potent mediators of platelet aggregation (Kato et al., 2008, Suzuki-Inoue et al., 2007). The activation was identified to be through CLEC-2 stimulation due to the similar signalling cascade and kinetics seen following platelet activation by the exogenous CLEC-2 ligand rhodocytin. The interaction was confirmed using expressing Chinese hamster ovary cells (CHO) cells transfected to express podoplanin (Suzuki-Inoue et al., 2007). Human embryonic kidney (293T) cells which express podoplanin were later shown to bind and activate platelets and the paper also confirmed an interaction of human CLEC-2 and podoplanin using surface plasmon resonance (Christou et al., 2008). It has also been shown that endogenously expressed podoplanin on mouse and human lymphatic endothelial cells can cause platelet aggregation in a CLEC-2 dependant manner (Finney et al., 2012, Navarro-Nunez et al., 2015).

1.3.2 Binding partners and other endogenous ligands of Podoplanin

Podoplanin is known to associate with transmembrane domains of the tetraspanin CD9. CD9 is a tumour suppressor and has been shown inhibit some of podoplanin functions such as cell motility and its platelet aggregating ability (Nakazawa et al., 2008). However, podoplanin has also been shown to associate with the major hyaluronan receptor lyve-1 which is upregulated in cancer cell lines and thought to increase cell migration and motility (Noda et al., 2010, Bono et al., 2004).

Podoplanin has been shown to have a vast expression pattern so it is unsurprising that studies have proposed additional podoplanin ligands. Galectin-8 expressed on LECs is believed to interact with podoplanin to support the adhesion of LECs to surrounding extracellular matrix (Cueni and Detmar, 2009). LECs and FRCs also express the lymphatic chemokine CCL21 which binds to podoplanin with high affinity and may play a role in trafficking dendritic cells (DCs) to the T zone of lymph nodes (Kerjaschki et al., 2004, Astarita et al., 2012). Podoplanin has been found to be expressed on range of cell types and tissues (see Table 1.1).

Tissue	Alternative Name	Reference
Lymphatic endothelial cells (LECs) E11	E11	(Wetterwald et al., 1996)
Fibroblastic Reticular cells (FRCs)	Gp38	(Farr et al., 1992)
Alveolar type 1 cells	T1α	(Williams et al., 1996)
Kidney Podocytes	Podoplanin	(Breiteneder-Geleff et al., 1997)
Thymic Epithelial cells	Gp38	(Farr et al., 1992)
Choroid Plexus (throughout brain in development)	T1α/Podoplanin	(Williams et al., 1996, Lowe et al., 2015a)
Ciliary Epithelium	T1α	(Williams et al., 1996)
Oesophagus and Intestine	T1α/podoplanin	(Williams et al., 1996, Scholl et al., 1999)
Osteoblasts	E11/OTS-8	(Wetterwald et al., 1996, Nose et al., 1990)
Mucosal Epithelium of Salivary glands and Tongue	Podoplanin	(Hata et al., 2010, Noda et al., 2010)
Myocardium, pericardium and epicardium of the heart	Podoplanin	(Mahtab et al., 2008, Gittenberger-de Groot et al., 2007)
Skin Keratinocytes	T1α/podoplanin	(Scholl et al., 1999)
TH17 cells	Gp38	(Peters et al., 2011)
Macrophages	Podoplanin/Gp38	(Kerrigan et al., 2012, Hou et al., 2010)
Colorectal and lung squamous carcinoma cells tumour cells	Aggrus/T1α/Podoplanin	(Kato et al., 2003, Kato et al., 2005, Suzuki-Inoue et al., 2007)

Table 1.1: Tissue Expression of podoplanin

List of cell types discovered to express podoplanin and the names used for the protein. Highlighted bold are cells which can be induced to express podoplanin during development or in response to an inflammatory stimulus.

1.3.3 Podoplanin Signalling

Podoplanin consists of a single transmembrane (TM) domain, a short cytoplasmic tail consisting of 9 amino acids and a heavily glycosylated extracellular domain (Astarita et al., 2012). There are homologues of podoplanin in many species including humans, mice, rats, dogs and hamsters. The TM and cytoplasmic tail are highly conserved between species (Martin-Villar et al., 2005). The amino acid sequence in the platelet aggregation stimulation domain (PLAG) of the ED is largely similar between podoplanin homologues in humans, mice and rats (Kaneko et al., 2006). However, in the sequence of the PLAG domain it was found that T52 is critical to the platelet aggregating capacity of human podoplanin, whereas T34 is critical in mouse podoplanin (Kaneko et al., 2006, Kato et al., 2003). Crystallography experiments confirmed the T52 (attached to an o-glycan) binds directly the extracellular domain of CLEC-2 in the same region as rhodocytin (Nagae et al., 2014).

Intracellularly podoplanin is known to colocalise with ezrin, radixin and moesin (ERM) family proteins (Martin-Villar et al., 2006). A conserved motif of three basic residues in the cytoplasmic tail of podoplanin is needed for the direct association with ezrin and moesin and overexpression of podoplanin was shown to result in phosphorylation of ERM proteins (Martin-Villar et al., 2006, Wicki et al., 2006). ERM proteins are the connectors between integral membrane proteins and the actin cytoskeleton. Phosphorylation of ERM leads the activation of Rho GTPases which in turn exposes binding sites for actin and other cytoskeletal proteins (Fehon et al., 2010). Podoplanin signalling is therefore believed to increase cell motility and its expression is often found on the leading edge of tumours where it can enhance tumour metastasis (Takagi et al., 2013). Podoplanin

has been proposed to influence tumour biology through the induction of epithelial-mesenchymal transition (EMT). EMT causes cells to lose polarity and cell-cell adhesion allowing for a more invasive phenotype which is believed to be necessary in wound healing as well as secondary metastasis (Martin-Villar et al., 2006, Wicki et al., 2006). However, the validity of the ability of podoplanin to cause this shift has been questioned as well as groups reporting differences on the influence podoplanin has on the activity levels of GTPases such as RhoA, Rac-1 and Cdc-42 (Navarro et al., 2011, Wicki et al., 2006). It is possible that podoplanin has different effects depending on the cell type in which it is expressed.

1.4 Role of CLEC-2 and Podoplanin in embryonic development

1.4.1 Development of lymphatic system

The lymphatic system is a complex network of vessels connected by hundreds of lymph nodes (~450) in the human body. It serves many functions including the return of protein rich fluid back to the blood, lipid absorption and immune cell trafficking. The development of this system begins during week 6-7 in human embryonic development and at E9.5 in mice after the blood vascular system is fully formed (Tammela and Alitalo, 2010, Schulte-Merker et al., 2011). It was proposed in the early 1900s to develop from the venous system and later studies tracing the fate of venous/endothelial cells (Tie2-Cre-based lineage tracing) revealed that the majority of lymphatic progenitor cells are of venous origin (Srinivasan et al., 2007). However, there was some lymphatic progenitor cells which did not follow the same path of origin which indicates that the development of the lymphatic system also stems from an undetermined non-venous origin (Martinez-Corral et al., 2015). Briefly described the lymphatic system develops from lymphatic progenitor cells are induced to express Prox-1 by the transcription factor Sox18 and can be detected at the cardinal vein at E10.0 in mice (Francois et al., 2008, Wigle et al., 2002). These prox-1 expressing cells are stimulated to migrate to the dorsal side of the cardinal vein by vascular endothelial growth factor 3 (VEGFR-3), axon guidance receptor neuropilin-2 (Nrp-2) and the vascular endothelial growth factor C (VEGF-C) (Xu et al., 2010, Dumont et al., 1998, Karkkainen et al., 2004). At this stage the immature LECs are expressing podoplanin which co-insides with the development of superficial lymph vessels and dermal lymphatic at E12.0. At the same time the

thoracic duct, an integral draining point of lymph to the venous system, develops alongside the cardinal vein from a subset of aggregating LECs (Hagerling et al., 2013, Yang et al., 2012).

1.4.2 The role of CLEC-2 and Podoplanin in lymphatic vasculature development

One of the first discovered functions for platelet CLEC-2 interaction with a podoplanin expressing cells was its role in the development of the lymphatic system. The first indications of this function came from the discovery that mice deficient in proteins necessary for CLEC-2 downstream signal propagation, such as Syk, SLP-76 and PLCy2, presented with subcutaneous haemorrhaging in the skin and oedema during embryonic development (Turner et al., 1995, Cheng et al., 1995, Clements et al., 1999, Clements et al., 1998, Wang et al., 2000). The phenotype was subsequently explained to be from erroneous connections between the blood and lymphatic systems within these mice (Ichise et al., 2009, Abtahian et al., 2003). Podoplanin deficient mice, which were separately discovered to die shortly after birth from respiratory failure, also present with lymphedema and blood filled lymphatic vessels in their skin and intestines (Schacht et al., 2003, Uhrin et al., 2010). It was later discovered that CLEC-2 deficient mice phenocopied the defects seen in podoplanin deficient mice (Bertozzi et al., 2010, Finney et al., 2012, Suzuki-Inoue et al., 2010).

Further studies into the mechanism of this phenotype highlighted a requirement for podoplanin expressed on an endothelial cell type is required for normal lymphatic development to occur (Fu et al., 2008). It was also shown that mice lacking T-synthase which is responsible for the

glycosylation of the extracellular domain of podoplanin is also necessary for normal lymphatic development (Fu et al., 2008, Xia et al., 2004).

The PF4-Cre mouse model is used to specifically delete genes from cells of megakaryocyte/platelet specific origin (Tiedt et al., 2007). This mouse model demonstrated that lack of CLEC-2 in platelets present with a blood lymphatic mixing phenotype (Bertozzi et al., 2010, Finney et al., 2012). The same mixing phenotype was also present in PF4- Cre models lacking the tyrosine kinase Syk or adaptor protein SLP-76. It is believed to be platelet specific due to the inhibitory effects which platelets have on LEC behaviour and the lack of a mixing phenotype in megakaryocyte specific CLEC-2 deficient mice (Finney et al., 2012, Nakamura-Ishizu et al., 2015).

1.4.3 Mechanism behind the blood lymphatic mixing phenotype

The question of how podoplanin expressing LECs interact with platelets to mediate correct separation of the blood and lymphatic system remains to be conclusively answered. Many different proposal have been put forward, including direct platelet and LECs interaction and the release of growth factors from platelets (Bertozzi et al., 2010, Uhrin et al., 2010, Suzuki-Inoue et al., 2010). The research done in this area has also demonstrated that platelet CLEC-2 is needed in order to maintain blood-lymphatic separation. This is evidenced by the presence of blood-lymphatic shunts which are visible in radiation chimeric mice reconstituted with CLEC-2 or Syk deficient bone marrow whose lymphatic system is fully developed. There is also blood-lymphatic mixing present in platelet specific CLEC-2 deficient mice (PF4-Cre.CLEC-$2^{fl/fl}$) around mesenteric vessels and the chylous fluid of the intestine (Finney et al., 2012).

It has also been proposed that CLEC-2 stimulated thrombus formation at the junction between the thoracic duct and subclavian vein is necessary to prevent lymphatic fluid backflow into the venous system throughout development and adulthood (Hess et al., 2014). This study however, failed to explain how the thrombus prevents backflow without affecting flow through from the lymphatic system. The mechanism behind how the separation of the blood-lymphatic system is maintained by CLEC-2 and podoplanin remains to be answered.

1.4.4 Role of CLEC-2 and Podoplanin in lymph node function

Studies on the hemITAM receptor CLEC-2 has revealed that it is involved in the regulation of the immune system and inflammation in many settings. Lack of platelet CLEC-2 has also been demonstrated to result in the development of blood filled lymph nodes and fibrosis as well as a reduced number of naïve CD4 T cells and B cells within the lymph nodes following repeated immunisations (Benezech et al., 2014). It has been demonstrated that platelet CLEC-2 secures the integrity of high endothelial venules (HEV) during lymphocyte trafficking to lymph nodes through interaction with podoplanin expressing fibroblastic reticular cells. Loss of either platelet CLEC-2 or podoplanin leads to bleeding in MAdCAM1 expressing mucosal lymph nodes (Herzog et al., 2013). Platelet CLEC-2 binding on FRCs was shown to induce the release of sphingoshine 1 phosphate (S1P) from platelets which induces VE-cadherin expression needed to maintain adherens junctions in HEVs. Podoplanin expression on LECs and FRCs has been shown to aid the entry and trafficking of CLEC-2 expressing DCs to lymph nodes in mice (Astarita et al., 2012). Later work revealed that podoplanin expression on FRCs is needed to maintain lymph node architecture

and CLEC-2 expressing DCs allow for reduced stiffness of this architecture during an immune reaction (Astarita et al., 2015).

1.4.4 The role of CLEC-2 and Podoplanin in cerebral vasculature development

A lack of CLEC-2 and podoplanin has been reported to result in the development of cerebral haemorrhages during embryonic development. The first report of this phenotype using CLEC-2 deficient mice was in Tang et al. 2010 who reported multiple haemorrhages in the midbrain parenchyma at E12.0 (Tang et al., 2010). Syk deficient mice also display brain haemorrhages at E14.0 (Cheng et al., 1995). It was later observed that megakaryocyte/platelet CLEC-2 and Syk deficient mice similarly developed brain haemorrhages although they were less severe (Finney et al., 2012). The development of these brain haemorrhages was studied in detail by Lowe et al 2015 (Lowe et al., 2015a). This study found that platelet interaction with podoplanin expressing neuroepithelium is necessary to prevent haemorrhage. Podoplanin is expressed throughout the brain during development and becomes localized to the choroid plexus. The involvement of pericytes and platelet released mediators such as S1P was also postulated to play a role. The study proposed that podoplanin induces platelet aggregation through the receptor CLEC-2 which supports the integrity and maturation of the developing vasculature in the brain based on the fact haemorrhaging was also seen in mice deficient in the integrin subunit αIIb.

1.5 Infection and immunity

The presented thesis deals in part with the involvement of platelet CLEC-2 and its ligand podoplanin in infection, inflammation and the immune system. As such the sections below explain the general principles of the immune system, in particular the innate response, the role of the lymphatic system and immune cell recruitment.

1.5.1 Innate and adaptive immune system

The innate immune system is the first line of defence against an immune stimulus. The system includes skin and mucosal barriers to prevent entry and well as phagocytic cells designed to “eat” and destroy an invader. There are many types of tissue resident cells such as dendritic cells (DCs) and mast cells which can stimulate recruitment of phagocytes such as monocytes and neutrophils through release of inflammatory signals such as cytokines. If these initial lines of defence fail to rid the body of the stimulus, the adaptive immune response begins to respond. The adaptive immune system recognises a pathogen specifically and responds with the release of antibodies by B lymphocytes and specific recognition and destruction by T lymphocytes.

1.5.2 Inflammation and Sepsis

Inflammation is a protective response by the body to a harmful stimulus which allows for the rapid recruitment of immune cells to a site of injury. The response helps ensure the removal of damaging agents as well as aiding in the healing process. Inflammation can be caused by a range of factors including tissue damage or pathogenic infection. Macroscopic effects of inflammation such as tissue swelling are due to increased vascular endothelium permeability which allows for

serum leakage and extravasation of immune cells. The response is normally tightly regulated to prevent damage from persistent inflammation. However, in recent years uncontrolled chronic inflammation is believed to be a factor in the pathogenesis of many diseases such as sepsis, atherosclerosis, and inflammatory bowel disease with elevated blood levels of C-reactive protein and other markers of inflammation seen in these patients (Laveti et al., 2013, Takeuchi and Akira, 2010).

Sepsis is a host's overwhelming response to infection and shock that triggers a dangerously uncontrolled inflammatory response. In fact, the mortality rates of patients who develop sepsis range between 30 to 70% with very little success by pharmaceutical companies to develop effective treatment. The lack of success is thought to be due to the involvement of not just classical inflammatory mediators such as cytokines and chemokines but the triggering of systems such as the coagulation cascade which can result in disseminated intravascular coagulopathy (DIC) and excess release reactive oxygen species which both cause tissue damage and eventually organ failure. The persistence activation of the immune system later leads to excess anti-inflammatory signals and immune paralysis that make re-infection likely in patients (Riedemann et al., 2003, Schouten et al., 2008). A schematic of the stages of sepsis can be seen in Figure 1.4.

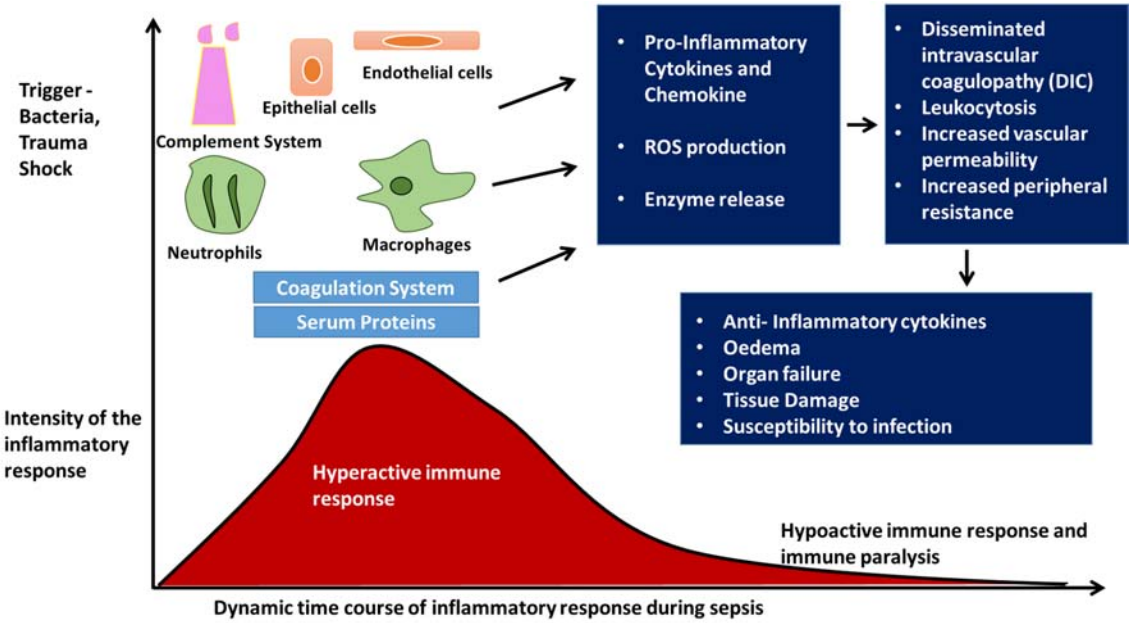

Figure 1.4: Inflammatory responses during sepsis

The initiation of sepsis is caused by an excess production of inflammatory mediators and activation of the coagulation and complement systems. Platelets also contribute to the pathology through DIC, the release of cytokines, recruitment of immune cells and activation of NETs. Leukocytes release a large amount of reactive oxygen species (ROS) and there is an upregulation of adhesion molecules on endothelial cells. Thus, there is increased vascular permeability, tissue damage and organ failure and essential innate immune functions become ineffectual leading to an inability for patients to recover. Image adapted from Riedemann et al (Riedemann et al., 2003).

1.5.3 Pattern Recognition receptors

For the body to respond to an unwanted invader such as bacteria, its presence must first be recognised. Pattern recognition receptors (PRRs) play an integral part in innate immune sensing which is necessary to mount the initial immune response. These receptors function to recognize pathogen-associated molecular patterns (PAMPs) such as lipopolysaccharide (LPS) found on the surface of gram negative bacteria or danger associated molecular patters (DAMPs) which are signals released by damaged endogenous cells. PRRs can be expressed intracellular compartments, on the cell surface or secreted in the blood stream and intercellular spaces. There are four classes of PRR families, including the transmembrane Toll-like receptors (TLRs) and C-type lectin receptors (CLRs) as well as cytoplasmic proteins such as the Retinoic acid-inducible gene (RIG)-I-like receptors, and NOD-like receptors (Takeuchi and Akira, 2010).

TLR4 is once such receptor which is expressed on many different cells of the innate system including epithelial cells, macrophages and platelets. Ligand stimulation ultimately causes the NF-κB transcription factor to translocate to the nucleus and drives the expression of pro-inflammatory cytokine genes critical for the recruitment of immune cells to the site of infection. Many of the other TLRs follow a similar downstream signalling pathway (Janeway and Medzhitov, 2002).

1.5.4 Cytokines and chemokines

The type of immune cells and their relative numbers recruited to a site of inflammation has been shown to vary considerably depending on the immune stimulus. Small peptide molecules known as cytokines and chemokines mediate the immune cell recruitment and trigger complex intracellular signalling that characterizes inflammation. Chemokines tend to be involved in the orchestration of leukocyte trafficking in many tissues. These chemotactic agents signal through G protein coupled receptors. They are spilt into two major subfamilies, CXC and CC based on their structural properties with several that belong to neither family. In general, CXC chemokines attract neutrophils whereas CC chemokines mainly attract monocytes. Cytokines however have more wide ranging functions. The families of cytokines tend to be broken down into interleukins (IL), tumour necrosis factors (TNF), interferons (IFN) and colony stimulating factors. Key pro-inflammatory cytokines are TNFα, IL-1 and IL-6. They signal through structurally distinct type 1 cytokine receptors which are often found to be upregulated in a range of inflammatory disorders. The biological effects of cytokines range from phagocytic cell activation to immune cell production from stem cells. Anti-inflammatory cytokines such as IL-10 are equally important in dampening the responses of immune cells following clearance of an infection (Turner et al., 2014).

1.5.5 Immune cell recruitment

Cells of the innate system include myeloid cells such as monocytes, macrophages, dendritic cells, mast cells and granulocytes (neutrophils, eosinophils and basophils). The system also includes innate lymphoid cells (ILCs) such as NK cells which derive from lymphoid progenitor cells like T and B cells (Figure 1.1) but lack antigen specific receptors. Tissue resident cells such as embryonic progenitor cell derived macrophages can produce chemokines which recruit monocytes and neutrophils to a site of infection. These macrophages are common near sites of primary exposure such as the lungs and intestines and are critical for the initiation of the inflammatory response. One study demonstrated that trafficking of neutrophils to an inflamed uroepithelium was only possible following the stimulation of chemokine CXCL2 release from tissue resident macrophages by monocyte derived Ly6C+ macrophages (Schiwon et al., 2014). It has also been shown that tissue resident mast cells aid in the recruitment of recruitment of neutrophils by the CXC chemokine macrophage inflammatory protein 2 through their release of the cytokine TNFα (Wang and Thorlacius, 2005). In particular, intraperitoneal mast cells are a main source of TNFα and implicated in early neutrophil recruitment (Malaviya et al., 1996).

The short-lived effector cells, neutrophils, are among the first cells to be called to an inflammatory site. As well their ability to phagocytose foreign matter and dead debris in the body, neutrophils also regulate the immune response through the recruitment of other types of immune cells. The type of cytokines that neutrophils release depends on the stimulus they receive. For example, neutrophils express IL-12 in response to LPS, whereas they release IL-13 and IL-33 in response to helminth infection. Neutrophils have also been found to influence macrophage activity such as

during *Leishmania* infection in which neutrophils enhance macrophage activity via TNFα and superoxide production. Macrophage response can also vary depending on the environment. M1 macrophages are highly phagocytic and associated with antimicrobial nitric oxide production, whereas M2 which can be stimulated during helminth infections have immunoregulatory functions through their ability to metabolise the local arginine supply needed by effector T cells to function (Rivera et al., 2016). In recent years, studies have highlighted the role of platelets as immune cells and how they might influence immune cell recruitment through interaction with cells such as neutrophils and influence the body's response to infection (Deppermann and Kubes, 2016). As this is an integral part of my thesis I will discuss it in more detail in a later section (Section 1.6.1).

1.5.6 Adhesion and transmigration of recruited cells

Another key part of immune cell function are the molecules utilized to tether immune cells to the endothelium and allow them to roll along the surface before arresting firmly at injured sites. Once arrested the cells can then leave the vasculature and migrate to the site of infection. For cells of the innate immune system this process is driven by expression of complementary trafficking receptors on leukocytes and endothelial cells. Selectin adhesion molecule such as P-selectin and E-selection are expressed by inflamed endothelium and allow for the initial tethering and rolling of cells such as neutrophils in the post capillary venules of the peripheral vasculature. (Hickey and Kubes, 2009). The lymphatic system is key to the recruitment and activation of lymphocytes as well as immune system surveillance and will be discussed in the following section.

1.5.7 Secondary lymphatic organs

The lymphatic system is involved in immune cell trafficking and surveillance. The system is integral to the mounting an adaptive immune response. Most of the activity of the lymphatic system happens within secondary lymphoid organs. These organs include lymph nodes localized all around the body, the spleen and gut-associated lymphoid tissue (GALT) which includes the tonsils and the Peyer's patches of the small intestine, which each connected by blood and lymphatic vasculatures.

Lymphatic vessels begin as blind ended valve containing tubes which collect DCs and excess interstitial fluid from surrounding tissues. These initial lymphatic vessels drain into collecting vessels that converge at lymph nodes. The lymph fluid flows into the node through afferent lymphatic vessels and travels through the sinuses of the node to bring DCs in contact with naïve lymphocytes such as B and T cells. Lymphocytes enter lymph nodes from the circulatory system through specialized blood vessels known as high endothelial venules (HEV). These entry sites are located within a fibroblastic reticular cell network (FRC) in the T lymphocyte rich paracortex (Figure 1.5). The FRC network is lined with antigen presenting cells (APCs) such as macrophages which T lymphocytes can survey in search of a "non-self" antigen. Following recognition of a foreign antigen, APCs will stimulate a T lymphocyte to proliferate, or if none are encountered the T cell will leave the re-enter the blood system through efferent lymphatics to make their way to other lymphatic organs. Surrounding the paracortex are follicles where follicular DCs are the main APCs and present to B lymphocytes. Recognition of an antigen by a B lymphocyte will

cause it to rapidly clone itself, and these cells further transform into antibody secreting plasma cells upon secondary stimulation by helper T cells (Girard et al., 2012).

The spleen is arranged differently to lymph nodes but is also separated into zones arranged to maximize the interaction between APCs and lymphocytes as well as an environment for B and T cell maturation. The spleen also differs in that it does not contain HEVs. Instead lymphocytes enter into the marginal zone through the afferent artery. B lymphocytes are directed to B cell follicles while T cells migrate to the T cell zone, directed by chemokines. DCs can then activate T lymphocytes which then surround the periphery of B cell follicles to activate B lymphocytes. Similar to lymph nodes these B lymphocytes can then produce specific antibodies to opsonize an invader and aid its removal from the body (Mebius and Kraal, 2005).

1.5.8 Immune cell recruitment to Gut Associated Lymphoid Tissue (GALT).

The intestines are an area of the body which is continuously exposed to foreign antigens in food as well having a thriving population of commensal bacteria believed to be essential for its function. As such the immune environment needs to be tightly regulated to prevent unwarranted immune system reactions while stopping the entry of a pathogen through this exposed organ system. The secondary lymphoid organ of the intestines, GALT, consists of both isolated and aggregated lymphoid follicles and contains up to 70% of the body's immunocytes. The largest of the lymphoid follicles are the Peyer's patches (PP) of the small intestines which are surrounded by specialized epithelium known as follicle–associated epithelium (FAE) that is the interface between the GALT and the luminal environment (Jung et al., 2010).

Similar to lymph nodes, naïve and memory lymphocytes are recruited to the GALT through HEVs. However, GALT HEVs are dissimilar in that they express high levels of mucosal vascular addressin cell adhesion molecule 1 (MAdCAM1). Migratory retinoic acid–presenting DCs travel from the intestinal lamina propria to the mesenteric lymph nodes (MLNs) once presented with an antigen. These DCs then upregulate integrin α4β7, the ligand for MAdCAM1, ligand on lymphocytes. This integrin allows for activated B and T lymphocytes specific for gut antigens to travel towards the GALT or the intestine lamina propria itself. The HEVs specific adhesion molecule L-selectin and the B-cell lectin CD22 are also believed to be ligands of MAdCAM1 and bind to its mucin domain which is linked with O-linked carbohydrates. Peripheral lymph node (PLNs) express peripheral lymph node addressin which consists of branched high-affinity, high-avidity L-selectin binding sites. In contrast, PP HEVs have lower affinity L-selectin binding sites as well as a reduced number of sites. Consequently, this form of L selectin supports loose and rapid rolling of lymphocytes and the engagement of MAdCAM1 with integrin a4B7 is required to arrest the rolling cells sufficiently to allow chemokine signals to trigger integrin α4β7 and lymphocyte function–associated antigen-1 intercellular adhesion molecule-1 (ICAM1)-dependent arrest (Habtezion et al., 2016). These details are important because platelet CLEC-2 has been shown to maintain the vascular integrity of HEVs (Herzog et al., 2013). However, the bleeding has been shown to spontaneously occur in MAdCAM-1 expressing lymph nodes and therefore CLEC-2 may influence the immune cell recruitment to these areas.

Another unique aspect of PPs is the existence of specialized enterocytes called M-cells which form part of their specialized epithelium cap. The M-cells work to transport luminal antigens

and bacteria towards the underlying lymphoid aggregate resulting in the activation or inhibition of the immune response. PPs also highly express PRR receptors, such as Nod2 on follicle associated cells. Nod2 recognises component of the peptidoglycan bacterial wall present in most Gram positive and Gram negative bacteria known as muramyl dipeptide (MDP). Studies of shown that lack of Nod2 in mice leads to a strong immune reaction to the commensal bacteria in the gut and NOD2 variants are associated with Crohn's disease. PPs are therefore critical to determining whether an intestinal luminal antigen will trigger either tolerance or a systemic immune response (Jung et al., 2010).

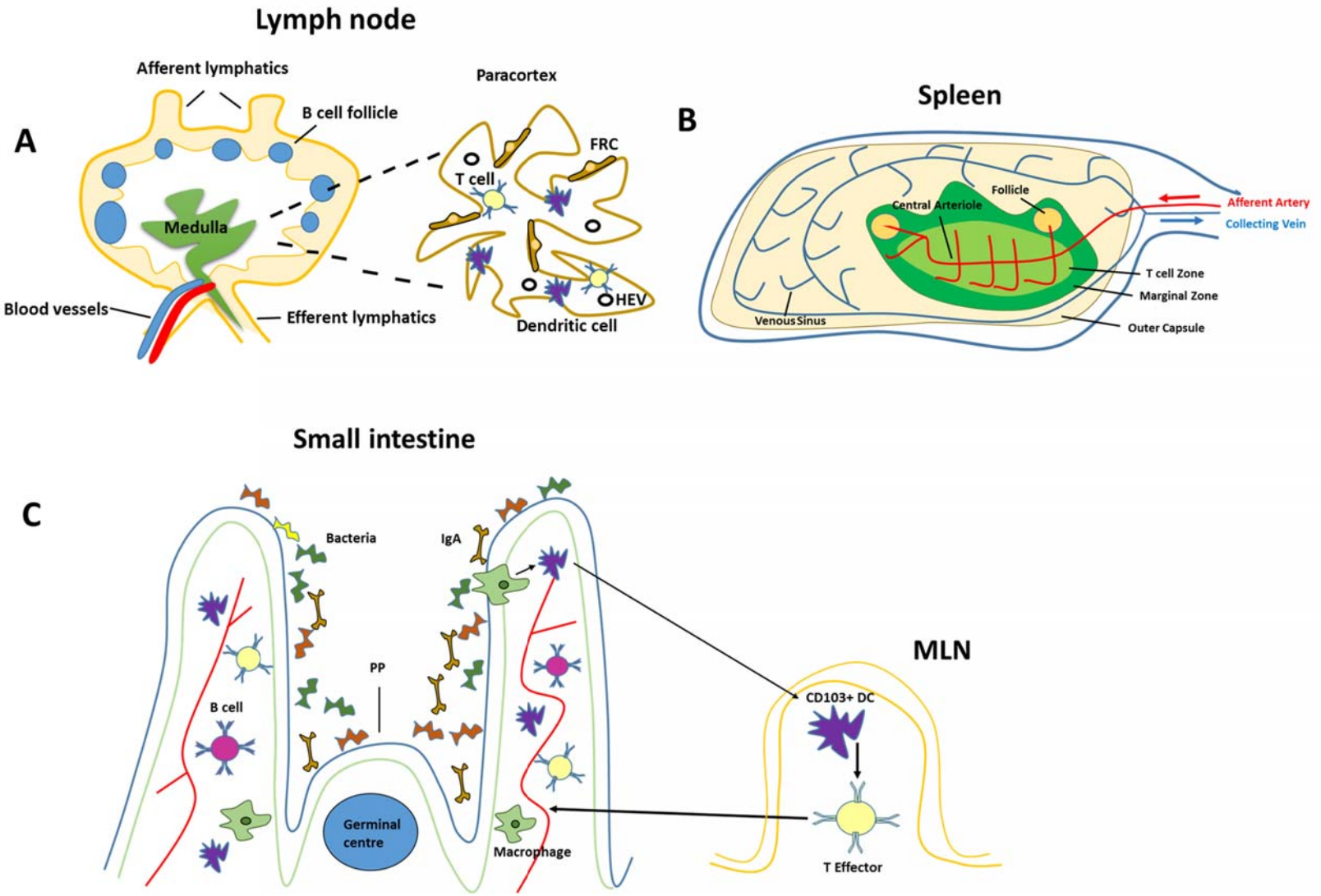
Lymph node
A
Afferent lymphatics
B cell follicle
Paracortex
FRC
T cell
Medulla
HEV
Blood vessels
Efferent lymphatics
Dendritic cell
B
Spleen
Follicle
Central Arteriole
Afferent Artery
Collecting Vein
T cell Zone
Marginal Zone
Venous Sinus
Outer Capsule
Small intestine
C
Bacteria
IgA
PP
B cell
Germinal centre
Macrophage
MLN
CD103+ DC
T Effector

Figure 1.5: Immune cell trafficking to lymph nodes and the intestines.

A. Immune cells enter lymph nodes through afferent lymphatic vessels and travel through the parenchymal tissue lined with phagocytic macrophages before entering the B cell rich follicles or T cell rich paracortex. Lymphocytes enter through high endothelial venules in the paracortex where they come into contact with APCs with the fibroblastic reticular cell network. Platelet CLEC-2 has been shown to be integral in the maintaining the vascular integrity of high endothelial venules through interaction with podoplanin expressing fibroblastic reticular cells. Immune cells leave lymph nodes through the efferent lymphatics and can continue to the body for foreign bodies.
B. Arterial blood enters the spleen into the "red pulp" where aged erythrocytes can be phagocytosed by macrophages. B and T lymphocytes enter into the marginal zone from afferent blood vessels. B cells mature in the germinal centres of the spleen to become antibody producing plasma cells. The spleen acts as an immune surveillance organ similar to lymph nodes, screening for foreign antigens and providing an environment for the adaptive system to mount an attack.
C. Intestinal APCs can sample the microbial environment of the intestine and display these antigens to tissue resident dendritic cells (DCs). Dendritic cell then travel to mesenteric lymph nodes (MLN) to stimulate lymphocytes such T cells to express the integrin α4β7 allowing the cells to transmigrate into the intestinal tissue. Peyer's patches (PP) also serves as immune sensors of the intestine and contain germinal centres for B cell proliferation. Modified from (Habtezion et al., 2016) and (Girard et al., 2012).

1.6 Platelets in disease

1.6.1 Platelets in acute infection

Over the last number of years there has been an increasing body of evidence indicating that platelets play an active role in the immune system as well as mediators of haemostasis. Within the three types of platelet granules, α-granules, dense granules and lysosomes, platelets contain proteins such as chemokines and mitogenic factors. Platelets are also said to contain a limited amount of mRNA and the translational machinery to synthesise proteins. Proteomic analysis revealed that platelets can secrete up to 300 different proteins following activation including interleukin-1 (IL-1), monocyte chemotactic protein-1 (MCP-1) and transforming growth factor β (TGFβ) which do not play a role in blood clotting but are instead believed to be involved in inflammation and tissue repair processes (Coppinger et al., 2007).

Platelets are thought to interact with immune cells during an infection to influence their behaviour and promote their recruitment. For instance, platelets can bind to LPS through TLR4 and present it to neutrophils to stimulate their activation (Clark et al., 2007). This neutrophil activation was shown to cause degranulation and release of DNA in mice which forms structures known as neutrophil extracellular traps (NETs) which trap and isolate the infecting bacteria. It was also found that plasma from septic patients leads the formation of NETs through promotion of platelet-neutrophil interaction (Clark et al., 2007). Trapping bacteria this way may be beneficial in stopping the spread of the infection but the by product release of substances such as reactive oxygen species may be damaging to the underlying tissue (Brinkmann et al., 2004).

One of the common consequences in patients with sepsis is the development of thrombocytopenia, and this is strongly associated with increased mortality. During sepsis, platelets as well as leukocytes become activated which contributes to DIC, decreased blood and oxygen delivery and eventual multi-organ failure. Activated platelets are also thought to release platelet microparticles which express various molecules found on platelets such as integrin αIIbβ3 (Ogura et al., 2001). These microparticles can readily interact and adhere to endothelial cells, leukocytes or other platelets. They therefore may be responsible for increasing the inflammatory signals during sepsis (Ogura et al., 2001, Mause et al., 2005). There is also a disruption of the endothelial barrier in septic patients with thrombocytopenia which results in increased vascular permeability. Platelets may be responsible in maintaining this barrier through direct contact with the endothelium or the release of stabilising factors. It is not yet clear whether platelets contribute to death by sepsis or are if they are one of the main causes of mortality (Li et al., 2011, Semple et al., 2011).

Platelets have been shown to interact with certain bacteria strains directly via receptors such as glycoprotein GPIb and integrin αIIbβ3. In fact, the absence of the GPIb-IX-V complex was shown recently to lead to reduced platelet–neutrophil and platelet–monocyte interactions and evaluated serum cytokine levels using the cecal ligation mouse model of sepsis (Corken et al., 2014). It has also been shown that *Staphylococcus epidermis* can induce human platelet aggregation via direct interaction with αIIbβ3 (Brennan et al., 2009).

As well as the involvement platelets have in releasing inflammatory mediators and interacting with leukocytes, multiple studies have shown that they are critical to the maintenance of vascular integrity during inflammation (Boulaftali et al., 2013, Goerge et al., 2008). Models of dermatitis and LPS induced lung inflammation revealed the development of haemorrhages at the site of inflammation in thrombocytopenic mice (Goerge et al., 2008). Later studies have since revealed that platelet ITAM signalling is critical in securing vascular integrity during leukocyte recruitment, as mice transfused with platelets lacking signalling through GPVI, CLEC-2 or SLP-76 developed haemorrhages in the skin and lungs following inflammatory stimulus (Boulaftali et al., 2013). The collagen receptor GPVI has since been revealed to be critical in preventing bleeding caused by neutrophil transmigration during immune complex mediated inflammation (Gros et al., 2015). A depiction of the varying roles that platelets play in infection and inflammation can be seen below in Figure 1.6.

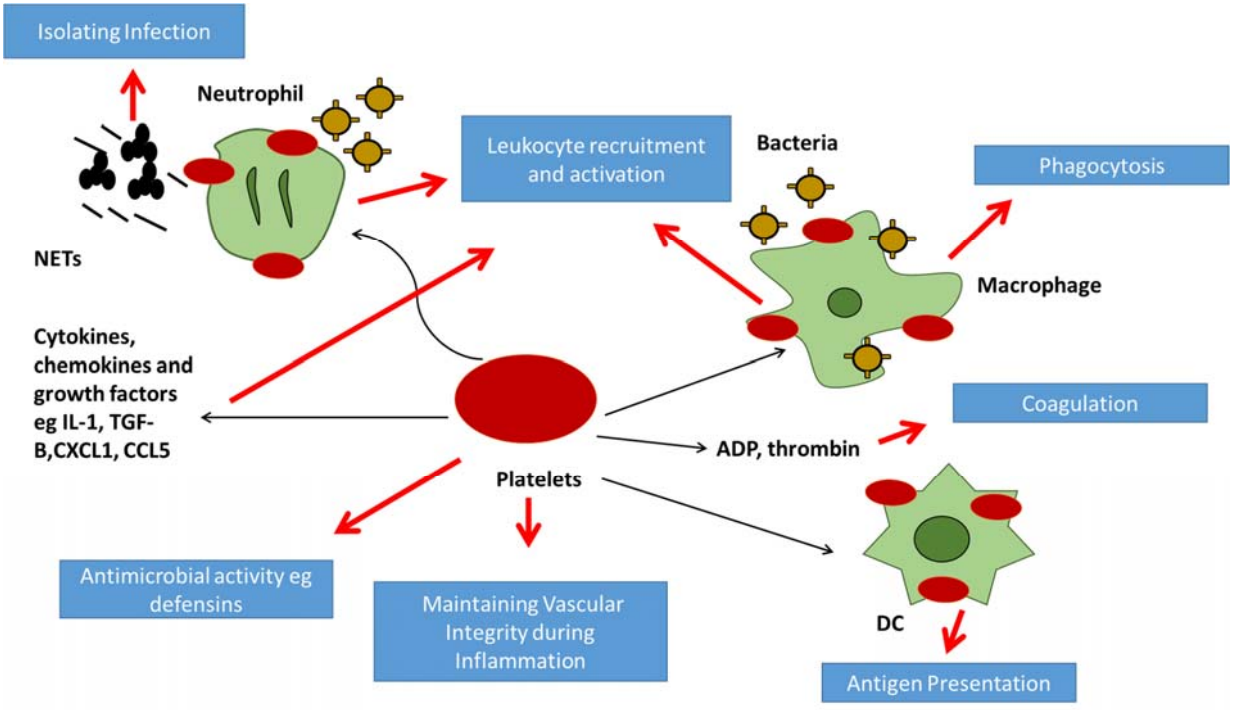

Figure 1.6: Role of platelets in infection

Platelets play a multi-faceted role in the innate immune system. As well the direct release of mediators such as cytokines and defensins, platelets interact and support the function of innate leukocytes. Platelets also activate leukocytes through supporting formation of thrombin and aid the adaptive immune response through interaction with DCs. Image adapted from (Mantovani and Garlanda, 2013).

1.6.2 Role of CLEC-2 and Podoplanin in infection and inflammation

Podoplanin and CLEC-2 interaction have been demonstrated to directly affect a range of inflammatory diseases and infections. However, the influence which CLEC-2 and podoplanin play in these different conditions, whether beneficial or deleterious, is highly dependent on the specific infection, inflammatory state and nature of the interaction. It was first discovered in 1990 that the Human Immunodeficiency Virus (HIV-type1) is internalised by megakaryocytes and platelets (Zucker-Franklin et al., 1990). Later it was discovered that platelet CLEC-2 mediates this internalisation through an interaction with a macrophage cell line expressing podoplanin and C-type lectin receptor DC-SIGN, which in turn facilitates the spread of infection (Chaipan et al., 2006). In a very different manner to HIV, CLEC-2 on platelets has also been shown to influence the pathology of salmonella infection. A recent study demonstrated that the infection leads to an upregulation of podoplanin within the liver driven by TLR4 and IFNγ dependant inflammation. This inflammation driven upregulation causes the formation of occlusive thrombi. The potentially life threatening venous thrombosis is inhibited in the absence of CLEC-2 expressing platelets or macrophages, which are suspected to be the podoplanin expressing cell (Hitchcock et al., 2015).

The influence these molecules have in inflammatory disorders is also variable. Rheumatoid arthritis (RA) is a chronic systemic inflammatory disease which leads to progressive degradation of the articular cartilage and bone. Platelet CLEC-2 has been shown to interact with synovial fibroblasts during this disease and increase the levels of proinflammatory IL-6 and IL-8. Platelet microvesicles from RA patients have also been shown to express CLEC-2 and are thought to have pro-inflammatory effects within the synovial fluid (Gitz et al., 2014). Coinciding with this discovery

is the presence of podoplanin expression in areas of inflammation, and synovial fibroblast activation and transformation (Del Rey et al., 2014). CLEC-2 and podoplanin may therefore be interacting and causing the progression of the pathology of this disease.

However, in the case of multiple sclerosis (MS), which is an inflammatory disease of the central nervous system (CNS), podoplanin has been suggested to enhance the resolution of inflammation. Using a mouse model of MS, known as spontaneous experimental autoimmune encephalomyelitis (EAE), it was shown that podoplanin is expressed on a subset of CD4+ effector T cells known as Th17 cells. A T cell specific deletion of Pdpn leads to exacerbated EAE due to an increase in the number of effector T cells within the CNS. Podoplanin was shown to increase expression of other inhibitory molecules and downregulate survival factors and is therefore believed to promote tissue tolerance (Peters et al., 2015). However, podoplanin expression has not been found the lymphocytic infiltrates of glioblastoma multiforme (GBM), an aggressive malignant primary brain tumour indicating that the upregulation is dependent on the autoimmune environment of MS.

1.7 Platelets in chronic inflammatory diseases

1.7.1 Atherosclerosis and platelets

Atherosclerosis is a chronic inflammatory disease of blood vessels and is one the main risk factors of cardiovascular disease, a leading cause in mortality worldwide. In this section I will discuss how platelets are involved in the development of atherosclerosis as well as in in potential plaque rupture.

For many years, it was believed that atherosclerosis was caused by a passive accumulation of cholesterol on the vessel wall. It is now appreciated that the disease involves many complex factors involving the innate and adaptive immune system. The lesions start as “fatty streaks” of subendothelial deposition of lipids such as low density lipoprotein (LDL) and macrophages filled with cholesterol known as foam cells. These lesions develop over time into atherosclerotic plaques containing an infiltration of immunocytes such as macrophages, T cells, and mast cells usually contained within a fibrous cap. The fibrous cap is mainly made up of collagen and is generated from vascular smooth cells, whose numbers increase during plaque formation. As plaques grow they can cause a narrowing of the lumen that leads to ischemia of the surrounding tissue. Overtime the fibrous cap of a plaque can become thinner and lead to unstable plaques. The exposure of collagen as well as the inflammatory cells and signals within the plaque is what leads to platelet aggregation and clot formation. These clots can then embolise to different areas of the body such as the coronary arteries or the arteries of the brain and result in cardiac arrest or stroke (Hansson and Hermansson, 2011).

Research has found that platelets are also involved in the development of atherosclerosis. Platelet activation, as defined by P-selectin expression, can be found at different stages of atherosclerosis. It is unclear what contributes to platelet activation during the early stages of atherosclerosis but it may be factors such as an increase in pro-thrombotic and pro-inflammatory mediators such as tissue factor and chemokines or a decrease in endothelial antithrombotic factors such as nitric oxide and prostacyclin production. Studies have shown that platelet activation is a key influence in plaque development. Inhibition of platelets through the use of aspirin, indomethacin or inhibition of thromboxane A_2 receptors have all shown to drastically reduce the formation of atherosclerotic lesions (Huo and Ley, 2004).

As mentioned previously in this chapter, platelets can release a large range of adhesive and pro-inflammatory substances. For instance, activated platelet can bind to and regulate monocyte functions which may be promoting their recruitment to plaques. Also the platelets can release the chemokine PF-4 which enhances the binding of oxidised LDL to vascular endothelium and smooth muscle cells and platelets are also capable of depositing the strong monocyte and memory T lymphocyte chemokine CCL5 (also known as RANTES) on the surface of atherosclerotic plaques (Lievens and von Hundelshausen, 2011, Weber, 2005).

Interestingly for this thesis, the CLEC-2 ligand podoplanin has been found to be expressed in advanced atherosclerotic lesion from human aortic samples on both macrophages and smooth muscle cells (Hatakeyama et al., 2012).

1.7.2 Inflammatory bowel disease and platelets

Inflammatory bowel disease (IBD) is a chronic relapsing inflammatory disease of the intestine. It is classified into two forms: Crohn's disease (CD) which happens throughout the entire gastrointestinal tract (GI) focused mainly in the terminal ileum and colon and ulcerative colitis (UC) which displays as mucosal inflammation of the colon and rectum. These diseases result in similar symptoms cause by epithelial injury and recurring intestinal inflammation. The underlying causes of this disease are believed to stem from a mixture of several factors such as genetic predisposition and other environmental factors such as diet or mediations which initiates disturbances in the epithelial lining of the gut. The lack of a robust epithelial barrier allows for luminal antigens, such as antigens from commensal bacteria, to enter the intestinal tissue. Failure to resolve the acute inflammation that ensues, results in chronic inflammation that further damages the intestinal tissue (Neurath, 2014).

Many platelet abnormalities have been found in patients with IBD. Similar to the case of atherosclerosis, platelets from IBD patients are often found in an activated state regardless of the disease activity. It has also been reported that IBD platelets are reduced in size and circulate in higher numbers. Platelet count has in fact been suggested as a method of distinguishing between IBD and infectious diarrhoea. IBD platelets are also capable of spontaneous aggregation and are more sensitive to platelet agonist such as ADP and collagen. It is also important to note that intravascular microthrombi are frequently found with the intestinal mucosa of CD and UC patients but rarely if ever found in healthy tissue (Danese et al., 2004).

A recent paper has also reported a role for platelets in the lymphangiogenesis seen in IBD (Sato et al., 2016). It has long been reported that lymphatic remodelling occurs during active IBD and blocking lymphangiogenesis results a worsening of murine colitis (Alexander et al., 2010). Sato et al. also demonstrated that more lymphatic vessels are present in samples from inflamed ulcerative colitis patients and a mice model of colitis treated with dextran sulfate sodium. However depleting platelets was shown to increase lymphangiogenesis in the colons of these mice and resulted in a less severe colitis phenotype. Platelets are seen within the mucosal layer of DSS treated mice and in a colitis model in rats, and the hypothesis that they cause the inhibition of lymphatic vessel formation was backed up by *in vitro* data showing platelets inhibiting LEC proliferation. The interaction between platelets and LECs has been previously shown to be dependent on CLEC-2 and podoplanin (Finney et al., 2012, Bertozzi et al., 2010).

1.8 Aims

In recent years, there has been an increase in research into the role of platelets beyond their involvement in classical haemostasis and thrombosis. Studies have shown that the platelet receptor CLEC-2 is involved in many of these newly emerging roles. In this thesis, I investigated the interaction of platelet CLEC-2 with its ligand podoplanin using *in vitro* and *in vivo* models.

An in vitro flow model was used to investigate the interaction of the mouse forms of these proteins under the conditions of shear stress. Previous work in our lab using this model using human platelets lead us to believe that mouse platelets would interact with recombinant mouse podoplanin solely under the conditions of venous shear rates.

The role of the CLEC-2-podoplanin axis was also investigated using *in vivo* mouse models of inflammation. Recent studies highlighted that CLEC-2 is involved in maintaining vascular integrity during inflammation. CLEC-2 has also been shown to play a role in inflammatory disorders such as rheumatoid arthritis and multiple sclerosis. Interestingly, the CLEC-2 ligand podoplanin has been shown to upregulated on cells such as macrophages following an inflammatory stimulus. The role of platelet CLEC-2 was previously investigated and found to play a role in atherosclerosis. I further investigated how podoplanin may be involved in this phenotype. I also focused on the hypothesis that CLEC-2 may influence acute inflammation using a sterile inflammatory stimulus (LPS peritonitis) and a model of ulcerative colitis.

The specific aims were:

1. To investigate the interaction of recombinant mouse podoplanin with mouse platelets under the conditions of shear stress.

2. To investigate the influence of platelet CLEC-2 in a sterile of acute inflammation, in particular, a potential influence on early immune cell recruitment.

3. To investigate the role of platelet CLEC-2 using a non-sterile form of acute inflammation, namely DSS induced ulcerative colitis.

4. To investigate the influence of the CLEC-2 ligand podoplanin in an atherosclerosis mouse model.

Chapter 2

Materials and Methods

2.1 Antibodies

Table 2.1 Antibodies

Antibody	Clone number	Host species	Dilution	Source
	PRIMARY			
Podoplanin	8.1.1	Hamster	IF -1/200, WB - 1/200	EBioscience (Hatfield,UK)
CLEC-2	17D9	Rat	WB -1/1000	Biolegend (USA)
His tag	-	-	WB -1/1000	Cell Signaling Technology, USA
CD45	OX-1	Rat	IF -1/200	BioRad (Hertfordshire)
CD68	KP-1	Mouse	IF -1/200	Abcam (Cambridge, UK)
Smooth Muscle Actin	1A4	Mouse	IF -1/200	Abcam (Cambridge, UK)
F4/80	BM8	Rat	IF -1/200	EBioscience (Hatfield,UK)
Lyve-1 Biotin	ALY7	Rat	IF -1/200	EBioscience (Hatfield,UK)
CD326 (EpCAM)	G8.8	Rat	IF -1/200	EBioscience (Hatfield,UK)
Rat IgG	-	Rat	WB- 1/1000	Santa Cruz Biotechnology (Santa Cruz, US)
Rabbit IgG	-	Rabbit	WB- 1/1000	Santa Cruz Biotechnology (Santa Cruz, US)
Hamster IgG	-	Hamster	IF- 1/200 WB- 1/200	EBioscience (Hatfield,UK)
Mouse IgG	-	Mouse	IF -1/200	Santa Cruz Biotechnology (Santa Cruz, US)
Podoplanin- PE	8.1.1	Hamster	FC- 1/100	EBioscience (Hatfield,UK)
CD45-FITC	2D1	Rat	FC- 1/100	EBioscience (Hatfield,UK)
CD45-APC	2D1	Rat	FC -1/100	EBioscience (Hatfield,UK)

CD45- APCCy7	2D1	Rat	FC -1/100	EBioscience (Hatfield,UK)
CD11b-Biotin	M1/70	Rat	FC -1/2000	EBioscience (Hatfield,UK)
CD31- Biotin	390	Rat	FC -1/2000	EBioscience (Hatfield,UK)
F4/80-FITC	BM8	Rat	FC -1/100	EBioscience (Hatfield,UK)
F4/80-APC	BM8	Rat	FC -1/100	EBioscience (Hatfield,UK)
Ly6G-APCCy7	RB6-8C5	Rat	FC -1/100	EBioscience (Hatfield,UK)
Ly6C-PerCP-Cy5.5	HK1.4	Rat	FC -1/100	EBioscience (Hatfield,UK)
CD11c-PECy7	3.9	Rat	FC- 1/200	EBioscience (Hatfield,UK)
CD4- PECy5.5	GK1.5	Rat	FC -1/100	EBioscience (Hatfield,UK)
CD8-PB	SK1	Rat	FC -1/100	EBioscience (Hatfield,UK)
CD19-PECy7	1D3	Rat	FC -1/100	EBioscience (Hatfield,UK)
MHCII-PB	M5/114.15.2	Rat	FC- 1/50	EBioscience (Hatfield,UK)
CD206-FITC	MR6F3	Rat	FC -1/100	EBioscience (Hatfield,UK)
CLEC-2-FITC	17D9	Rat	FC-1/30*for platelet microvesicles	BioRad (Hertfordshire)
CD41- APC	MWReg30	Rat	FC-1/30*for platelet microvesicles	EBioscience (Hatfield,UK)
Hamster IgG-PE	-	Hamster	FC- 1/200	EBioscience (Hatfield,UK)
Rat IgG-PB	-	Rat	FC- 1/200	EBioscience (Hatfield,UK)
	SECONDARY			
Anti-Rat HRP	-	Goat	WB- 1/10,000	Santa Cruz Biotechnology (Santa Cruz, US)
Anti-Rabbit HRP	-	Goat	WB- 1/10,000	Santa Cruz Biotechnology (Santa Cruz, US)

Anti-Human HRP	-	Goat	WB-1/10,000	Santa Cruz Biotechnology (Santa Cruz, US)
Anti-Hamster HRP	-	Goat	WB-1/10,000	Santa Cruz Biotechnology (Santa Cruz, US
IgG-H&L-Cy3® (Hamster)	-	Goat	IF -1/500	Invitrogen (Paisley,UK)
AlexaFluor® 488 (Rat)	-	Goat	IF -1/500	Invitrogen (Paisley,UK)
AlexaFluor® 488 (Mouse)	-	Goat	IF -1/500	Invitrogen (Paisley,UK)
AlexaFluor® 647 (Mouse)	-	Goat	IF -1/500	Invitrogen (Paisley,UK)
AlexaFluor® 488 (Hamster)	-	Goat	IF -1/500	Invitrogen (Paisley,UK)
Streptavidin-PE	-	Goat	FC -1/400	EBioscience (Hatfield,UK)
Streptavidin-FITC	-	Goat	FC -1/400	EBioscience (Hatfield,UK)

Table 2.1: Antibodies

Details of all antibodies used in the methods described in this thesis. WB= Western Blotting HRP=Horseradish peroxidase IF= Immunofluorescence, FC= Flow Cytometry

2.2 Mice

2.2.1 Mice strains

All animal experimentation was performed under approved licenses from the UK Home Licence. Conditional deletion of CLEC-2 was generated first by insertion of loxP sites flanking exons 3 and exons 4 of the CLEC-2 (Clec1b) gene (CLEC-$2^{fl/fl}$). The mice were then bred with PF4-Cre recombinase mice bought from Jackson Laboratories (C57BL/6-Tg(Pf4-icre)Q3Rsko/J) which deleted CLEC-2 expression from cells of platelet and megakaryocyte lineage (PF4-Cre.CLEC-$2^{fl/fl}$). An inducible CLEC-2 deficient mouse model (ER^{T2}-Cre.Clec-$2^{fl/fl}$) was generated by the breeding of Clec-$2^{fl/fl}$ mice to mice expressing ER^{T2} Cre recombinase driven by the ROSA26 locus bought from Jackson Laboratories (B6.129-Gt(ROSA)26Sortm1(cre/ESR1)Tyj/J) and backcrossed 8 times onto a C57BL/6 background.

$ApoE^{-/-}$ mice (B6.129P2-Apoetm1Unc/J) were purchased from Charles River. $ApoE^{-/-}$ mice were crossed to ER^{T2}-Cre.Clec-$2^{fl/fl}$ to generate an inducible CLEC-2-deficient mouse model on an athero-prone background.

Mice with a conditional deletion of podoplanin ($Pdpn^{fl/fl}$) were generated by Taconic Artemis on a C57BL/6 background. These $Pdpn^{fl/fl}$ were then crossed to mice expressing Cre recombinase driven by the Vav promotor (*Vav-iCre*) from Jackson Laboratories (B6.Cg-Tg(Vav1-icre)A2Kio/J) used for conditional deletion from haematopoietic cells and their progenitors. *Vav-iCre* mice were also crossed to R26-stop-EYFP mice which results in a mouse with Vav promotor directed EYFP expression (Vav-iCre. R26-stop-EYFP) mice previously described in (Siegemund et al., 2015).

2.2.2 Tamoxifen induced depletion of CLEC-2

ER^{T2}-Cre.Clec-$2^{fl/fl}$ and CLEC-$2^{fl/fl}$ control mice were aged to 6-8 weeks old before being placed on TAM 400 diet (contains 40mg/kg tamoxifen) for 2 weeks and weighted every day to check that the weight of the mice did not drop below 20% of the original weight. The mice were then put on normal diet for 4 weeks due to the anti-inflammatory effects of tamoxifen before being treated with DSS or LPS as later described.

2.2.3 Systemic Inflammatory Challenge

Different mice strains were aged to 12 -13 weeks old (to accommodate for the tamoxifen induced depletion described above) before being treated with an intraperitoneal (IP) injection of 50µg lipopolysaccharide (LPS O11:B4) diluted in sterile PBS. The mice were kept at 37^{o}C for 6 or 24 hours after the injection. The mice were then anaesthetised using isoflurane gas followed by a lethal dose of $C0_2$ gas. The Home Office licence used for this work allowed for a moderate severity limit. As such, animals were humanely killed if they show signs of ill health, such as continued piloerection, intermittent hunched posture and reduced activity. In addition, any animal that loses >20% of its body weight during an experiment was culled immediately. Peritoneal lavage fluid was collected by injection of 2ml of ice cold PBS 2mM EDTA into the peritoneal cavity and subsequently withdrawn. The spleens, small intestines and colons from these mice were also collected from these mice for flow cytometry analysis. Mouse injections and collection of organs was carried out by Dr. Sian Lax.

2.2.4 DSS Induced Colitis

Following a diet of tamoxifen and a 4 week interim period as described, the water supply of ER^{T2}-Cre.Clec-$2^{fl/fl}$ and CLEC-$2^{fl/fl}$ control mice was replaced with a 3% dextran sodium sulphate (DSS) solution for 6 days. The clinical score limits which were used for these mice are described in Table 2.2.

Table 2.2: Clinical Score measurements for DSS treated mice.

Weight loss (from baseline)	No weight loss or increase Weight loss of 1-5% Weight loss of 6-10% Weight loss of 11-15% Weight loss of >15%	0 1 2 3 4
Stool consistency	Well-formed pellets Semi-formed pellets (no anal adherence) Liquid stools (with anal adherence)	0 1 2
Bleeding	No blood by hemoccult Positive by hemoccult Gross bleeding	0 1 2
Appearance	Normal Ruffled coat Hunched Lethargic	0 1 2 3

Table 2.2: Clinical Score measurements for DSS treated mice.
Table and scores adapted from (Fattouh et al., 2013).

Mice will be weighed daily and any animal that has a cumulative clinical score of > 9 will be humanely killed. The mice were anaesthetised using isoflurane gas followed by a lethal dose of $C0_2$ gas and colons of these mice collected. Blood measurement within the stool of the mice was done using the Hemoccult test as per instructions on the kit (Hemoccult 40, Point of Care Testing Ltd, Angus). This work was done by Sian Lax.

2.2.5 Atherosclerotic mice

$ApoE^{-/-}$ mice were aged to 10 weeks old on normal chow diet before being placed on a high fat western diet for 6 weeks. Mice were then anaesthetised and culled using $C0^2$ gas. Hearts and aortas were removed for sectioning and RNA analysis respectively. Aortic sinus sections from $ApoE^{-/-}$ x ER^{T2}-Cre.Clec-$2^{fl/fl}$ were provided by Matt Harrison and Marie Lordkipanidze. These mice were aged similarly to $ApoE^{-/-}$ and subjected to tamoxifen injections at 9 weeks old before being put on high fat western diet for 6 weeks.

2.3 Recombinant protein expression and protein biochemistry

2.3.1 Recombinant Podoplanin expression

Fc mPodoplanin (mPdpn Fc) -The extracellular domain of mouse Podoplanin was amplified from cDNA generated from a C57BL/6 kidney with the primers mPodoHindFor (GATCAAGCTTATGTGGACCGTGCCAGTGTTG) and mPodoFcRev (GATCGGATCCACTTACCTGTCAGGGTGACTACTGGCAAGCC). The PCR product was cloned into IgFc vector pcDNA3Ig to yield a construct encoding the extracellular domain of Podoplanin fused at the C terminus to the Fc region of human IgG1. For the expression and purification of the protein the expression vector was transfected into 293T cells using the polyethylenimine transfection method. The fusion protein was then purified by affinity chromatography using protein A-Sepharose. mPdpn Fc containing fractions were dialysed into PBS. Purity was confirmed by sodium dodecyl sulfate-polyacrylamide gel electrophoresis and western blot using an anti- mouse Podoplanin antibody (Table 2.1).

His-tagged hPodoplanin (hPdpn-His) and His-tagged mPodoplanin (mPdpn-His)- The vector pHLsec was used for expression of these recombinant proteins and was designed by Maria Hoellerer. The primers used for hPdpn-His were hPDPNFor (GTACGAATTCGCCACCATGTGAAGGTG TCAGCTCTGC) and hPDPNRev (GATCAGGTACCGGTCACTGTGACAAACCATCTTTC). The primers used for mPdpn-His were mPDPNFor (GTACGAATTCGCCACCATTGGACCGTGCCAGTGTTG) and mPDPNRev (GAT TCAGGTACCGGTGATACTGGCAAGCCATC). The PCR products was cloned into the pHLSec vector and the expression vectors were transfected into 293T cells using the polyethylenimine transfection

method. The fusion proteins were purified from culture supernatants by affinity chromatography using Qiagen Ni-NTA beads, eluted with imadazole and dialyzed into phosphate-buffered saline (PBS). Purity was confirmed by sodium dodecyl sulfate-polyacrylamide gel electrophoresis and western blot using anti- His tag antibody and anti -mouse or anti human Podoplanin antibodies (Table 2.1). All three proteins were produced by the Protein Expression Facility in the University of Birmingham.

2.3.2 Recombinant CLEC-2 expression

A fusion protein of amino acids 55-229 of the ECD of mCLEC-2 fused to an N terminal 6xHIS tag was generated using the amplification primers GGAACCGGTCATCATCACCATCACCATCACCATACACAGCAAAAGTATCTA and CGTGGTACCTTAAAGCAGTTGGTCCACTCT, designed by Alice Pollitt. The PCR product was cloned into the expression vector pHLsec and expressed in 293T cells using polyethylenimine transfection method. The fusion protein was purified from culture supernatants by affinity chromatography using a 1ml HisTrap HP (GE Healthcare) and eluted using imidazole. Fusion protein purity was confirmed by sodium dodecyl sulfate-polyacrylamide gel electrophoresis and western blot using an anti-His antibody and an anti-Clec-2 antibody. The fusion protein was dialyzed into PBS.

2.3.3 SDS-PAGE and Western blotting

In the process of making recombinant proteins, unpurified and purified supernatant from transfected cells were tested. These protein samples were heated to 100^{o}C for 5 min and centrifuged at 8600g for 5 min, before being run on a 4-12% gradient BOLT gel (Invitrogen, UK).

Pre-stained molecular weight marker (Bio-Rad, Hemel Hempstead, UK) were run alongside the spun down samples to determine molecular weights of the proteins of interest. Following the sample separation by SDS-polyacrylamide gel electrophoresis, the gel was then stained using Instant Blue (Expedeon, Cambridge, UK) to visualise the protein separation or proteins were transferred onto a polyvinylidene difluoride (PVDF) membrane. Membranes were then blocked in 3%BSA in TBS-T (Tris-buffered saline (200mM Tris, 1.37M NaCl; pH 7.6) containing 0.2% Tween20 and 0.1% w/v sodium aside) for 1 hr at RT or overnight at 4^{o}C depending on antibody used. Membrane were subsequently incubated with primary antibody diluted in 3% BSA-TBS-T for 1 hr at RT or overnight at 4^{o}C. Primary antibodies used for western blotting are outlined in Table 2.1. Membrane were washed 3 times for 10 min in TBS-T before incubation with a HRP-conjugated antibody with the specificity to bind to the primary antibody for 1 hr at RT. Primary antibodies and secondary (HRP-conjugated) used for western blotting are outlined in Table 2.1.The membranes were then washed 3 times in TBS-1 before being incubated with an enhanced chemiluminescence reagent (ThermoScientific Paisley, UK) and then imaged on autoradiographic film or imaged with the Licor Odyssey-FC imager (Chemiluminescence channel; Cambridge, UK) for band quantitation.

2.3.4 Dotblot

Purified protein sample from transfected cells such as His-tagged mCLEC described in section 2.3.2 were spotted onto PVDF membrane and left to dry at RT. The membranes were then blocked

using either 5% milk powder in TBS-T for 1 hr at RT. The secondary binding protein diluted in 5% milk powder in TBS-T was incubated with the membranes for 1hr at RT. Following incubation the membranes were washed 3 times for 10 min in TBS-T followed by incubation with a diluted sample of primary antibody specific to the secondary binding protein. Following washing in TBS-T 3 times for 10 min, the membranes were subsequently incubated with a secondary HRP antibody, again diluted in 5% milk powder in TBS-T. The membranes were then washed 3 times in TBS-T for 10 min before being incubated with an enhanced chemiluminescence reagent (ThermoScientific Paisley, UK) and then imaged on autoradiographic film or imaged with the Licor Odyssey-FC imager (Chemiluminescence channel; Cambridge, UK).

2.3.5 Surface plasmon resonance

Surface plasmon resonance binding studies were conducted using a Biacore T200 machine (Biacore GE, Sweden). Proteins were attached to the carboxymethylated dextran-coated surface of CM5 biosensor chips, using amine coupling chemistry. Experiments were performed in 10mM Hepes pH 7.4; 150mM NaCl; 3mM EDTA and 0.005% polysorbate 20 surfactant. Non-specific interactions were controlled for by subtraction of the signal from a reference blank flow cell. To avoid avidity effects with podoplanin which was expressed as a dimeric Fc-fusion protein, experiments were only performed with podoplanin immobilized on the chip surface. Raw data was analysed using Scrubber2 (BioLogic Software Pty Ltd, Australia), and KD values were obtained by nonlinear curve fitting using Graphpad Prism 5.

2.3.6 Protein quantitation

Following blood perfusion and washing with Tyrode's buffer, cell lysates were collected using 50µl lysis buffer (150mM NaCl, 10mM Tris, 1mM EGTA, 1mM EDTA, 5mM Na3VO4, 1mM AEBSF, 10µg/ml leupeptin, 10µg/ml aprotinin, 1µg/ml pepstatin). The protein was determined using a Bio-Rad Protein Assay kit (Bio-Rad laboratories, Germany) using a BSA gradient for the standard curve. Protein measurement from the peritoneal lavage fluid supernatant of challenged and unchallenged mice was determined was also determined using the Bio-Rad Protein Assay kit using a BSA gradient for the standard curve. Haemoglobin measurement of the peritoneal lavage fluid before red blood cell lysis was carried out using a bovine haemoglobin protein (Sigma, Poole, UK) standard curve. All the assays were measured using the Versa Max Microplate reader (Molecular Devices, CA, USA).

2.4 *In vitro* flow assay and platelet spreading experiments

2.4.1 Mouse and Human blood preparation

Mouse blood was drawn from the inferior vena cava of anaesthetized and then CO_2-asphyxiated mice into 5 U/mL heparin and 40µM PPACK, stained with 2µM $DiOC_6$. This work was authorised under UK Home office licences. Ethical approval for blood donation from healthy volunteers was granted by Birmingham University Internal Ethical Review (ERN_11-0175). Venous blood was collected from consenting, healthy drug free volunteers. Blood was drawn into 3.2% trisodium citrate BD vacutainers (Becton Dickinson, Oxford, UK). The blood was used for washed platelet preparation and for in-vitro flow experiment described in sections 2.4.3 and 2.4.4. Blood was incubated with inhibitors for 10 min before perfusion. Inhibitors used were dasatinib (Sigma, Poole, UK), Cangrelor (Medicines company, Place, UK), indomethacin (Sigma, Poole, UK), p0p/B antibody (Emfret, Germany), Eptifibatide (Queen Elizabeth Hospital pharmacy, UK). Fab fragments (mAb) (10µg/ml) were added to the human blood to block Fc receptor.

2.4.2 Washed platelet preparation and platelet spreading

Anti-coagulated mouse blood was centrifuged at 2000 rpm for 5 min in a microcentrifuge (ThermoScientific, Paisley, UK). The platelet rich plasma (PRP) along with the top third of erythrocytes were taken and placed in a fresh tube before centrifugation at 200 g for 6 min (Sanyo Harrier). Modified Tyrode's buffer was added to the PRP extracted above to give a total volume of 1 ml. Prostacyclin (PGI_2; 1 µg/ml) was added to the sample before centrifugation at 1000 g for 6 min. Supernatant was removed, and platelet pellet was resuspended with Modified Tyrode's

buffer (with 5 mM glucose, and 1 mM $MgCl_2$; pH 7.3). Washed platelets were then resuspended to the required platelet concentration of $2x10^7$/ platelet spreading.

Human washed platelets were prepared by adding 10% acid citrate dextrose (ACD) to citrated blood before centrifugation at 200 g for 20 min. The top layer of PRP was removed, avoiding the buffy coat layer. Prostacyclin (PGI_2; 1 µg/ml) was added before centrifugation at 1000 g for 10 min. The supernatant was discarded and the platelet pellet was resuspended in Modified Tyrode's buffer (with 5 mM glucose, and 1 mM $MgCl_2$; pH 7.3). The pellet was then washed in Modified Tyrode's buffer containing ACD and PGI_2 (1 µg/ml) and again centrifuged at 1000 g for 10 min. washed platelets were then resuspended to the required platelet concentration; $2x10^7$/ platelet spreading. Both human and mouse washed platelets were rested for 30 min before experiments. Coverslips (13 mm) were coated with 200µl of agonist (collagen 10µg/ml, Fc-mPdpn 100µg/ml, PBS control) were coated overnight before use. Protein coated coverslips were washed 3 times with PBS and then blocked with heat inactivated BSA (5 mg/ml) blocking buffer for 1h at room temperature. The coverslips were then washed with PBS before incubation with 200 µl washed platelets ($2x10^7$/ml). The platelets were then allowed to spread for 45 min at 37^{o}C. The coverslips were then gently washed using Modified Tyrode's buffer and the remaining platelets were fixed using formalin (10 min at RT). The coverslips were washed with PBS and then mounted onto glass coverslips using hydromount (National Diagnostics, Atlanta, USA). The coverslips were imaged using a differential interference contrast (DIC) microscope (Zeiss Axiovert 200, 63x oil immersion) with at least 10 fields of view per condition.

2.4.3 Capillary Flow assay

Glass capillaries tubes used were from Camlab, Cambridge UK. The glass capillaries with internal dimensions of 1 x 0.1mm were coated with 100µg/ml fibrillar Horm collagen or 100µg/ml mPdpn-Fc overnight at 4°C rotating slowly and followed by blocking using 5mg/ml heat denatured BSA in phosphate buffered saline (PBS). Blood was incubated with the fluorescent dye $DiOC_6$ and inhibitors for 10 min at 37°C. Blood was placed in a syringe and perfused through a capillary at the desired shear rate for up to 10 min at 37°C using a syringe pump (Harvard Apparatus Ltd, Kent, UK). The pump flow rate is calculated by the equation:

$$\frac{desired\ shear\ rate\ x\ capillary\ width\ x\ (capillary\ height)^2}{6}$$

The capillary was perfused with Tyrode's buffer for 5 mins at the same shear rate and temperature. Live imaging of the capillary was done using was an inverted stage microscope (DM IRB, Leica Microsystems Ltd, Milton Keynes UK) equipped with a digital camera (CoolSnap ES, Photometrics, Huntington Beach, CA) under fluorescent light for the duration of the experiment. The videos from these experiments were analysed by masked the fluorescence created from platelet aggregation to calculate a percentage area coverage. This analysis was done using Image J. The capillary was perfused with Tyrode's buffer for 5 mins at the same shear rate and temperature and imaged using a DIC (Zeiss Axiovert 200M) microscope. The images taken using the DIC microscope were analysed using software on the Zeiss Axiovert 200M which masked the fluorescence created from platelet aggregation to calculate an area coverage in μm^2.

2.5 Microscopy

2.5.1 Organ preparation

Hearts are first flushed with PBS by needle insertion through the bottom half of the heart before removal. Hearts are then placed in 10% formalin for up to 1 hour before embedding in optimum cutting temperature (O.C.T) media (Tissue-Tek®, Thermo Fisher Scientific Loughborough, UK) and snap freezing using a container of 2-methylbutane in liquid nitrogen. The hearts are then cut for sections of the aortic sinus using a Cryostat (Bright Instruments, Huntington, UK) onto Polylysine® coated adhesion slides (VWR, Leicestershire, UK). The slides were then dried for 30 min at 37^{o}C before storing at -80^{o}C.

Colons were first flushed with PBS using a round headed needle to remove any faeces. The colons were then cut open to create a flat structure and from there the organ was rolled into a "swiss roll" shape with the anus lying in the centre of the structure and pinned to keep the shape. The prepared colon was then left in 30% sucrose overnight at 4oC before embedding in O.C.T media (Tissue-Tek®, Thermo Fisher Scientific Loughborough, UK) and snap freezing using a container of 2-methylbutane in liquid nitrogen. Samples were cut using a Cryostat (Bright Instruments, Huntington, UK) onto Polylysine® coated adhesion slides. The slides were then dried for 30 min at 37oC before storing at -80^{o}C.

2.5.2 Haematoxylin and Eosin staining

Slides were dried at room temperature for 30 min before fixing in formalin for 10 min. The slides were then washed in PBS before being washed in deionised water. Following this the slides were stained in Harris Haematoxillin (Sigma, Poole, UK) for 2.5 min, followed by a short wash in 0.3% acid alcohol (0.3% HCl in 70% ethanol) and then submerged in deionised water until a blue colour on the tissue sections was visible. The slides were then stained in Eosin (Sigma, Poole, UK) for 2.5 min and then back of the slides were washed in running tap water. The sections were then put through a series of dehydration steps, first in 75% ethanol, then 90% ethanol, and finally 100% ethanol, each for 3 min at a time. Finally, the slides were incubated in Histoclear overnight and then mounted using DPX Mountant (Sigma, Poole, UK) and coverslips. The histology of the DSS treated colons were scored blindly by Dr. Sian Lax. The method of scoring considers architectural derangements, epithelium changes, goblet cell depletion, ulceration, and degree of inflammatory cell infiltrates. scoring system was used to quantify the degree of colitis. The total histologic score ranged from 0 to 12, which represented the sum of scores from 0 to 3 for loss of epithelium (0 = none; 1=mild, 2=moderate and 3 =severe), for crypt damage (0 = none; 1=mild, 2=moderate and 3 =severe) for depletion of goblet cells (0 = none; 1=mild, 2=moderate and 3 =severe) and for infiltration of inflammatory cells (0 = none; 1=mild, 2=moderate and 3 =severe).

2.5.3 Immunofluorescence

Slides were dried at room temperature for 30 min before fixing in ice cold acetone for 15 min. Sections were then circled with an ImmEdge™ hydrophobic pen and incubated with a 20mM

ammonium chloride solution for 15 mins at room temperature (RT). The sections were permeabilised through immersion in 0.1% Tween-20 PBS (PBST) before blocking with 1% BSA 5% goat serum in PBST for 1 hour at RT. In the case of the smooth muscle actin and CD68 antibody an extra blocking step using Goat Anti-Mouse IgG (H+L) Fab fragments (Jackson ImmunoResearch Inc, USA). Primary antibody incubation was done in a solution of 1% BSA PBST and left overnight at 4^{o}C followed by washing in PBST. Secondary antibodies were diluted in PBST and incubated on slides for 1 hour at RT followed by washing in PBST. DNA staining was done using either TO-PRO-3 Iodide (Invitrogen, Paisley, UK) or Hoechst 33342 (Thermo Fisher Scientific Loughborough, UK) at a dilution of 1/1000 or 1/10,000 in PBS respectively, each left for 10 min at RT. Slides were then washed in PBS before mounting using Hydromount (National Diagnostics, Georgia, USA). Slides were imaged either by confocal microscopy or using a Leica SP2 confocal microscope or by wide field fluorescence imaging using Axio Scan Z1 (Zeiss). Quantification of fluorescence was done using the imaging software of the Axio Scan Z1 (Zeiss). The software allows for an area of interest (eg. plaques in the aortic sinus) to be outlined and the software generates a mean fluorescence intensity for each fluorescent channel. Slides stained using isotype control antibodies, along with the appropriate secondary antibody were used to find the base level mean fluorescent intensity of a channel of interest (eg. Podoplanin control = Anti-Hamster primary control and Alexa 647). This value was then used to calculate the true mean fluorescence intensity for the fluorescent channel. The same method was used to calculate the mean fluorescent intensity on immunofluorescent stained colons.

2.6 Flow Cytometry

2.6.1 Organ digestion

In order to stain organs and lavage fluid for flow cytometry analysis, a single cell suspension needed to be prepared. Peritoneal lavage fluid (PLF) cells were treated with ACK lysis buffer (ThermoFisher Scientific Loughborough, UK) for 1 min to lyse red blood cells, then suspended in cold PBS followed by centrifugation at 400g for 10 min. Supernatant was removed and the cells were resuspended in 2% BSA PBS. Spleen were macerated onto a 70μM cell strainer and suspended in cold PBS. Spleen cells were then spun down at 400g for 10 min followed by treatment with ACK buffer for 5 min, then suspended in cold PBS followed by centrifugation at 400g for 10 min. Supernatant was removed and the cells were resuspended in 2% BSA PBS. Both small intestine and colons were prepared by first flushing with PBS using a round headed needle to remove any faeces and undigested material. The tissue was then cut open to create a flat structure and cut into 2 cm segments. The tissue was then incubated in a solution of 5mM EDTA 2% FBS in RPMI media (All from Sigma, Poole) 25 min in a shaking 37^{o}C incubator. Following this, the tissue was washed 3 times with cold PBS and then cut up further. The tissue was then incubated with a digestion media containing 50μg/ml DNAase I (Roche Diagnostics, Burgess Hill, UK) and 0.4Wunsch units/ml Liberase™ TM Research Grade (Roche Diagnostics, Burgess Hill, UK) in RPMI media in a shaking 37^{o}C incubator for 40 min, stopping to mix the solution by pipetting every 10 min. The tissue was then put through a 70μM cell strainer to get a single cell solution followed by centrifugation at 400g for 10 min. The supernatant was then removed and cell suspended in 2%BSA PBS.

2.6.2 Cell Staining and Analysis

Once cell suspension of the tissues and lavage fluid was prepared, the cells were suspended in a blocking solution containing 5% mouse serum and a 1/100 dilution of Anti Mouse CD16/CD32 (EBioscience Hatfield,UK) in 2%BSA PBA for 15 min at RT. The cells were then washed once with PBS before being incubated with diluted primary conjugated antibodies and streptavidin (exact dilution vary depending on the antibody in question) for 15 min at RT. The cells were washed and fixed using 1/8 dilution of formalin in PBS. Between each step the cells were centrifuged at 400g for 4 mins and supernatant removed. Cell samples were then placed in CyAn specific flow cytometry tubes and analysed using CyAn™ ADP Analyser (Beckman Coulter, UK). The gating strategy used for tissue stained for the LPS peritonitis experiments (Chapter 4) is as follows: The cells were first gated on their forward scatter and side scatter on a log scale with the low value readings removed. The cells were then gated for single cells only using pulse width and side scatter. Leukocytes were selected using CD45, (leukocytes =CD45+) and all other cells were selecting through using CD45 and another molecule of specific expression for the cell type of interest - B cells (CD19+), Helper T cells (CD4+), Cytotoxic T cells (CD8+), Dendritic cells (CD11c+ MHCII+) Neutrophils (ly6G+ high), Monocytes (Ly6C+ high, F4/80+ low), Macrophages (F4/80+), Pdpn+ Macrophages (F4/80+ Pdpn+), M1 Macrophages (F4/80+ MHCII+), M2 Macrophages F4/80+ CD206+). Podoplanin expression was analysed by setting the gate at <1% using a Syrian hamster IgG isotype

For the flow cytometry experiment done using DSS treated mice (Chapter 5) done by Sian Lax cells were gated as follows: Epithelial cells (CD45-EpCAM+), Blood endothelial cells (CD45-EpCAM-

CD31+Pdpn-), and Lymphatic endothelial cells (CD45-EpCAM-CD31+Pdpn+). The gating protocol for both types of experiments was modified from (Fasnacht et al., 2014).

2.6.3 Cytokine and Chemokine Measurement

The concentration of a range of different cytokines and chemokines were tested for using the peritoneal lavage fluid supernatant of challenged and unchallenged mice were measured using the Firefly® mulitiplex assay (Abcam, Cambridge, UK) following the kit instructions. Samples were run through the Accuri™ C6 flow cytometer (BD Biosciences, CA, USA) and analysed using a Firefly® analysis software provided by Abcam or using the Luminex system (R&D Systems, MN, USA) and detected and analysed using the Luminex 200™ system (R&D Systems, MN, USA). The cytokines and chemokines measured were TNF-α, IL-6, IL-1β, IL-10, MCP-1/CCL2, MIP-2/CxCL2, IFN-γ, RANTES/CCL5, IL-4, CXCL1, GM-CSF, MIP1α, MIP1β.

2.7 Quantitative Real-Time PCR (qRT-PCR)

Aortic Arch from WT mice (C57BL/6) on normal diet, ApoE$^{-/-}$ fed on high fat diet for six weeks, ER^{T2}-Cre.Clec-2$^{fl/fl}$ and Vav-iCre.Pdpn$^{fl/fl}$ on normal diet were used for mRNA extraction. Nucleospin RNA isolation kit (Macherey Nagel, Duren, Germany) was used for mRNA extraction and kit instructions followed. cDNA was prepared from 200ng RNA and prepared using a kit called the High Capacity cDNA Reverse Transcription kit (ThermoFisher Scientific, Loughborough, UK). Taqman cDNA fluorescent probes for B-Actin (housekeeping control) and podoplanin were run separately (ThermoFisher Scientific, Loughborough, UK) in the Stratagene Mx3000P RT-PCR machine (Agilent Technologies, Cheshire, UK). The thermal cycle used for the experiments is outline in Table 2.2. The fold change in podoplanin mRNA levels was done using the following formula:

$$R = 2^{-(\Delta Ctsample - \Delta Ctcontrol)}$$

Table 2.2:

Temperature (°C)	Time (secs)	Cycles
50	120	1
95	600	1
95	15	40
60	60	

Table 2.2: Thermal cycle used for RT-qPCR experiments.
Temperatures, time and number of cycles used in real-time quantitative PCR experiments.

2.8 Statistical Analysis

Statistical analysis was performed as appropriate to the data distribution in each experiment described in this thesis. Details are described in individual methods sections or in figure legends. Where data did not show any significant difference, it is either referred to as not significant or not stated

Chapter 3

Mouse podoplanin supports adhesion and aggregation of platelets under arterial shear

3.1 Introduction

Since the discovery of podoplanin as the endogenous ligand for the platelet receptor CLEC-2 (Suzuki-Inoue et al., 2007), many years of research has gone into studying the influence of the interaction on the behaviour of platelets and podoplanin-expressing cells as well as the wider *in vivo* influence. Early work demonstrated that endogenously expressed podoplanin as well on a transfected cancer cell line, has the capacity to cause platelet activation including aggregation (Christou et al., 2008, Kerrigan et al., 2012, Suzuki-Inoue et al., 2007). Knockout mouse models demonstrated the necessity of the interaction of platelet CLEC-2 with podoplanin expressing lymphatic endothelial cells (LECs) in the development of the lymphatic system (Finney et al., 2012). Lack of podoplanin or CLEC-2 in a developing mouse embryo causes the appearance of subcutaneous bleeding because of blood-lymphatic mixing by E12.5 onwards (Suzuki-Inoue et al., 2010, Bertozzi et al., 2010, Finney et al., 2012, Uhrin et al., 2010)**.** Intracranial haemorrhages are seen in CLEC-2 and podoplanin deficient mice by E12.5 (Lowe et al., 2015a). Further investigation into the development of this phenotype revealed that podoplanin is expressed throughout the brain up to E12.5 before becoming restricted to the choroid plexus and brain lymphatic vessels by E14.5 (Lowe et al., 2015a). Mouse models with a neuroepithelial specific deletion of podoplanin (Nes-Cre.PDPN$^{fl/fl}$), or platelet specific deletion of CLEC-2 (PF4-Cre.CLEC-2$^{fl/fl}$) generated embryos with brain haemorrhaging similar to the constitutive knockout mice. Haemorrhaging was also found in mice deficient in the αIIb-subunit of the major platelet integrin αIIbβ3 demonstrating that the phenotype is due to a loss in platelet aggregation (Lowe et al., 2015a).

It is currently unclear if this discovery has relevance to the fact that 25–31% of preterm human infants born with a birthweight of below 1500 g exhibit a high rate of intraventricular hemorrhage (IVH) (Horbar et al., 2002). The main cause for this pathology is the presence of cardiovascular and respiratory instability. However, these infants often have a thrombocytopenic comorbidity and close temporal association between low platelet counts and the occurrence of clinical bleeding has been reported (Stanworth, 2012, Ferrer-Marin et al., 2013).

High shear rates ranging between $1000s^{-1}$ and $5000s^{-1}$ are present within healthy cerebral arterioles of neonatal and adult mice brains (Wang et al., 1992, Rovainen et al., 1992). It is speculated that high shear rates also exist in the cerebrovasculature of humans (Seymour et al., 2016). It is currently unclear how podoplanin on neuroepithelial cells is able to support platelet aggregation and prevent intracranial bleeding.

Previous work has shown the ability of both human and mouse podoplanin to induce platelet aggregation when using an aggregometer which is a low shear environment. Studies using an *in vitro* flow system highlighted that recombinant human podoplanin and podoplanin expressing human LECs can initiate human platelet aggregate formation solely at venous shear rates ranging from $50s^{-1}$ to $450s^{-1}$ (Navarro-Nunez et al., 2015). A similar finding of platelets forming aggregates on human LECs but not blood endothelial cells (BECs) at a low shear rate was also reported by Bertozzi et al. (Bertozzi et al., 2010). The reported affinity between human podoplanin and CLEC-2 is also relatively low at 24.5μM (Christou et al., 2008).

The interaction of mouse podoplanin and platelets under a high shear environment had not been investigated previously. Therefore, the aim of this chapter was to characterise the interaction of a recombinant form of mouse podoplanin with mouse platelets under a range of shear stress rates found in the developing brain. The results show that in contrast to human podoplanin, mouse podoplanin can support platelet adhesion and platelet aggregation at both venous and arterial rates of shear. Following this discovery, a further aim of this chapter was to characterise other platelet receptors involved in the formation of the aggregates and to further investigate the affinity between mouse podoplanin and CLEC-2 using surface plasmon resonance. The molecular basis of the aggregation is due to a much higher affinity between mouse CLEC-2 and mouse podoplanin relative to human CLEC-2 and human podoplanin.

In this chapter figures 3.1, 3.3 and 3.5 formed part of my Masters qualification (MRes in Biomedical research).

3.2 Results

3.2.1 Fc mPodoplanin supports the aggregation of mouse platelets at high shear

To investigate a possible role of podoplanin in platelet adhesion in the vasculature, we looked at the effect of a dimerised form of podoplanin in an *in vitro* blood flow system. Mouse blood was perfused over an immobilized monolayer of mPdpn-Fc, which is a recombinant Fc fusion of the mouse podoplanin extracellular domain. A range of venous and arterial shear rates were used, ranging from $100s^{-1}$ to $1000s^{-1}$ (Figure 3.1A). A recombinant Fc control did not support platelet adhesion (Figure 3.1B). Mouse platelets adhere and form small aggregates on the podoplanin-coated surface at a flow rate of $100s^{-1}$. At the greater shear rate of $500s^{-1}$, platelets form fewer but larger, distinct aggregates. At a higher, arterial rate of shear of $1000s^{-1}$, immobilized podoplanin supported the formation of large aggregates. There was no adhesion at flow rates of $2000s^{-1}$ (Figure 3.1B). Platelet coverage was quantified by calculation the percentage field of platelet after 4 min of perfusion. The calculated differences demonstrate a significant increase in percentage coverage at $1000s^{-1}$ compared with both $100s^{-1}$ and $500s^{-1}$ (Figure 3.1Ci). However, when adhesion was normalized to the percentage of coverage per ml of blood perfused, it was found that there was no significant difference in the level of adhesion between the shear rates (Figure 3.1Cii).

Figure 3.1

A

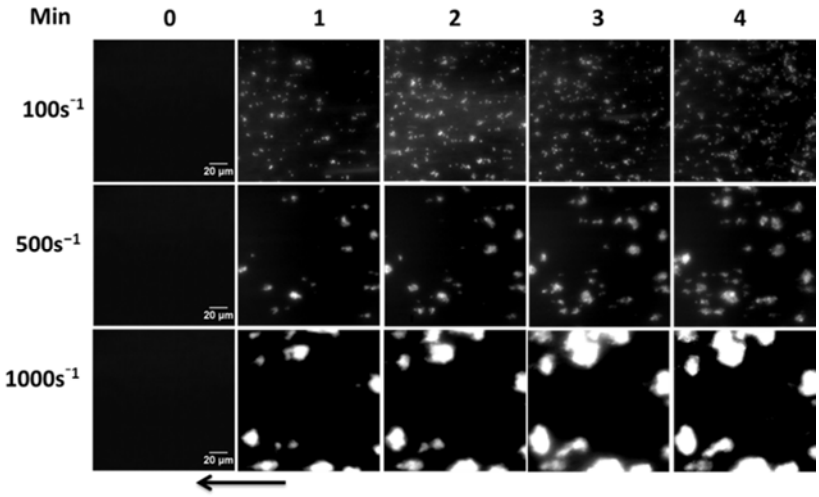

B

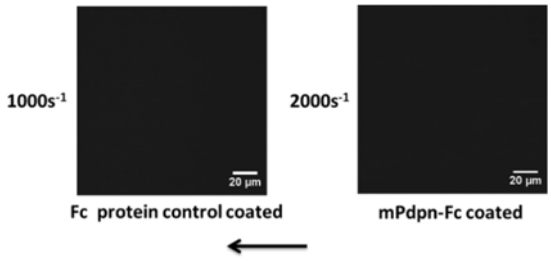

C

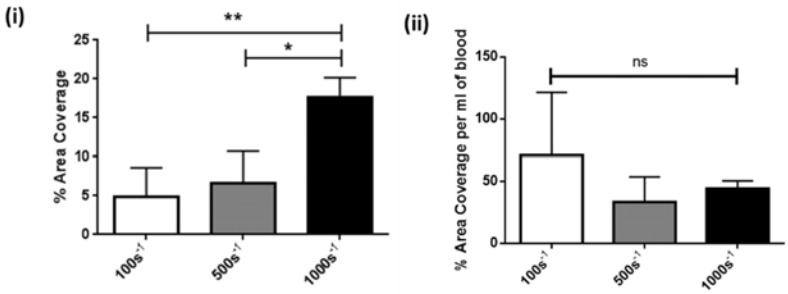

Figure 3.1: Fc mPodoplanin supports the aggregation of mouse platelets at high shear

A. Anticoagulated blood from wild-type mice was perfused over mPdpn-Fc -coated capillary tubes at the indicated shear rates. Platelets were fluorescently labelled with $DiOC_6$ before being perfused for 4 min. Representative images were taken in real time by fluorescence microscopy. Arrow indicates the direction of flow. Scale bar 20µm. Images are representative of 4 independent experiments.
B. Anticoagulated blood from wild-type mice was perfused over an Fc-protein control-coated capillary at $1000s^{-1}$ and over mPdpn-Fc -coated capillary at $2000s^{-1}$. Platelets were fluorescently labelled with $DiOC_6$ before being perfused for 4 min. Representative images were taken in real time by fluorescence microscopy. Arrow indicates the direction of flow. Scale bar 20µm. Images are representative of 3 independent experiments.
C. (i) Quantitation of mouse platelet area coverage following blood perfusion. Statistical analysis was performed using a one way ANOVA followed by a Dunnett's multiple comparisons test (*=$p<0.05$, **=$p<0.01$). (ii) Quantitation of mouse platelet area coverage normalised to the volume of blood perfused. Statistical analysis was performed using a one way ANOVA followed by a Dunnett's multiple comparisons test. Error bars represent standard deviation. This work formed part of my MRes in Biomedical Research qualification.

3.2.2 Platelet spreading on a mPdpn-Fc coated surface

One of the key characteristics of platelet activation is the change in shape from a discoid structure to a flat irregular shape with extending filopodia. We allowed washed platelets to adhere to a mPdpn-Fc coated surface to test if podoplanin can induce shape change (Figure 3.2). The platelets clearly spread in the presence of mPdpn-Fc (some marked with white asterisks for demonstration). Platelet adhesion was markedly reduced in the absence of mPDPN-Fc (PBS control), but the platelets that adhered failed to spread (marked with white arrows for demonstration).

Figure 3.2

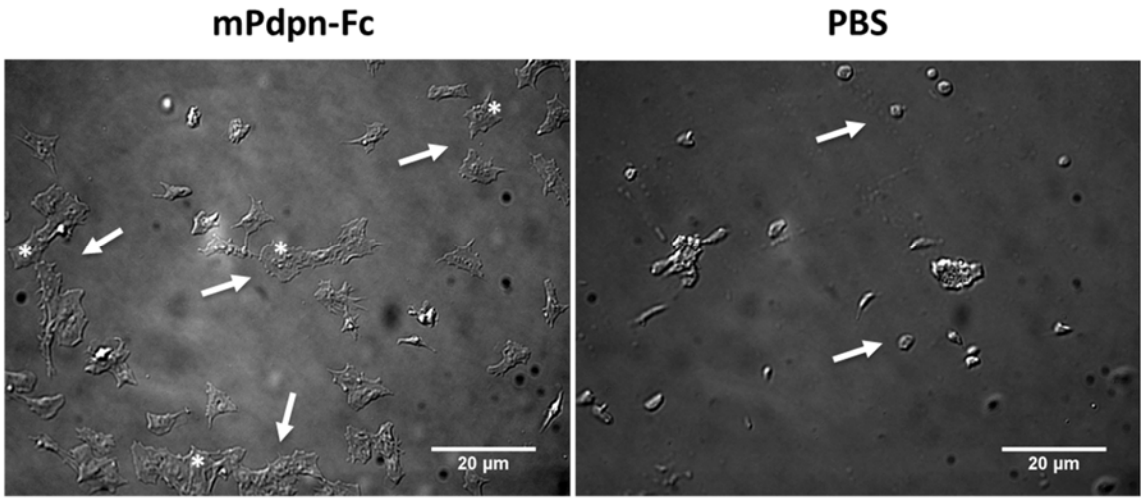

Figure 3.2: Mouse platelets spread on a podoplanin coated surface

Washed mouse platelets were incubated on coverslips coated with 100µg/ml mPDPN-Fc or PBS control. White arrows point to adhered platelet and white asterisks point to spread platelets. Scale bar 20µm. Images are representative of 3 independent experiments.

3.2.3 Platelet adhesion to Fc mPodoplanin is dependent on the platelet receptor CLEC-2

The PF4-Cre transgenic mouse model is an established technique for the generation of megakaryocyte and platelet specific knockout mice (Tiedt et al., 2007). A previous described CLEC-2 megakaryocyte/platelet specific knockout model was used to investigate if the platelet adhesion and aggregation seen in the *in vitro* flow system is dependent on CLEC-2. Blood from these mice (PF4-Cre.CLEC-$2^{fl/fl}$) was perfused over the mPdpn-Fc coated capillaries for 4 min at high and low shear rates. Lack of CLEC-2 expression on platelets abolished all platelet adhesion to mPdpn-Fc at both $100s^{-1}$ and $1000s^{-1}$ compared with the adhesion seen using blood from the Cre-negative littermates (Figure 3.3A). Quantification of platelet adhesion revealed that there is a significant difference at both $100s^{-1}$ and $1000s^{-1}$ between the CLEC-2 deficient platelets (PF4-Cre.CLEC-$2^{fl/fl}$) and their littermate controls (Figure 3.3Bii). Blood from both PF4-Cre.CLEC-$2^{fl/fl}$ mice and CLEC-$2^{fl/fl}$ was also tested by perfusion over a collagen coated capillary, and shown to aggregate normally (Figure 3.3A and 3.3Bi).

Figure 3.3

A

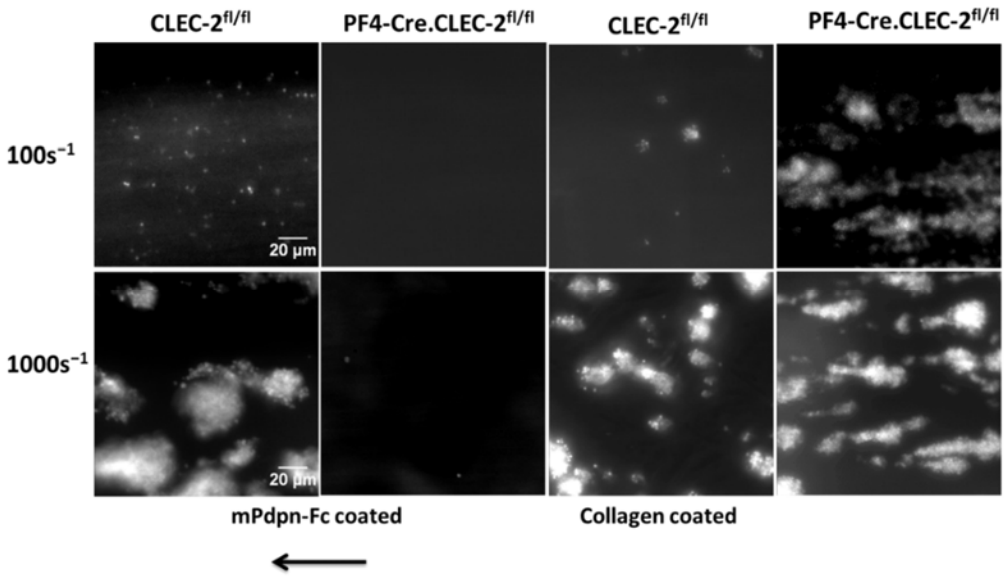
CLEC-2fl/fl
PF4-Cre.CLEC-2fl/fl
CLEC-2fl/fl
PF4-Cre.CLEC-2fl/fl
100s−1
1000s−1
20 µm
20 µm
mPdpn-Fc coated
Collagen coated

B

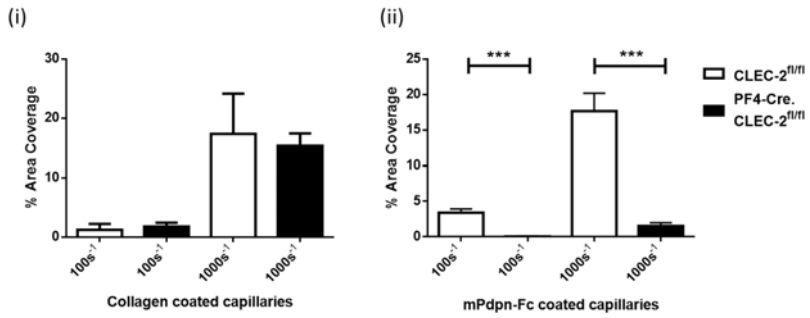
(i)
(ii)
% Area Coverage
% Area Coverage
***
***
CLEC-2fl/fl
PF4-Cre. CLEC-2fl/fl
100s−1
1000s−1
Collagen coated capillaries
mPdpn-Fc coated capillaries

Figure 3.3: Fc mpodoplain mediated platelet aggregation is dependent on the platelet receptor CLEC-2

A. Anticoagulated blood from PF4-Cre.CLEC-$2^{fl/fl}$ mice and CLEC-$2^{fl/fl}$ littermates was perfused through mPDPN-Fc -coated capillary tubes at the indicated shear rates for 4 min. Anticoagulated blood PF4-Cre.CLEC-$2^{fl/fl}$ mice was perfused over horm collagen coated capillaries to test platelet functionality. Platelets were fluorescently labelled with $DiOC_6$ before being perfused through the capillaries. Representative images were taken in real time by fluorescence microscopy. Arrow indicates the direction of flow. Scale bar 20μm. Images are representative of 3 independent experiments.

B. (i) Quantitation of platelet coverage following blood perfusion over collagen coated capillaries. (ii) Quantitation of platelet coverage following blood perfusion over mPdpn-Fc coated capillaries. Statistical analysis was performed using an unpaired one tailed t test (***=$p<0.001$). Error bars represent the standard deviation. This work formed part of my MRes in Biomedical Research qualification.

3.2.4 Effect of inhibitors on platelet aggregation on podoplanin under shear

Pharmacological inhibitors were used to investigate the role of platelet signalling pathways and receptors in CLEC-2 dependent platelet adhesion to immobilized podoplanin. Both the contribution of molecules previously implicated in the CLEC-2 signalling pathway and other receptors involved in the haemostatic role of platelets were assessed. The Src family kinase inhibitor dasatinib markedly reduced platelet aggregation on podoplanin (Figure 3.4 A, Bi), consistent with a critical role for Src kinases in CLEC-2 signalling as previously reported (Pollitt et al., 2014). CLEC-2 signalling is also dependent on feedback agonists thromboxane A_2 and ADP (Pollitt et al., 2010, Borgognone et al., 2014). In line with this, a combination of the cyclooxygenase inhibitor indomethacin and the $P2Y_{12}$ receptor antagonist, Cangrelor, blocked aggregation on mouse podoplanin at $1000s^{-1}$ (Figure 3.4A, Bi).

The platelet integrin αIIbβ3 mediates the formation of stable platelet aggregates. Inhibition of αIIbβ3 using eptifibatide blocked platelet aggregation on podoplanin at $1000s^{-1}$. Blocking of the GpIb subunit of the VWF receptor (GPIb-IX-V) using the antibody p0p/B also significantly reduced platelet aggregation compared to vehicle control (Figure 3.4A, Bi). Protein quantification of the capillary contents following blood perfusion revealed a significant difference in the presence of eptifibatide but not in the presence of the other inhibitors tested (Figure 3.4Bii). The lack of difference may be due to experimental variation or to single platelet adhesion which is still visible (Figure 3.4A). These results indicate that platelet aggregation on podoplanin is dependent on the interaction of CLEC-2 and podoplanin and involves Src kinase-driven platelet activation and

classical mediators of aggregation including the secondary platelet agonists ADP and TxA2, integrin αIIbβ3 and GPIb-IX-V complex.

Figure 3.4

A

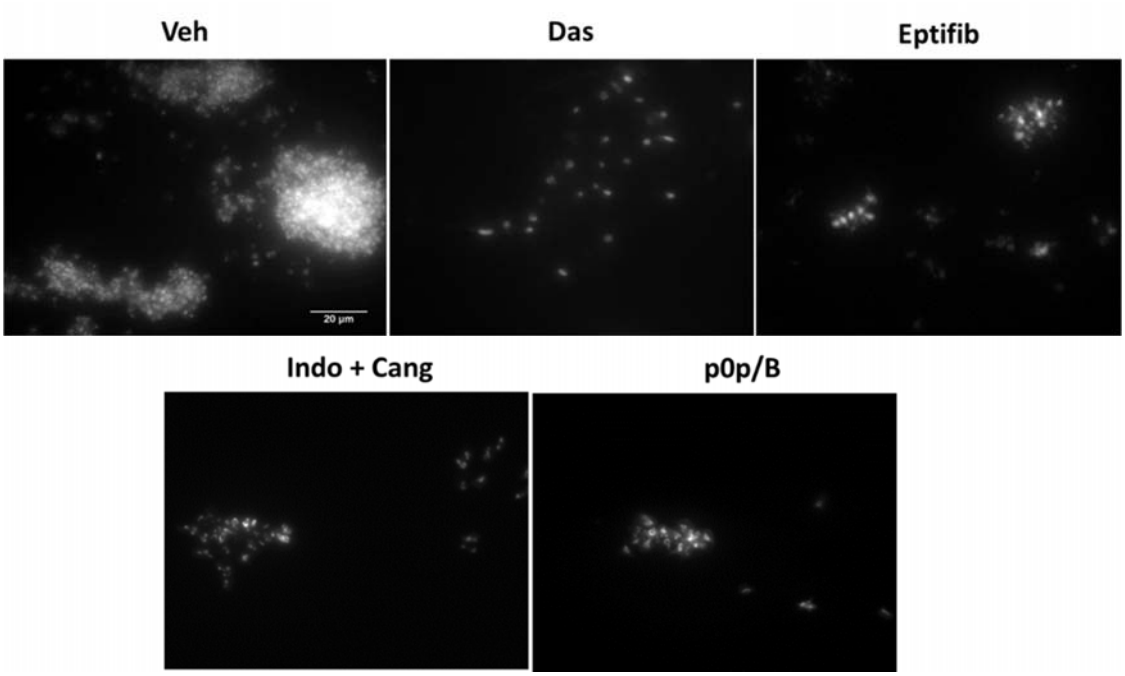
Veh
Das
Eptifib
20 µm
Indo + Cang
p0p/B

B

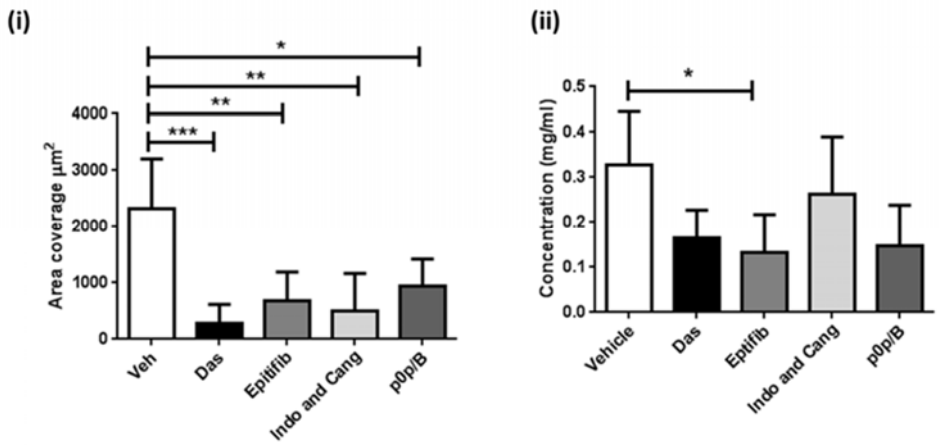
(i)
Area coverage µm²
4000
3000
2000
1000
0
*
**
**
***
Veh
Das
Epitifib
Indo and Cang
p0p/B
(ii)
Concentration (mg/ml)
0.5
0.4
0.3
0.2
0.1
0.0
*
Vehicle
Das
Eptifib
Indo and Cang
p0p/B

Figure 3.4: Effect of inhibitors on platelet aggregation on podoplanin under shear

A. Anticoagulated wild type (WT) mouse blood was perfused through mPdpn-Fc -coated capillary tubes at $1000s^{-1}$ for 4 min. Platelets were fluorescently labelled with DiOC6 before being perfused and ten representative images where taken post blood perfusion. Representative images were taken following 4 min of mouse blood perfusion with and without the indicated inhibitors at $1000s^{-1}$, Vehicle control image (Veh: DMSO), Dasatinib (Das: 10µM), eptifibatide (Eptifib: 9µM), Indomethacin (Indo: 10µM) and Cangrelor (Cang: 1µM), p0p/B antibody (50µg/ml). Scale bar 20µm. Images are representative of 4 independent experiments.

B. (i) Quantitation of platelet coverage following blood perfusion. (ii) Quantification of protein concentration within capillaries following perfusion. Statistical analysis was performed using a one-way ANOVA followed by a Dunnett's multiple comparisons test to the vehicle control, error bars represent standard deviation. *=$p<0.05$, **=$p<0.01$, ***=$p<0.001$.

3.2.5 Fc mPodoplanin supports the aggregation of human platelets at venous rates of shear

Human blood was perfused over the immobilized monolayer of mPdpn-Fc to investigate binding and aggregation of human platelets in the in vitro system. Human platelets were shown to form small aggregates on the mPdpn-Fc coated surface at the low shear rate of $100s^{-1}$ (Figure 3.5A). Inhibition of Src family kinases by dasatinib abolished formation of the aggregates on mPdpn-Fc coated surface at this shear rate, although adhesion of single platelets was preserved. Inhibition of integrin αIIbβ3 using eptifibatide demonstrated a critical role of the integrin. There was no adhesion at a higher shear rate of $300s^{-1}$ (not shown). Quantification of platelet coverage confirmed a significant reduction caused by dasatinib and eptifibatide at $100s^{-1}$ (Figure 3.5B).

Figure 3.5

A

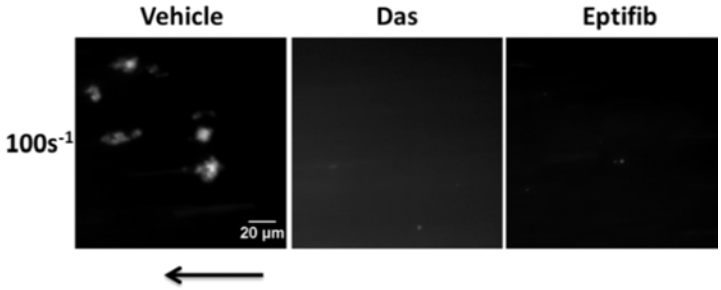

B

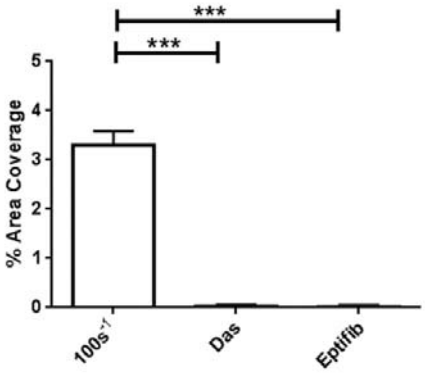

Figure 3.5: Fc mPodoplanin supports the aggregation of human platelets at low shear

A. Anticoagulated blood from humans was perfused through Fc mpodoplanin (mPdpn-Fc)-coated capillary tubes at the indicated shear rates for 4 min. Platelets were fluorescently labelled with DiOC6 before being perfused. Representative images were taken in real time by fluorescence microscopy at 100s-1, Vehicle control (Veh: DMSO), Dasatinib (Das: 10µM), eptifibatide (Eptifib: 9µM). Arrow indicates the direction of flow. Scale bar 20µm. Error bars represent standard deviation. Images are representative of 3 independent experiments.

B. Quantitation of human platelet coverage following blood perfusion. Statistical analysis was performed using a one-way ANOVA followed by a Dunnett's multiple comparisons test (*=p<0.05, **=p<0.01). Error bars represent standard deviation. This work formed part of my MRes in Biomedical Research.

3.2.6 Cloning and sequencing of recombinant mCLEC-2

Following the discovery of the ability of mouse podoplanin to induce platelet capture and aggregation under high rates of shear, I set out to determine the binding affinity between mouse podoplanin and mouse CLEC-2 in order to investigate if it was consistent with a direct effect. In order to do this, we needed to produce a recombinant form of mCLEC-2. Primers for the extracellular domain of mCLEC-2 where used with the addition of a N terminal 6xHIS tag to aid in the later process of protein purification. The amplified product was first cloned into a pGEMTeasy vector and the mCLEC-2-His band was cut from an agarose gel following restriction enzyme digestion (Figure 3.6Ai). The DNA was then extracted from the gel and cloned into the mammalian vector pHLsec (Figure 3.6Aii).

The pHLsec vector contains a secretory signal peptide allowing the expressed protein to be translocated across the endoplasmic reticulum membrane and into the supernatant in which transfected cells grow which simplifies the purification process. The pHLsec vector containing mCLEC-2 was sequenced and the reads compared against the known mRNA mCLEC-2 sequence (Figure 3.6Bi). Following this confirmation, the Signal P4.0 software was used to predict the amino acid sequence of the secreted mCLEC-2 sequence (Petersen et al., 2011).

The Signal P4.0 is a software program that is trained to distinguish between hydrophobic transmembrane regions and secretory signal peptide. The recognition of where the signal peptide is located is then used to predict the length of the secreted peptide. The results come in the form

of three prediction scores, which are the C-score or predicted cleavage site, S score showing the predicted signal peptide value and the Y score represents a combination of the C+S score.

The software program predicted a peptide of 183 amino acids long, containing the desired N terminal 6xHIS tag followed by amino acid number 55-229 of the mCLEC-2 sequence which encompasses the extracellular domain of mCLEC-2 (Figure 3.6Bii).

Figure 3.6

A

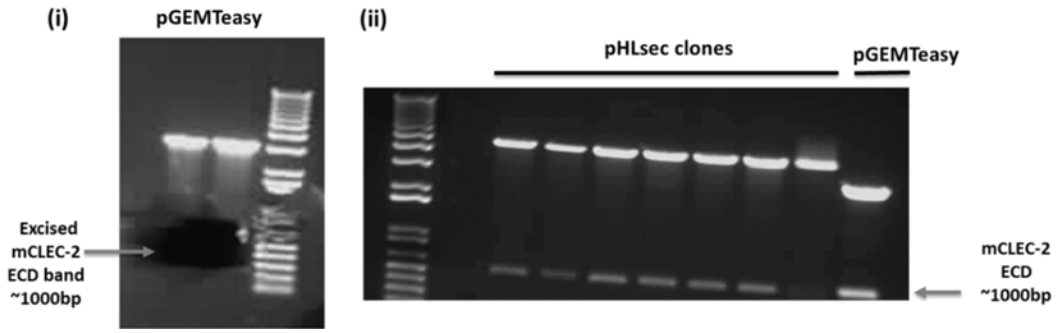

B

(i)

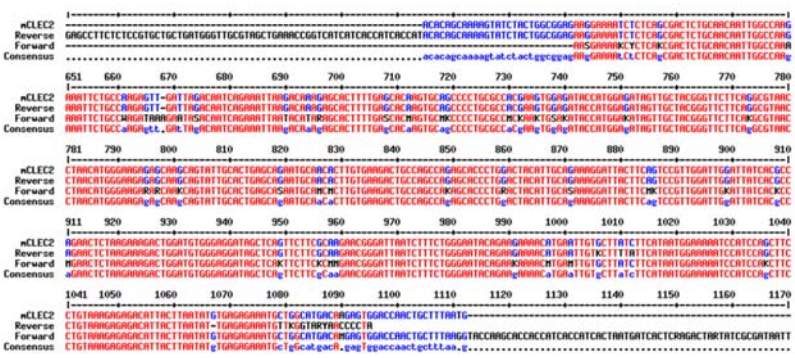

(ii)

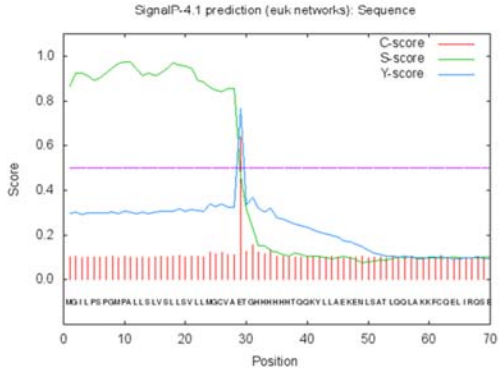

ECD of mCLEC-2 (aa 55-229) fused with 6xHIS at N terminus

Figure 3.6: Cloning and sequencing of recombinant mCLEC-2 protein (mCLEC-2-His)

A. (i) The DNA sequence of the ECD (extracellular domain) of mCLEC-2 fused to an N terminal 6xHIS tag was amplified and cloned into the vector pGEMTeasy. The vector was then digested and mCLEC-2 sequence cut from an agarose gel. (ii) The mCLEC-2 was cloned into the pHLsec vector which contains a mammalian peptide secretion signal. Restriction digest was carried out to confirm DNA insertion into the vector.

B. (i) The forward and reverse sequence reads of the cloned vector was compared to the mRNA sequence of mCLEC-2 and confirmed the vector contained the correct sequence for the extracellular domain of mCLEC-2. (ii) Sequence was entered in SignalP 4.0 server which is a prediction software for cleavage site of a protein. C-score is the predicted cleavage site, S score represents the predicted signal peptide value and the Y score represents a combination of the C+S score. The software predicted that the secreted peptide would be from a total of 182 amino acids long. The peptide consists of an N terminal 6xHIS tag and amino acids 55-229 of the coding sequence of mCLEC-2.

3.2.7 Expression and purification of recombinant mCLEC-2

The confirmed pHLsec vector containing mCLEC-2 was transfected into HEK 293T cells for protein expression and later purification. The supernatant was taken after 4 days and purified through a HIS column. A band at around 32kDa was visible on a coomassie gel from an elution concentration of 60mM imidazole (Figure 3.7A). The eluted samples were then tested by western blot using an anti-mCLEC-2 and an anti-His tag antibody, confirming the identity of the purified protein (Figure 3.7Bi and ii). The predicted weight of the secreted protein from sequence alone is approximately 22kDa, however the presence of smears on the western blot point to glycosylation of the protein which may account for the added weight. The functionality of the purified protein was then tested using a dotblot. It was found that mCLEC-2-His can successfully bind to both mPdpn-Fc and mPdpn-His (Figure 3.7C). Isotype controls did not show any binding confirming the specificity. Significantly, no binding was seen to hPdpn-His (3.7C).

Figure 3.7

A

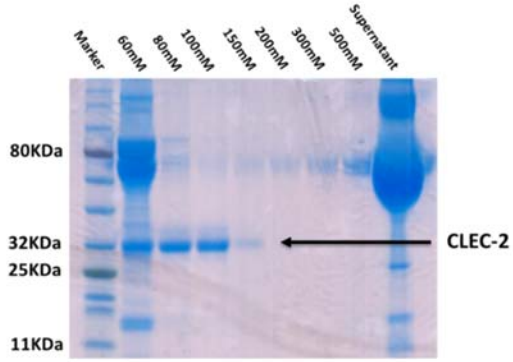

B

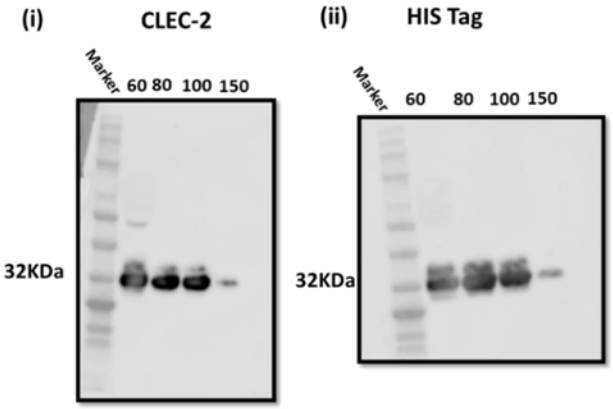

C

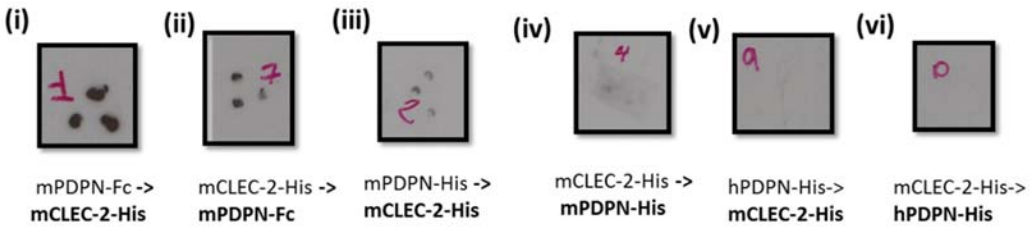

Figure 3.7: mCLEC-2 expression and confirmation of functionality

A. The cloned and sequence vector containing the ECD of mCLEC-2 within the pHLsec vector was transfected into HEK 293T cells. The supernatant was collected and put through a HIS tag column for purification. The coomassie gel indicates concentrations of imidazole tested to elute the protein
B. The elution fractions were examined by western blot. (i) HIS tag antibody used to detect the protein (ii) Mouse CLEC-2 antibody used to detect the protein.
C. Dotblots used to test the functionality of 6xHIS mCLEC-2 purified protein through its capability to bind to recombinant forms of mpodoplanin. (i) Fc mpodoplanin (mPDPN-Fc) binding to His tagged mCLEC-2 (mCLEC-2-His) on the membrane (ii) mCLEC-2-His binding to mPDPN-Fc on the membrane (iii) His tagged mpodoplanin (mPDPN-His) binding to mCLEC-2-His on the membrane (iv) mCLEC-2-His binding to mPDPN-His on the membrane. No binding of His tagged hpodoplanin (hPDPN-His) to mCLEC-2-His (v) or mCLEC-2-His to hPDPN-His was seen. No binding seen using isotype controls for each combination (not shown).

3.2.8 Mouse CLEC-2 and mouse podoplanin interact with high affinity

The results of the experiments discussed so far indicate that an interaction between mouse CLEC-2 and podoplanin is sufficient to trigger platelet adhesion and aggregation at arterial shear. To investigate these findings further, we determined the binding affinity between mouse CLEC-2 and mouse podoplanin using surface plasmon resonance (Figure 3.8). Surface plasmon resonance is a method used to detect the interaction between two molecules without the use of labels. A light source is passed through a sensor chip surface and light energy is absorbed by an interaction causing a change in the energy of the reflected beam. This change can be detected and used to calculate the affinity between the molecules. Human podoplanin has a 46% protein sequence identity with mouse podoplanin (Figure 3.8A) and was also tested to investigate the cross-species interaction between mouse CLEC-2 and human podoplanin. Monomeric His-mCLEC-2 was bound to the surface and podoplanin was perfused over at increasing concentrations ranging from 5.6nM to 4.5µM. Two forms of recombinant podoplanin were tested, the previously described dimerized mPdpn-Fc and a single extracellular domain of podoplanin connected to a His tag (mPdpn-His). Both forms of mouse podoplanin showed a similar strong affinity to mCLEC-2-His of 15.3 ± 3.2 nM for mPdpn-Fc and 10.6 ± 1.3 nM when using mPdpn-His. The human form of monomeric podoplanin, expressed as a His tag (hPdpn-His) did not bind specifically to mCLEC-2-His coinciding with the results from the dotblot (Figure 3.8A). The result confirmed a specific high affinity interaction between mouse CLEC-2 and mouse podoplanin.

Figure 3.8

A

Range 1: 1 to 172 GenPept Graphics Next Match Previous Match

Score	Expect	Method	Identities	Positives	Gaps
126 bits(317)	2e-42	Compositional matrix adjust.	79/172(46%)	99/172(57%)	10/172(5%)

```
Query  1    MWKVSALLFVLGSASLWVLAEGASTGQPEDDTETTGLEGGVAMPGAEDDVVTPGTSEDRY  60
            MW V  L +VLGS   W  A+G + G  EDD  T G   G+  PG ED + T G +
Sbjct  1    MWTVPVLFWVLGSVWFWDSAQGGTIGVNEDDIVTPGTGDGMVPPGIEDKITTTGATGGLN  60

Query  61   KS-GLTTLVATSVNSVTGIRIEDLPTSESTVHAQEQSPSATASNVATSHSTEK-------  112
            +S G   LV T     T   +E+L TS ++ H   +  S T   V TSHS +K
Sbjct  61   ESTGKAPLVPTQRERGTKPPLEELSTSATSDHDHREHESTTTVKVVTSHSVDKKTSHPNR  120

Query  113  --VDGDTQTTVEKDGLSTVTLVGIIVGVLLAIGFIGGIIVVVMRKMSGRYSP  162
              +TQTT +KDGL  VTLVGIIVGVLLAIGF+GGI +VVM+K+SGR+SP
Sbjct  121  DNAGDETQTTDKKDGLPVVTLVGIIVGVLLAIGFVGGIFIVVMKKISGRFSP  172
```

B

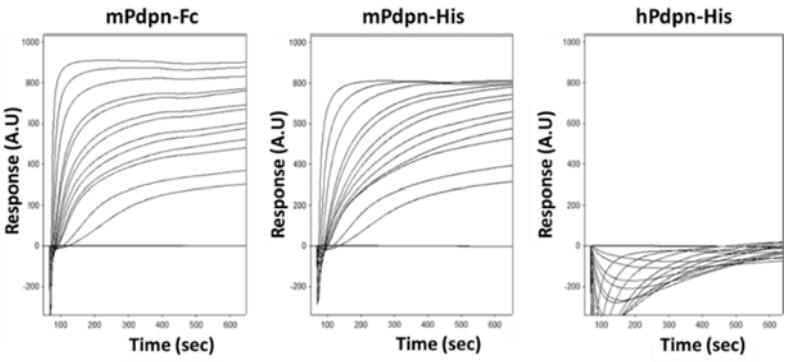

C

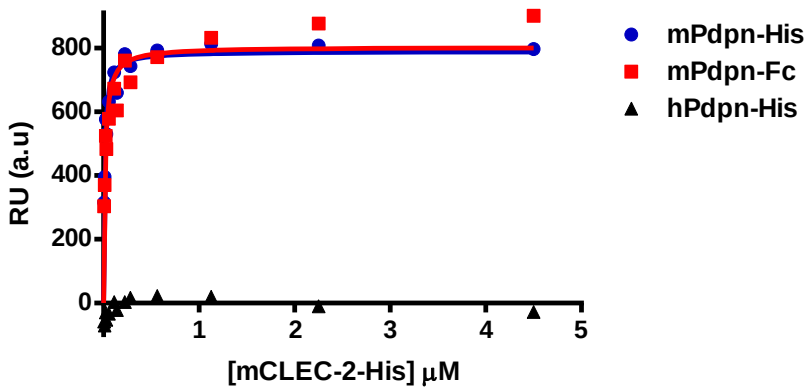

Figure 3.8: Mouse CLEC-2 and mouse podoplanin interact with high affinity

A. Blast protein sequence comparison between human podoplanin (Query 1) and mouse podoplanin (Sbject 1) showing a 46% sequence identity.
B. Sensorgram from equilibrium–based binding experiment after subtraction of the signal from a control flow cell surface. Increasing concentrations of CLEC-2 (ranging from 5.6nM to 4.5µM) were injected over surfaces coupled with Fc mpodoplanin (mPDPN-Fc), His tagged mpodoplanin (mPDPN-His) and His tagged hpodoplanin (hPDPN-His).
C. Plot of the equilibrium binding response from the sensorgram of mPDPN-Fc, mPDPN-His and hPDPN-His as a function of CLEC-2 concentration. The curve is the best fit to the experimental data as calculated by GraphPad Prism 5. The affinity between mouse CLEC-2 and mouse podoplanin was calculated to be 15.3nM ± 3.2nM when using mPDPN-Fc and 10.6nM± 1.3nM when using mPDPN-His. Plots and calculations taken from one experiment.

3.3 Discussion

The results of this chapter demonstrate the ability of immobilised dimeric mouse podoplanin to initiate platelet adhesion and aggregation at arterial and venous rates of shear blood flow. Platelet adhesion and subsequent aggregation is dependent on the platelet receptor CLEC-2. The dimerised form of podoplanin is also likely to reflect the *in vivo* situation as there is evidence to suggest that podoplanin is expressed as a dimer and higher oligomers (Martin-Villar et al., 2010).

Platelet aggregation on immobilized podoplanin is dependent on integrin αIIbβ3, the VWF receptor complex GPIb-IX-V, and the feedback mediators ADP and thromboxane A_2 indicating that it involves classical hemostasis. Inhibition of Src family tyrosine kinases, which initiate CLEC-2 signalling, also blocks aggregate formation consistent with aggregation being initiated by the C-type lectin-like receptor. In contrast, mouse podoplanin can only capture and induce aggregation in human platelets at venous rates of shear. These aggregates are also dependent on Src kinase activation and the integrin αIIbβ3.

We have determined that the affinity between mouse podoplanin and mouse CLEC-2 to be within the nanomolar range. Human podoplanin did not show any specific affinity to mouse CLEC-2. However, CLEC-2 clustering has previously been reported to increase the avidity of platelets to podoplanin which may account for the in vitro flow adhesion of human platelets (Pollitt et al., 2014). Clustering is mediated through Src (and Syk) family kinases which would explain the inhibitory effect of dasatinib.

The involvement of integrin αIIbβ3, GPIb-IX-V and ADP and thromboxane A2 indicates a classical pattern of platelet aggregation. The process generally involves several stages. Firstly, platelets interact via GPIb with VWF immobilized to collagen and in turn collagen triggers platelet activation through the collagen GPVI. VWF is integral to the capture of platelets in the high shear environment in arteries and arterioles (Du, 2007, Lopez and Dong, 1997, Savage et al., 1996). The feedback agonists ADP and thromboxane A_2 reinforce platelet activation (Ren et al., 2008, Reed et al., 2000). A process of "inside out" signalling leads to activation of αIIbβ3 to an active confirmation and platelet-platelet interaction mediated through binding of fibrinogen to the activation integrin (Coller and Shattil, 2008, Shattil et al., 2010). It has been demonstrated that CLEC-2 signalling triggers similar steps in platelet activation to GPVI, including the activation of Src and Syk tyrosine kinases. CLEC-2 signalling also relies on the release of the secondary mediators ADP and thromboxane A_2 to sustain receptor phosphorylation, although previous work highlighted these mediators are less important in mouse platelet signalling than in human platelet signalling to CLEC-2 (Borgognone et al., 2014). The work presented demonstrates that podoplanin can capture mouse platelets under high shear stress, and trigger platelet aggregation through CLEC-2 in a pathway that is dependent on granule secretion and thromboxane A_2 formation. Additionally, the interaction between GPIb and VWF plays a key role in podoplanin-mediated platelet aggregation *in vitro*, suggesting that VWF may bind to the sialylated protein or to adhered platelets and in this way, initiate the recruitment of additional platelets into the aggregate as the initial stage of adhesion is lost.

A significant difference in protein quantification from the capillaries was only seen in the presence of eptifibatide. However, this may be due to the single platelets still visible in the presence of all the inhibitors tested. Taken together, this data points to podoplanin acting as an adhesion receptor which subsequently set off the series of events discussed above necessary in the classical pattern of platelet aggregation. Experiments using washed platelets also highlighted the ability of the dimerised form of podoplanin to trigger platelet activation and spreading which additionally adds to this hypothesis that podoplanin acts as an adhesion receptor.

Podoplanin is not present in adult blood vessels but is expressed on the neuroepithelium lining the blood vessels in mid-gestation (Lowe et al., 2015a). We speculate that neuroepithelial cells expressing podoplanin come in to contact with platelets under these conditions in the high shear forces of the developing brain (Wang et al., 1992, Rovainen et al., 1992). Loss of podoplanin expression on neuroepithelial cells at this stage of development phenocopies loss of CLEC-2 on platelets and leads to haemorrhaging. It has been proposed that platelet aggregation, initiated through a podoplanin-CLEC-2 interaction, is needed to prevent haemorrhaging in the rapidly growing vessels (Lowe et al., 2015a). Mice lacking the αIIb-subunit of the integrin αIIbβ3 also develop brain haemorrhages although it is noticeable that they are not as severe as those in mice deficient in CLEC-2 or podoplanin. It is possible that that this difference reflects a non-haemostatic role for CLEC-2 in development of the cerebral vasculature.

There are homologues of podoplanin in many organisms including humans, mice, rats, dogs, and hamsters. The sequence similarity between human and other primates is well conserved, however there is only a 46% protein sequence similarity between humans and mice. The

divergence in sequence similarity may explain the reported lower affinity between human podoplanin and CLEC-2, of 24 ± 3.7μM (Christou et al., 2008), which is three orders of magnitude weaker than our calculated affinities for the interaction of the two mouse proteins. Previous work also demonstrated that human platelets interact with podoplanin-expressing human lymphatic endothelial cells or a recombinant form of human podoplanin at low shear rates, but not at intermediate or high shear rates (Navarro-Nunez et al., 2015).

The difference between mouse and human podoplanin leads to uncertainty as to whether the findings in the present study can be extrapolated to the development of the cerebrovasculature in humans where high shear rates are also likely (Seymour et al., 2016). IVH is however a common pathology in preterm neonatal babies who often exhibit low platelet counts (Horbar et al., 2002, Stanworth, 2012, Ferrer-Marin et al., 2013). It is possible that platelet CLEC-2 is important for the development of the human cerebrovasculature in a similar way to mice, but it may involve additional platelet agonists and receptors along with podoplanin to exert its effects in view of the lower affinity of interaction.

In conclusion, this study demonstrates the novel ability of mouse podoplanin to initiate formation of stable platelet aggregates at high shear. It is likely that podoplanin acts as the initial platelet adhesion and activation receptor triggering a classical pattern of platelet activation. We speculate that this aggregation is important during the development of the cerebrovasculature when triggered by podoplanin on neuroepithelial cells under conditions of arterial shear rates which accounts for the haemorrhaging in developing brains of podoplanin and CLEC-2 deficient mice.

Chapter 4

The role of platelet CLEC-2 and podoplanin in a model of acute inflammation

4.1 Introduction

The most extensively studied aspect of platelet function has been their integral role in haemostasis. However, a growing number of studies have begun to shed light on the role that platelets play in inflammatory processes ranging from acute infection to chronic inflammatory diseases such as atherosclerosis (Morrell et al., 2014).

Platelets have been shown to play a role in leukocyte recruitment and activation through the release of factors such as chemokines and growth factors as well as in the presentation of antigens to leukocytes such as T cells (Chapman et al., 2012, Smyth et al., 2009). Platelets therefore can function as immune cells as well as haemostatic regulators. Their role in the body's response to an infection is highlighted by the occurrence of thrombocytopenia following the development of an uncontrolled response to a systemic infection which is known as sepsis or septic shock. Studies have shown that unresolved thrombocytopenia is associated with an increase in mortality (Venkata et al., 2013).

Studies have revealed that platelets maintain haemostasis during inflammation, albeit in a different manner to classical haemostasis. An inflammatory reaction which triggers mass movement of leukocytes to the site of infection or injury and to lymph nodes for activation Leukocytes therefore need to transmigrate and pass through blood vessel and the maintenance of vascular integrity while this occurs is critical. Data suggest that platelets, through the ITAM receptors GPVI and CLEC-2, prevent the development of haemorrhages in the skin and lungs after an inflammatory trigger (Boulaftali et al., 2013). Platelet CLEC-2 has also been shown to maintain

high enodothelial venule (HEV) vascular integrity through its interaction with fibroblastic reticular cells (FRCs) which express podoplanin (Herzog et al., 2013).

The CLEC-2 ligand podoplanin is upregulated during many inflammatory conditions and on many cell types. For instance, macrophages upregulate podoplanin following an inflammatory stimulus such as lipopolysaccharide (LPS) and have the ability to induce platelet aggregation through a CLEC-2-podoplanin interaction (Kerrigan et al., 2012). Other studies have highlighted a role for platelet CLEC-2 interacting with podoplanin-expressing cells and effecting the auto-inflammatory disease rheumatoid arthritis. Podoplanin expression has been found to be upregulated on synovial fibroblasts of rheumatoid arthritis patient samples; it was shown that platelet CLEC-2 interaction with synovial fibroblasts induces a higher expression of the pro- inflammatory cytokines IL-6 and IL-8 (Del Rey et al., 2014).

This chapter focuses on the role of CLEC-2, and its binding partner podoplanin, in a model of systemic inflammation. For this model, we used a major component of the outer membrane of Gram-negative bacteria, LPS, to trigger an immune reaction through an intraperitoneal injection. The reactions of two different types of CLEC-2 transgenic models, a platelet specific CLEC-2 deficient model, and an inducible CLEC-2 deficient model were used to investigate the role of the C-type lectin receptor in inflammation. CLEC-2 was depleted from the inducible model once the mice were past development through treatment with tamoxifen whereas the platelet specific mouse model lacked platelet CLEC-2 from inception. Importantly previous work performed in our lab by Dr. Kate Lowe has shown that two weeks of tamoxifen diet given to the ER^{T2}-Cre.CLEC-$2^{fl/fl}$ mouse is sufficient to delete CLEC-2 solely from platelets and not from other CLEC-2 expressing

cell such as dendritic cells. The immune cell recruitment to the peritoneal lavage, spleen, and intestines of these mice were examined and compared to littermate controls. Blood counts and cytokine and chemokine quantities in the peritoneal lavage fluid of both models were examined. Additionally, a haematopoietic specific podoplanin deficient model was also examined using the same inflammatory trigger.

4.2 Results

4.2.1 Summary of the reaction of a platelet specific CLEC-2 knockout mouse model (PF4-Cre.CLEC-2$^{fl/fl}$), an inducible CLEC-2 knockout mouse model (ER^{T2}-Cre.CLEC-2$^{fl/fl}$) and a haematopoietic cell specific knockout mouse model (Vav-iCre.PDPN$^{fl/fl}$) to LPS-induced systemic inflammation

Before any inflammatory stimulus, PF4-Cre.CLEC-2$^{fl/fl}$ mice present with thrombocytopenia and splenomegaly (Figure 4.1B and 4.2). Both ER^{T2}-Cre.CLEC-2$^{fl/fl}$ mice (after two weeks of tamoxifen diet) and Vav-iCre.PDPN$^{fl/fl}$ mice do not present with any phenotypic different in comparison to their corresponding littermate control.

All three mouse models were injected with 50µg of LPS into the peritoneum and reactions were compared to their corresponding floxed littermate controls. Table 4.1 shows a comparison of all parameters measured in these mice. PF4-Cre.CLEC-2$^{fl/fl}$ mice present with blood accumulation within the peritoneal lavage fluid and in the Peyer's patches of the small intestine (Figure 4.1). These mice also show a significant increase in spleen size and a significant drop in platelet count, although this is likely due to the thrombocytopenia and splenomegaly present in unchallenged PF4-Cre.CLEC-2$^{fl/fl}$ as previously mentioned. PF4-Cre.CLEC-2$^{fl/fl}$ also present with a significant increase of a range cytokines and chemokines within their peritoneal lavage fluid compared to littermate controls (Figure 4.3). However, this increase did not translate to a significant increase in leukocytes recruited to the peritoneum of PF4-Cre.CLEC-2$^{fl/fl}$ mice and there was in fact a downward trend in the recruitment of neutrophils, monocytes and macrophages (Figure 4.4)

ER^{T2}-Cre.CLEC-$2^{fl/fl}$ mice present with blood accumulation within the peritoneal lavage fluid and in the Peyer's patches of the small intestine after 6 hours of LPS stimulation in a similar manner to PF4-Cre.CLEC-$2^{fl/fl}$ mice (Figure 4.7). However, haemoglobin levels were not significantly different in the ER^{T2}-Cre.CLEC-$2^{fl/fl}$ mice compared to littermate controls when the mice were culled 24 hours after the LPS stimulus suggesting that the phenotype is recoverable over time. PF4-Cre.CLEC-$2^{fl/fl}$ and Vav-iCre.PDPN$^{fl/fl}$ mice could not be examined at a similar time point because both mice models reached a moderate severity level 6 hours post-LPS and therefore had to be culled within the terms of the animal licence. Blood filled Peyer's patches were still present after 24 hours in ER^{T2}-Cre.CLEC-$2^{fl/fl}$ mice (Figure 4.7). In contrast to PF4-Cre.CLEC-$2^{fl/fl}$ mice, ER^{T2}-Cre.CLEC-$2^{fl/fl}$ mice did not present with a significant difference in cytokine and chemokine levels within their lavage fluid at the same time point (Figure 4.9). However downward trend in the recruitment of neutrophils and monocytes to the peritoneum was found in ER^{T2}-Cre.CLEC-$2^{fl/fl}$ mice (Figure 4.10).

Vav-iCre.PDPN$^{fl/fl}$ mice presented with blood in their peritoneum 6 hours post-LPS in a similar manner to the CLEC-2 deficient models (Figure 4.12). Beyond this phenotype, no other significant differences were found in the phenotype of the Vav-iCre.PDPN$^{fl/fl}$ mice. No significant differences were seen in the leukocyte recruitment to the spleen, colon, or small intestine of PF4-Cre.CLEC-$2^{fl/fl}$, ER^{T2}-Cre.CLEC$^{fl/fl}$ or Vav-iCre.PDPN$^{fl/fl}$ mice before or after LPS (Table 4.1).

Table 4.1

Mouse Model	PF4-Cre.CLEC-2$^{fl/fl}$	ER^{T2}-Cre.CLEC-2$^{fl/fl}$		Vav-iCre.CLEC-2$^{fl/fl}$
Time since I.P LPS	**6 Hrs**	**6 Hrs**	**24 Hrs**	**6 Hrs**
Blood filled PLF	Yes	Yes	No	Yes
Blood filled PPs	Yes	Yes	Yes	No
Spleen Weight	Increased	NS	NS	NS
Platelet Count	Decreased	NS	NS	NS
Cytokine and Chemokine levels	Increased	NS	NS	NS
Leukocyte recruitment to:				
PLF	Trend of lower no. of Nϕ, MO, and Mϕ	NS	Trend of lower no. of Nϕ and MO	NS
Spleen	NS	NS	NS	NS
Colon	NS	NS	NS	NS
Small Intestine	NT	NT	NS	NS

Table 4.1: Summary of all three mouse models used following LPS-induced systemic inflammation.

Non-significance (NS) denotes a lack of difference between the reaction of the floxed littermate controls and the knockout mice in question at the time points noted. NT= Not tested, PLF= Peritoneal lavage fluid, PPs=Peyer's patches, Nϕ= Neutrophils, MO= Monocytes, Mϕ= Macrophages. The cytokines and chemokines measured were TNF-α, IL-6, IL-1β, IL-10, MCP-1/CCL2, MIP-2/CxCL2, IFN-γ, RANTES/CCL5, IL-4, CXCL1, GM-CSF, MIP1α, MIP1β.

4.2.2 Splenomegaly and the presence of blood in the peritoneal lavage, lymph nodes and Peyer's patches in platelet specific CLEC-2 knockout mice (PF4-Cre.CLEC-2$^{fl/fl}$) compared to littermate controls after LPS treatment

The first notable difference in the phenotype of platelet specific CLEC-2 deficient mice (PF4-Cre.CLEC-2$^{fl/fl}$) compared to littermate controls was the development of blood filled inguinal and mesenteric lymph nodes post-LPS (Figure 4.1A). This finding correlates with studies that demonstrated the role of platelet CLEC-2 in lymph node vascular integrity during development and after an immune stimulus (Benezech et al., 2014, Herzog et al., 2013). However, a novel finding is the presence of blood filled Peyer's patches in all PF4-Cre.CLEC-2$^{fl/fl}$ mice (Figure 4.1B). The peritoneal fluid also presented with blood not seen in the floxed littermate controls (Figure 4.1B) and measured by a haemoglobin assay in Figure 4.1C. No significant difference was measured in the weight loss induced by LPS but a significant difference is seen in spleen weight in the CLEC-2 platelet specific knockout mice compared to littermate controls. This difference however is likely due to the splenomegaly seen in untreated PF4-Cre.CLEC-2$^{fl/fl}$ mice.

Figure 4.1

A

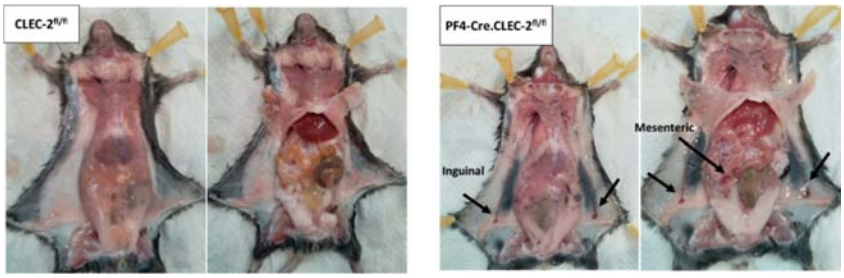

B

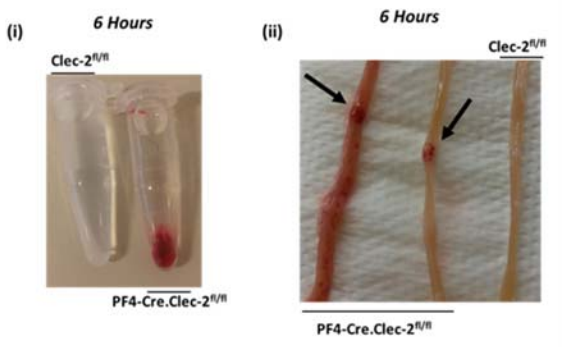

C

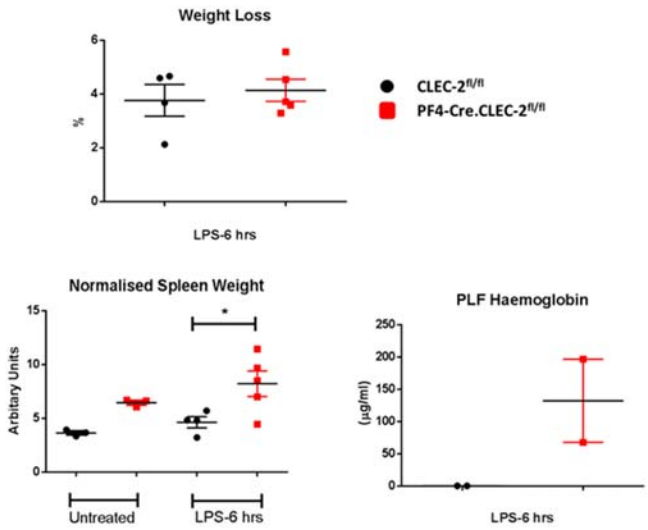

Figure 4.1: Phenotype of platelet specific CLEC-2 deficient mice (PF4-Cre.CLEC-2$^{fl/fl}$) and littermate controls following LPS treatment.

A. PF4-Cre.CLEC-2$^{fl/fl}$ and their littermate controls were culled 6 hours after an injection of 50µg LPS. Pictures display a representative comparison of the internal phenotype following the LPS stimulus. Arrows point to area of blood accumulation within the mesenteric and inguinal lymph nodes of PF4-Cre.CLEC-2$^{fl/fl}$ mice.
B. Representative peritoneal lavage fluid (PLF) samples and small intestines of PF4-Cre.CLEC-2$^{fl/fl}$ and the CLEC-2$^{fl/fl}$ littermate controls after 6 hours of LPS treatment. Blood accumulation was observed in the peritoneal lavage (i) and Peyer's patches of the small intestine (ii) following LPS treatment in PF4-Cre.CLEC-2$^{fl/fl}$ and not in control mice (arrows). Some PF4-Cre.CLEC-2$^{fl/fl}$ present with more severe blood accumulation within the small intestine than others.
C. Graphs display the percentage weight loss 6 hour post- LPS treatment in PF4-Cre.CLEC-2$^{fl/fl}$ and CLEC-2$^{fl/fl}$ littermate controls as well as spleen weight (normalised to body weight) and PLF haemoglobin quantification. Statistical analysis performed by two way ANOVA followed by a Bonferroni multiple comparison test for comparison between the untreated and LPS treated groups and Mann Whitney U test for a two sample group comparison, * =$p<0.05$

4.2.3 Lower platelet count in untreated and LPS-treated platelet specific CLEC-2 knockout mice (PF4-Cre.CLEC-2$^{fl/fl}$) compared to littermate controls.

Figure 4.2 displays the platelet and white blood cell (WBC) count as well as the percentage of lymphocytes, monocytes and neutrophils in the blood of untreated and LPS treated platelet specific CLEC-2 deficient mice (PF4-Cre.CLEC-2$^{fl/fl}$) compared to littermate controls. In the untreated mice, the only significant difference noted is the previously reported lower platelet count in the PF4-Cre.CLEC-2$^{fl/fl}$ mice. The lower platelet count is the untreated PF4-Cre.CLEC-2$^{fl/fl}$ is believed to be the result of blood lymphatic mixing present in these mice (Bender et al., 2013).

Following LPS treatment the PF4-Cre.CLEC-2$^{fl/fl}$ and CLEC-2$^{fl/fl}$ mice follow the known trajectory blood cell count changes which is reported in (Copeland et al., 2005). Most circulating cells in mouse blood are lymphocytes and after an LPS immune stimulus there is a significant drop WBC count and percentage of lymphocytes and an increase in the percentage of neutrophils which can been seen in Figure 4.2. There is also a significant drop in platelet count. However, the LPS treated platelet specific CLEC-2 knockout mice experienced a significantly greater in platelet count compared to the littermate controls, which is most probably due to the lower count present in these mice before treatment.

Figure 4.2:

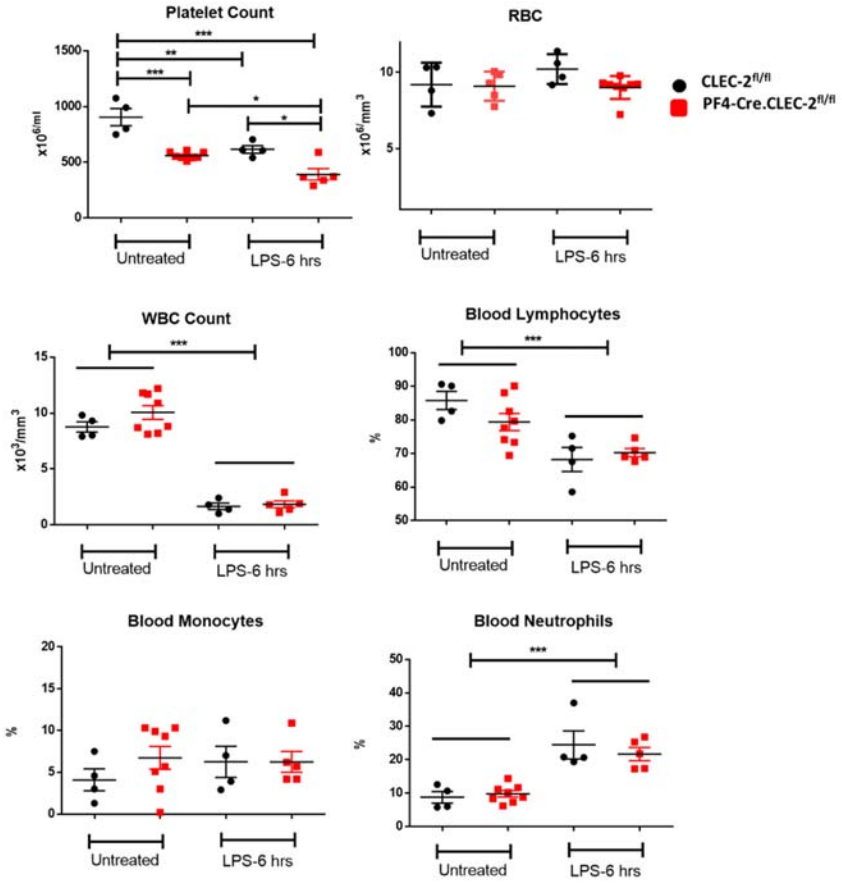

Figure 4.2: Blood count measurements of untreated and LPS-treated platelet specific CLEC-2 knockout mice (PF4-Cre.CLEC-2$^{fl/fl}$) compared to littermate controls

Graphs display the platelet count, red blood cell count (RBC), white blood cell (WBC) count and lymphocyte, neutrophil and monocyte percentage in the blood of untreated and 6 hour LPS treated PF4-Cre.CLEC-2$^{fl/fl}$ and CLEC-2$^{fl/fl}$ mice. Statistical analysis performed using a two way ANOVA followed by a Bonferroni multiple comparison test for comparison between the untreated and LPS treated groups and a Mann Whitney U test for a two sample group comparison * =$p<0.05$, ** = $p<0.01$, *** =$p<0.001$. Lines above two sample groups indicate a statistical comparison of both groups together with another group.

Table 4.2

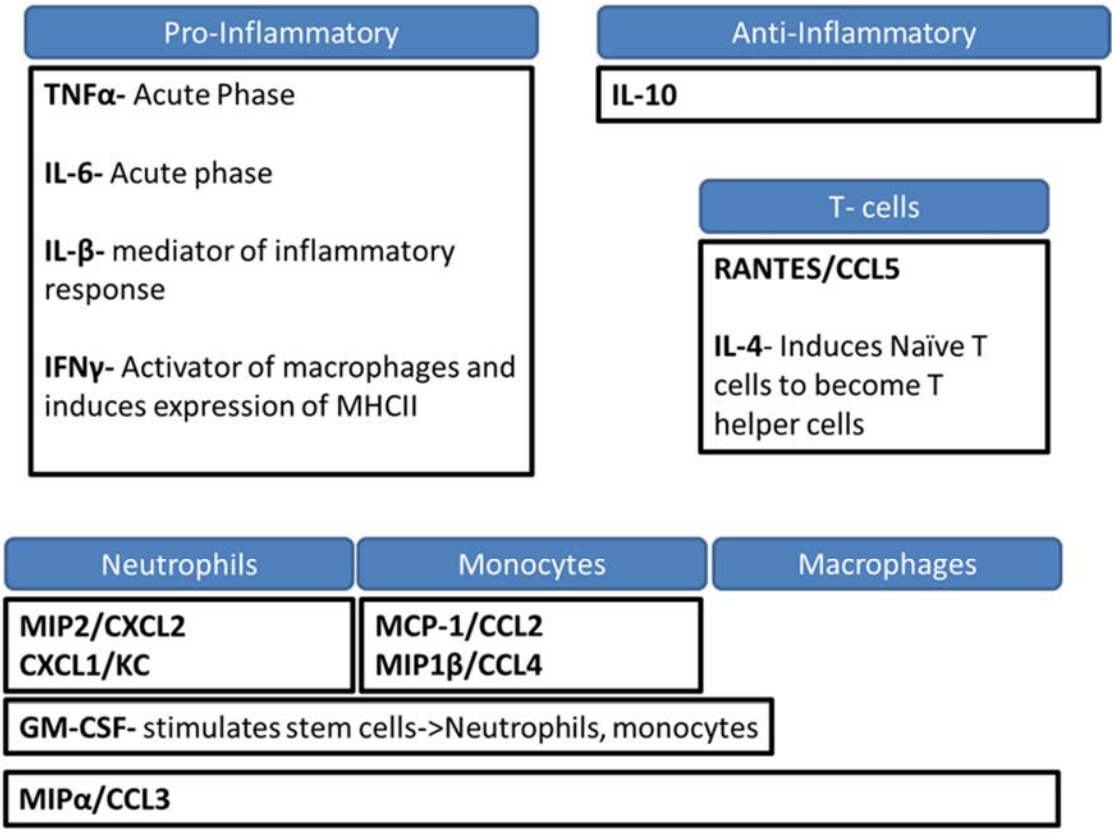

Table 4.2: Key cytokines and chemokines involved in LPS-induced inflammation.

Blue boxes represent the generalised function or cell type which the molecules can cause behaviour modification to, recruit or increase cell production.

4.2.4 Significantly higher quantity of protein and cytokine and chemokine levels in LPS-treated platelet specific CLEC-2 knockout mice (PF4-Cre.CLEC-2$^{fl/fl}$) compared to littermate controls

The quantity of protein and the levels of a range of cytokines and chemokines (Table 4.2) were measured in the peritoneal lavage of untreated and LPS treated platelet specific CLEC-2 deficient mice (PF4-Cre.CLEC-2$^{fl/fl}$) and is compared to littermate controls in Figure 4.3. No differences are seen between the knockout and littermate controls before LPS treatment but significant differences are seen between the two groups following LPS treatment. An increase in protein levels and many the cytokines and chemokines in the PLF was observed in littermate controls as would be expected to occur following an injection of LPS. However, the levels of protein and both anti-inflammatory (eg. IL-10) and pro inflammatory (eg. IL-1β) cytokines were significantly greater in the platelet specific CLEC-2deficient mice (Figure 4.3). There was also a significant increase seen in many of cytokines and chemokines involved in the recruitment of specific leukocytes such as neutrophils, monocytes and macrophages. These data could indicate a role for platelet CLEC-2 in regulating the immune response by preventing the production of excess cytokines which has been referred to as a 'Cytokine storm' (Tisoncik et al., 2012).

Figure 4.3

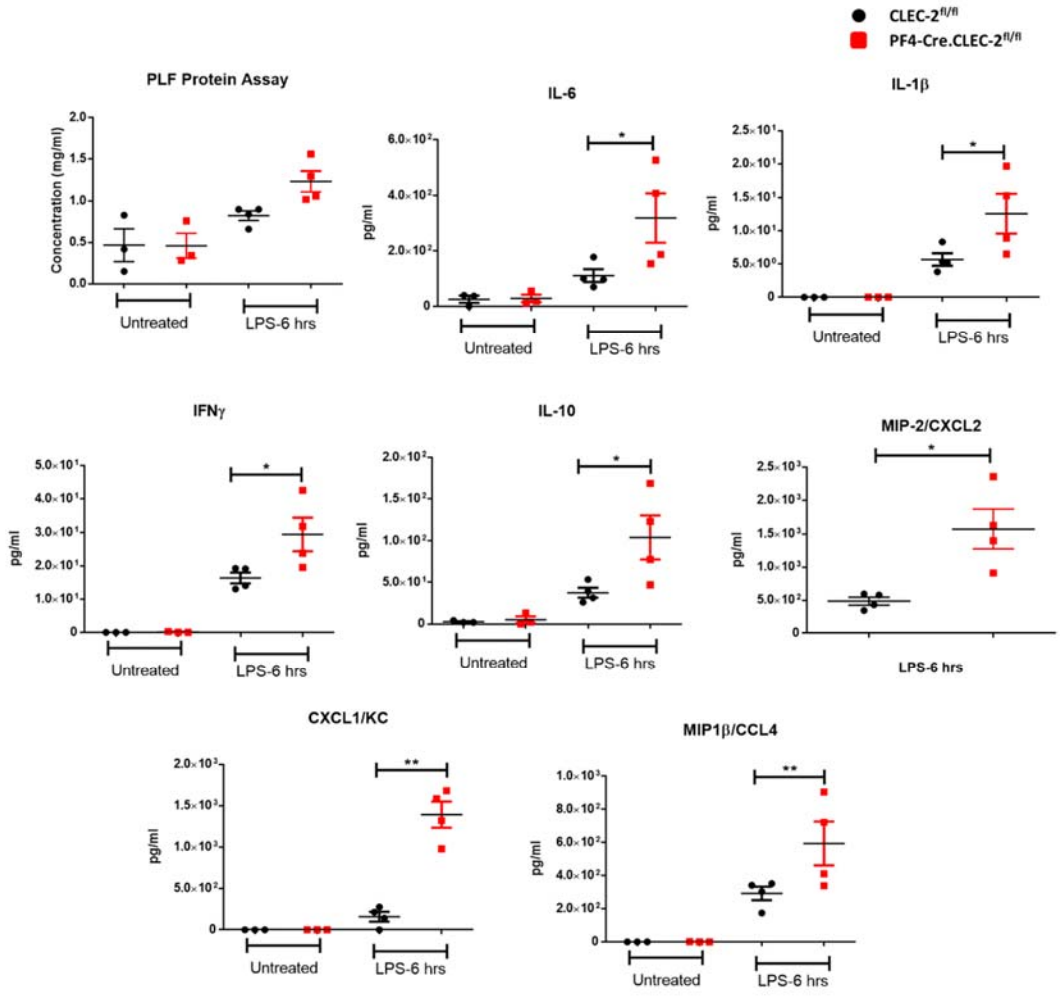

Figure 4.3: Analysis of total protein and inflammatory mediators present in the peritoneal lavage of unchallenged and 6 hour LPS-treated platelet specific CLEC-2 knockout mice and littermate controls

Graphs display the protein and cytokine and chemokine quantification from the peritoneal lavage of untreated and 6 hour LPS treated PF4-Cre.CLEC-2$^{fl/fl}$ and CLEC-2$^{fl/fl}$ mice. The cytokines and chemokines measured were TNF-α, IL-6, IL-1β, IL-10, MCP-1/CCL2, MIP-2/CxCL2, IFN-γ, RANTES/CCL5, IL-4, CXCL1, GM-CSF, MIP1α, MIP1β. Non-significant cytokines and chemokines which were quantified are not shown. Protein was measured using a protein assay and cytokine and chemokines were measured using a Firefly or Luminex assay. Statistical analysis performed using a two way ANOVA followed by a Bonferroni multiple comparison test for comparison between the untreated and LPS treated groups and a Mann Whitney U test for a two sample group comparison, * = $p<0.05$, ** = $p<0.01$, ***=$p<0.001$. Lines above two sample groups indicate a statistical comparison of both groups together with another group.

4.2.5 No significant difference found in leukocyte recruitment to the peritoneal lavage, spleen or colons of untreated and LPS-treated platelet specific CLEC-2 knockout mice (PF4-Cre.CLEC-$2^{fl/fl}$) compared to littermate controls

Despite the finding that there are greater quantities of a range of cytokines and chemokines present in the peritoneum of LPS-treated platelet specific deficent mice, no significant differences were found in the percentage or number of leukocytes in the peritoneal lavage fluid (PLF), spleen or colons of these mice (Figure 4.4 and Figure 4.5). There was in fact evidence of a trend towards a lower number of leukocytes in the PLF of the knockout mice compared to littermate controls but remained non-significant. The number of leukocytes found in the PLF can be variable therefore the testing of greater number of mice may show this trend to be significant. Despite the increase in spleen weight no significant increase in leukocytes was seen (percentage and number) when comparing the untreated mice to each other or the LPS treated mice groups to each other (Figure 4.5). The proportional percentage of the different leukocyte groups (B cells, T cells, macrophages etc) also remained the same (not shown). Equally no significant shifts were seen in the leukocyte percentage and numbers collected from the colons of these mice.

Figure 4.4

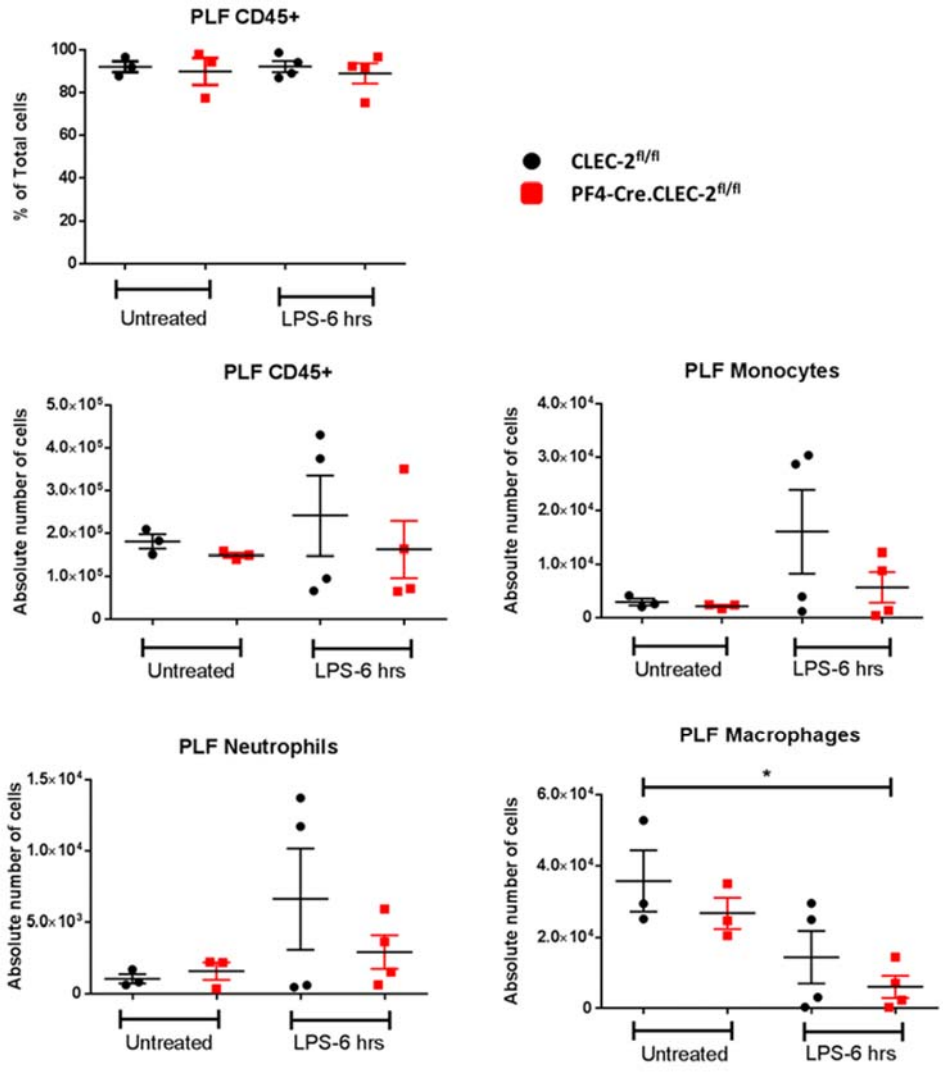

Figure 4.4: Leukocyte recruitment to the peritoneal lavage of untreated and LPS treated mice of a platelet specific CLEC-2 knockout mouse model (PF4-Cre.CLEC-2$^{fl/fl}$) compared to littermate controls

Graphs display the percentage and number of leukocytes (CD45+ cells) in the peritoneal lavage (PLF) of untreated and LPS treated PF4-Cre.CLEC-2$^{fl/fl}$ and CLEC-2$^{fl/fl}$ mice. The numbers of quantified neutrophils (CD11b+ Ly6G+), monocytes (CD11b+ Ly6C+) and macrophages (CD11b+ F4/80+) in the PLF of these mice is also shown. Statistical analysis performed using a two way ANOVA followed by a Bonferroni multiple comparison test for comparison between the untreated and LPS treated groups and a Mann Whitney U test for a two sample group comparison, * = $p<0.05$, ** = $p<0.01$, *** =$p<0.001$.

Figure 4.5

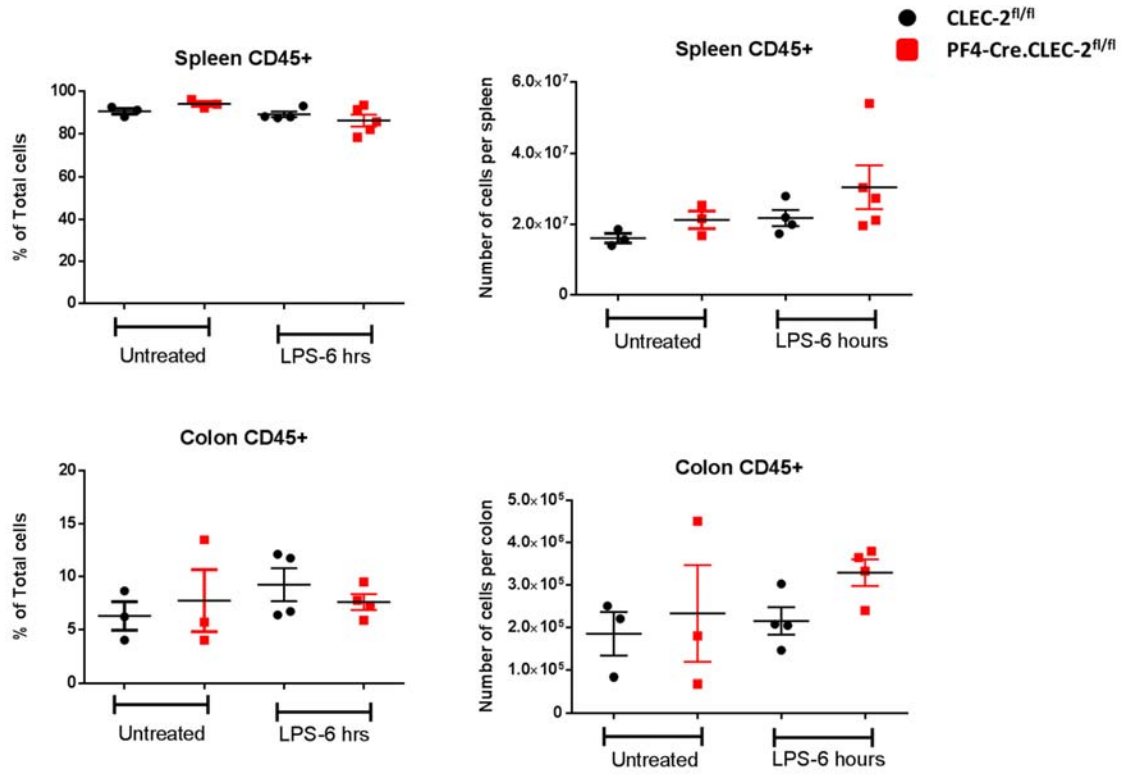

Figure 4.5: Leukocyte recruitment to the spleens and colons of untreated and LPS treated mice of a platelet specific CLEC-2 knockout mouse model (PF4-Cre.CLEC-2$^{fl/fl}$) compared to littermate controls

Graphs display the percentage and number of leukocytes (CD45+ cells) in the spleen and colons of untreated and LPS treated PF4-Cre.CLEC-2$^{fl/fl}$ and CLEC-2$^{fl/fl}$ mice. Statistical analysis performed using a two way ANOVA followed by a Bonferroni multiple comparison test for comparison between the untreated and LPS treated groups and a Mann Whitney U test for a two sample group comparison.

4.2.6 Blood accumulation in the peritoneal lavage and Peyer's patches of inducible CLEC-2 knockout mice (ER^{T2}-Cre.CLEC-$2^{fl/fl}$) compared to littermate controls after LPS treatment

Lack of platelet CLEC-2 during development has been shown to result in incomplete separation in the blood and lymphatic system. This defect is present in PF4-Cre.CLEC-$2^{fl/fl}$ mice and we therefore wanted to compare the immune reaction of a CLEC-2 deficient mouse model which can develop normally before removal of CLEC-2 expression. Any significant differences seen in this inducible CLEC-2 knockout mouse model can therefore be attributed to the involvement of platelet CLEC-2 in the reaction of the immune system and not due to an underlying developmental defect. Figure 4.6 displays the phenotypic differences seen in the ER^{T2}-Cre.CLEC-$2^{fl/fl}$ mice compared to the CLEC-$2^{fl/fl}$ littermate controls. The mice were given two weeks of tamoxifen diet to induce the removal of CLEC-2 from their genome, and subsequently placed on normal chow diet for four weeks to prevent the anti-inflammatory effects of tamoxifen from affecting the results (Tapia-Gonzalez et al., 2008, Suuronen et al., 2005). These ER^{T2}-Cre.CLEC-$2^{fl/fl}$ mice did not reach the moderate severity until 24 hours post-LPS which is the same time limit as wild type mice. However, they presented with blood within their peritoneal lavage fluid (PLF) 6 hours post-LPS injection similar to PF4-Cre.CLEC-$2^{fl/fl}$ mice (Figure4.6Ai). This phenotype was no longer visible or measurable 24 hour post LPS (Figure 4.6Ai, B). Blood filled Peyer's patches were visible in the small intestines of the knockout mice both 6 hour and 24 hour post LPS (Figure 4.5ii). There were no differences seen in the weight loss or spleen weight at each time point between the knockout mice and their littermate controls. However, the spleen weight of the ER^{T2}-Cre.CLEC-$2^{fl/fl}$ mice was seen to be seen be significantly greater 24 hour post LPS than untreated mice. This difference could be an

indication that these mice develop larger spleen than their littermates in a similar way to the PF4-Cre.CLEC-2$^{fl/fl}$ mice but the change does not occur until a later time point.

Figure 4.6

A

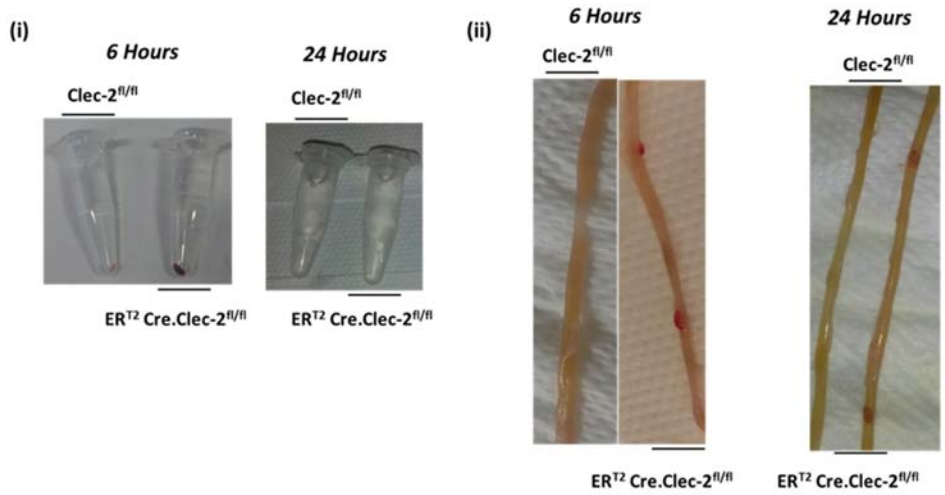
(i)
6 Hours
24 Hours
Clec-2fl/fl
Clec-2fl/fl
ERT2 Cre.Clec-2fl/fl
ERT2 Cre.Clec-2fl/fl
(ii)
6 Hours
24 Hours
Clec-2fl/fl
Clec-2fl/fl
ERT2 Cre.Clec-2fl/fl
ERT2 Cre.Clec-2fl/fl

B

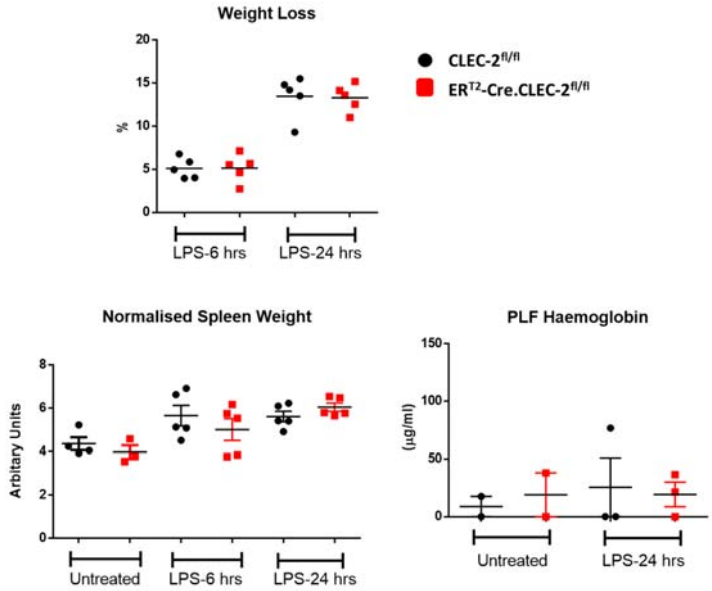
Weight Loss
%
20
15
10
5
0
LPS-6 hrs
LPS-24 hrs
CLEC-2fl/fl
ERT2-Cre.CLEC-2fl/fl
Normalised Spleen Weight
Arbitary Units
8
6
4
2
0
Untreated
LPS-6 hrs
LPS-24 hrs
PLF Haemoglobin
(µg/ml)
150
100
50
0
Untreated
LPS-24 hrs

Figure 4.6: Phenotype of inducible CLEC-2 knockout mice (ER^{T2}-Cre.CLEC-$2^{fl/fl}$) and littermate controls following LPS treatment

A. Representative peritoneal lavage fluid (PLF) samples and small intestines of ER^{T2}-Cre.CLEC-$2^{fl/fl}$ and the CLEC-$2^{fl/fl}$ littermate controls 6 and 24 hours after an injection of 50µg LPS. These mice were given two weeks of tamoxifen diet to induce the remove of CLEc-2 expression followed by four weeks of normal diet before LPS treatment. Blood accumulation was observed in the peritoneal lavage (i) and following 6 hours LPS treatment but not after 24 hours of LPS treatment. Blood accumulation was also seen in Peyer's patches of the small intestine (ii) following both 6 and 24 hours of LPS treatment

B. Graphs displays the percentage weight loss 6 and 24 hours post-LPS treatment in ER^{T2}-Cre.CLEC-$2^{fl/fl}$ and the CLEC-$2^{fl/fl}$ littermates, as well as body weight normalised spleen weight (6 and 24 hour) and peritoneal lavage fluid (PLF) haemoglobin quantification (24 hour) between untreated and LPS treated ER^{T2}-Cre.CLEC-$2^{fl/fl}$ and the CLEC-$2^{fl/fl}$. Statistical analysis performed by two way ANOVA followed by a Bonferroni multiple comparison test for comparison between the untreated and LPS treated groups and a Mann Whitney U test for a two sample group comparison, * = $p<0.05$, ** = $p<0.01$, *** =$p<0.001$. Lines above two sample groups indicate a statistical comparison of both groups together with another group.

4.2.7 No significant differences in the blood count of untreated and LPS-treated inducible CLEC-2 knockout mice (ER^{T2}-Cre.CLEC-$2^{fl/fl}$) compared to littermate controls.

As previously discussed in reference to the platelet specific CLEC-2 deficient mice (PF4-Cre.CLEC-$2^{fl/fl}$) there are changes in the blood cell counts in mice post-LPS. The inducible CLEC-2 knockout mice (ER^{T2}-Cre.CLEC-$2^{fl/fl}$) and littermate controls were seen to exhibit similar changes (Figure 4.7). One notable difference is the ER^{T2}-Cre.CLEC-$2^{fl/fl}$ mice did not show a significant difference in platelet count until 24-hour post LPS. This lack of difference however may be due to low n numbers. The graphs show that the percentage of neutrophils begin to drop 24 post LPS whereas the monocyte percentage increases. This change is likely due to neutrophils begin to extravagate into the bodies' tissues.

Figure 4.7:

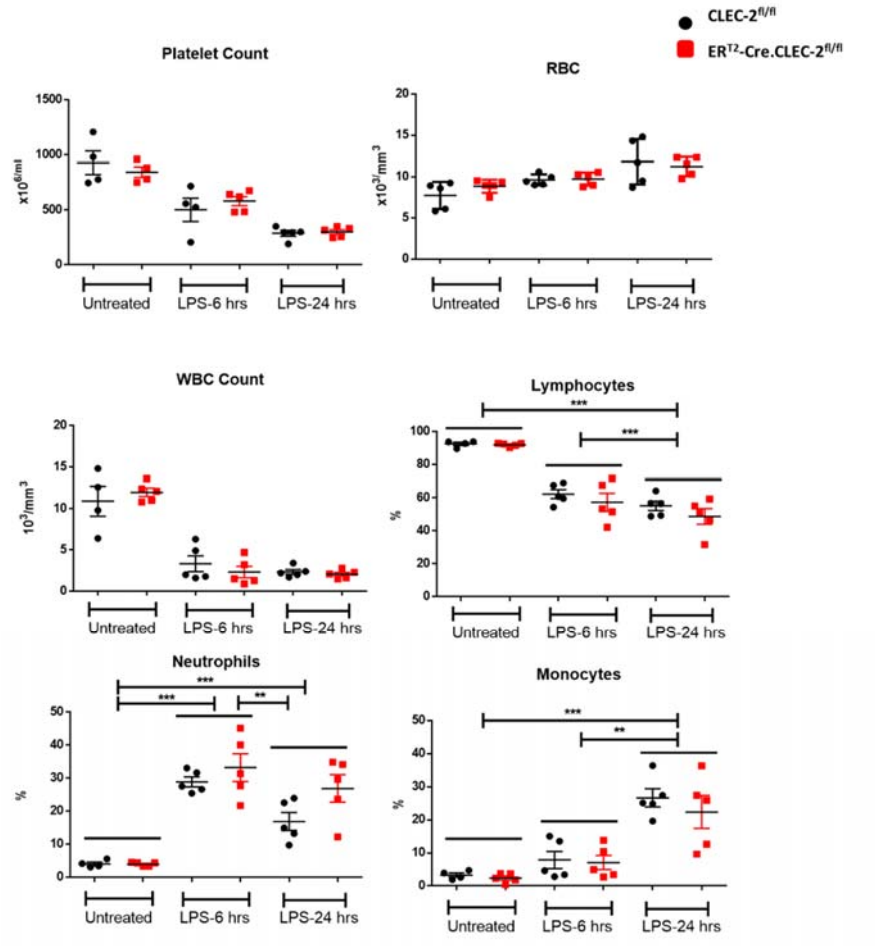

Figure 4.7: Blood count measurement of untreated and LPS treated mice of an inducible CLEC-2 knockout mouse model (ER^{T2}-Cre.CLEC-$2^{fl/fl}$) compared to their littermate controls

Graphs display the platelet counts, red blood cell count (RBC), white blood cell count (WBC) and lymphocyte, neutrophil and monocyte percentage in the blood of untreated and 6 and 24 hour LPS treated ER^{T2}-Cre.CLEC-$2^{fl/fl}$ and the CLEC-$2^{fl/fl}$. Statistical analysis performed using a two way ANOVA followed by a Bonferroni multiple comparison test for comparison between the untreated and LPS treated groups and a Mann Whitney U test for a two sample group comparison, ***=$p<0.001$. Lines above two sample groups indicate a statistical comparison of both groups together with another group.

4.2.8 No significant differences in the quantity of protein or levels of cytokines and chemokines in the peritoneal lavage fluid between inducible CLEC-2 knockout mice and littermate controls.

The quantity of protein was measured in the peritoneal lavage fluid of untreated, and LPS treated inducible CLEC-2 knockout mice and littermate controls 6 and 24 hours post-LPS (Figure 4.8). A range of cytokines and chemokines levels were also measured in the peritoneal lavage fluid inducible CLEC-2 knockout mice and littermate controls 6 hours post-LPS. No significant differences were seen in the quantity of protein between the knockout and littermate controls at any of the time points measured. In addition and in contrast to the platelet specific CLEC-2 knockout mice (PF4-Cre.CLEC-$2^{fl/fl}$), no significant increases in cytokines and chemokines were measured 6 hours post-LPS.

Figure 4.8

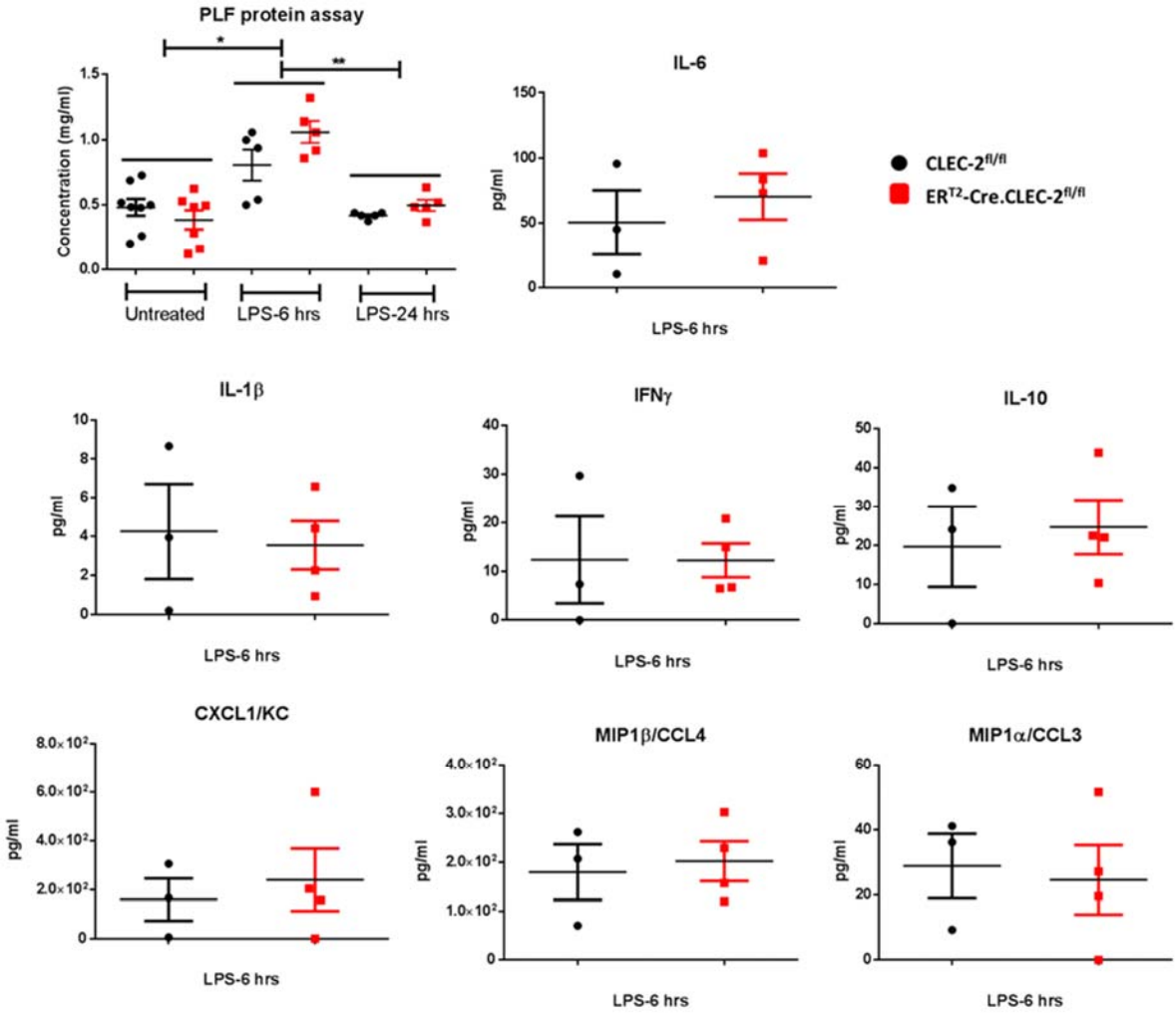

Figure 4.8: Peritoneal lavage protein and cytokine measurements from LPS treated mice of an inducible CLEC-2 knockout mouse model (ER^{T2}-Cre.CLEC-$2^{fl/fl}$).

The above graphs display the protein quantification from the peritoneal lavage of untreated, 6 and 24 hour LPS treated ER^{T2}-Cre.CLEC-$2^{fl/fl}$ and the CLEC-$2^{fl/fl}$ mice and cytokine and chemokine measure from 6 hour LPS treatment of the same mice. Cytokine and chemokine graph measurement shown of the same molecules displayed in Figure 4.5 for comparison to the platelet specific CLEC-2 mouse model. Protein was measured using a protein assay and cytokine and chemokines were measured using a Firefly or Luminex assay. Statistical analysis performed using a two way ANOVA followed by a Bonferroni multiple comparison test for comparison between the untreated and LPS treated groups and a Mann Whitney U test for a two sample group comparison, * = $p<0.05$, ** = $p<0.01$, *** =$p<0.001$. Lines above two sample groups indicate a statistical comparison of both groups together with another group.

4.2.9 No significant difference in leukocyte recruitment to the peritoneal lavage between inducible CLEC-2 knockout mice and littermate controls

Figure 4.9 shows the leukocyte recruitment to the peritoneal lavage of untreated and LPS treated inducible CLEC-2 knockout mice compared to littermate controls. No significant differences were seen between the knockout mice and controls at each time point. The numbers of cells were variable at all time points. However, a significant increase in neutrophil and monocyte numbers was seen in the littermate controls 24 hours post-LPS compared to the untreated mice, while the same increase in not seen in the inducible CLEC-2 deficient mice. There is also a notable increase in number of podoplanin expressing macrophages recruited to the peritoneum 24 hours post-LPS but no significant differences were seen between the inducible CLEC-2 knockout mice and littermate controls.

Figure 4.9:

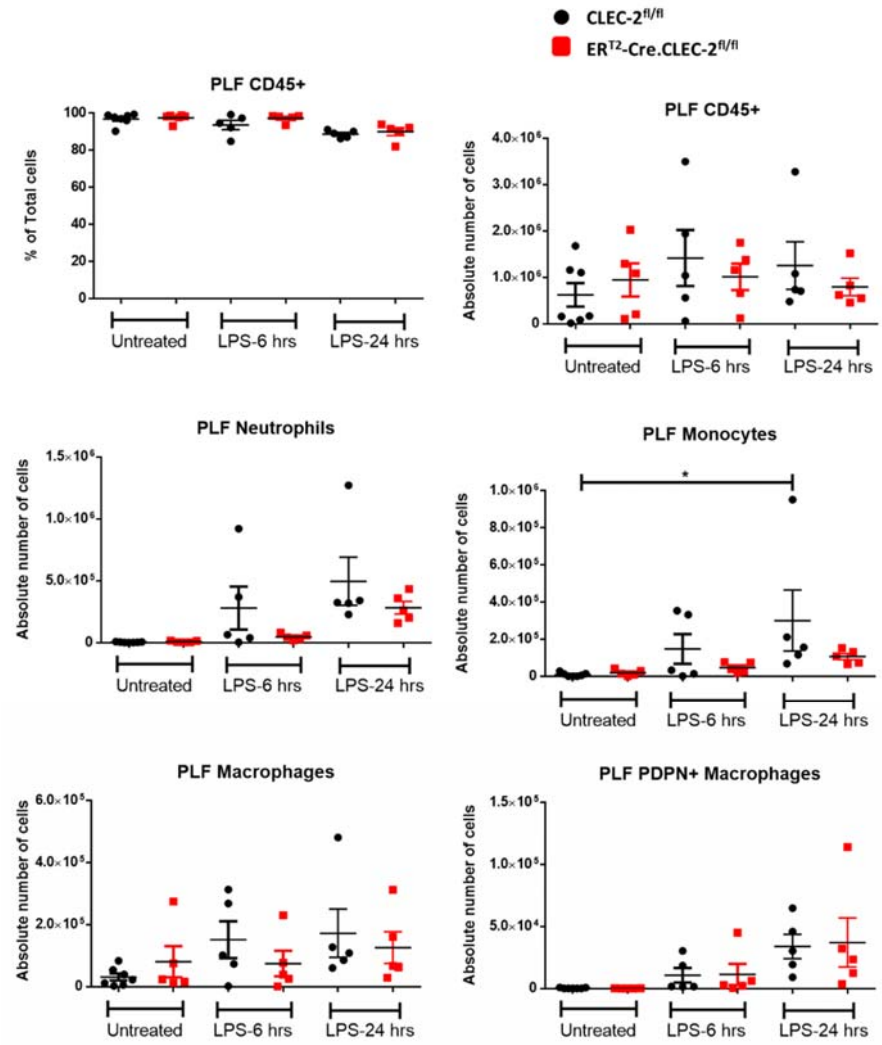

Figure 4.9: Leukocyte recruitment to the peritoneal lavage of untreated and LPS treated mice of an inducible CLEC-2 knockout mouse model (ER^{T2}-Cre.CLEC-$2^{fl/fl}$) compared to their littermate controls

Graphs display the percentage and number of leukocytes (CD45+ cells) in the peritoneal lavage (PLF) of untreated and 6 and 24 hour LPS treated ER^{T2}-Cre.CLEC-$2^{fl/fl}$ and the CLEC-$2^{fl/fl}$ mice. The numbers of quantified neutrophils (CD11b+ Ly6G+), monocytes (CD11b+ Ly6C+) and macrophages (CD11b+ F4/80+) and podoplanin positive macrophages (CD11b+ F4/80+ PDPN+) in the PLF of these mice is also shown. Statistical analysis performed using a two way ANOVA followed by a Bonferroni multiple comparison test for comparison between the untreated and LPS treated groups and a Mann Whitney U test for a two sample group comparison * = $p<0.05$, ** = $p<0.01$, *** =$p<0.001$

4.2.10 No significant difference seen in leukocyte recruitment to the spleen, colons or small intestines between LPS treated inducible CLEC-2 knockout mice and littermate controls.

Leukocyte percentage and numbers in the spleen, colon and small intestine of untreated and LPS treated inducible CLEC-2 deficient mice were compared to littermate controls. Spleen and colons were examined in untreated mice and in mice 6 and 24 hours post-LPS while small intestines were examined only in untreated mice and in mice 24 hours post-LPS (Figure 4.10). The changes in leukocyte numbers in the spleen and colon of these mice were not significantly different between the knockout mice and littermate controls. No fluctuations were seen in the percentage or number of leukocytes in the small intestine after LPS.

Figure 4.10

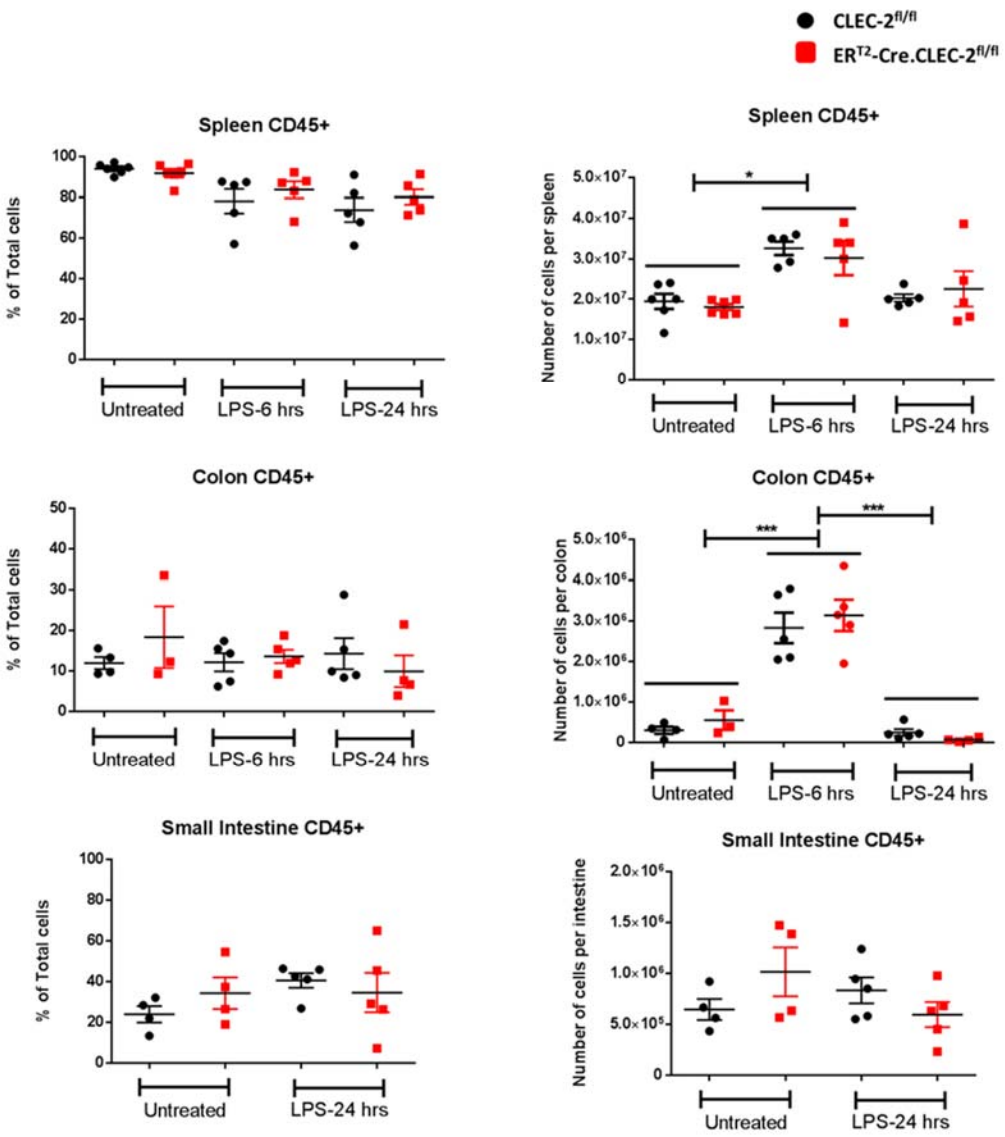

Figure 4.10: Leukocyte recruitment to the spleens, colons and small intestines of untreated and LPS treated mice of an inducible CLEC-2 knockout mouse model (ERT2-Cre.CLEC-2fl/fl) compared to littermate controls

Graphs display the percentage and number of leukocytes (CD45+ cells) in the spleen, colon and small intestine of untreated and 6 (excluding small intestine) and 24 hour LPS treated ER^{T2}-Cre.CLEC-$2^{fl/fl}$ and the CLEC-$2^{fl/fl}$ mice. Statistical analysis performed using a two way ANOVA followed by a Bonferroni multiple comparison test for comparison between the untreated and LPS treated groups and a Mann Whitney U test for a two sample group comparison, * = $p<0.05$, ** = $p<0.01$, *** = $p<0.001$. Lines above two sample groups indicate a statistical comparison of both groups together with another group.

4.2.11 Blood accumulation in the peritoneal lavage fluid of LPS treated haematopoietic lineage specific podoplanin knockout mice (Vav-iCre.PDPN$^{fl/fl}$) compared to littermate controls

To compare to the results using the two CLEC-2 knockout mouse models, a haematopoietic lineage specific podoplanin deficient mice (Vav-iCre.PDPN$^{fl/fl}$) was treated with the same amount of LPS and compared to its littermate controls. Similar to the CLEC-2 knockout models, blood was present in the peritoneal lavage fluid of Vav-iCre.PDPN$^{fl/fl}$ and the quantity of haemoglobin was significantly greater than littermate controls 6 hours post-LPS (Figure 4.11Ai, and B). However, in contrast to the CLEC-2 knockout models, no obvious accumulation of blood within the Peyer's patches of the LPS treated haematopoietic podoplanin specific knockout mice was seen (Figure 4.11Aii). No significance differences were seen in weight loss and a similar significant increase in spleen weight was seen in both in the Vav-iCre.PDPN$^{fl/fl}$ mice and PDPN$^{fl/fl}$ littermate controls. No significant differences were seen in any other parameters measured as described in Table 4.1.

Figure 4.11

A

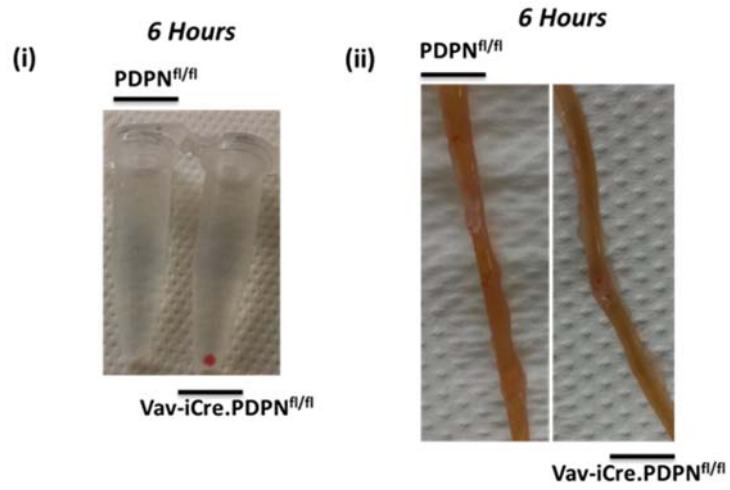

B

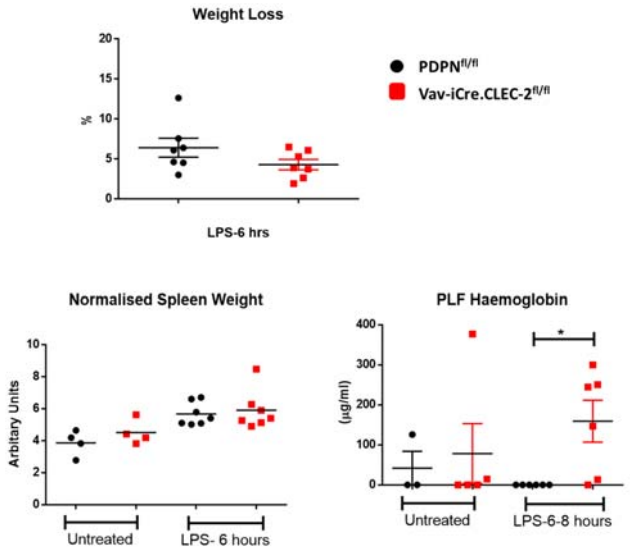

Figure 4.11: Phenotype of haematopoietic specific podoplanin knockout mice (Vav-iCre.PDPN$^{fl/fl}$) and littermate controls following LPS treatment.

A. Representative peritoneal lavage fluid (PLF) samples and small intestine of Vav-iCre.PDPN$^{fl/fl}$ and PDPN$^{fl/fl}$ littermate controls 6 hours after an injection of 50µg LPS. Blood accumulation within the peritoneum was observed in the peritoneal lavage (i) following LPS treatment in Vav-iCre.PDPN$^{fl/fl}$ mice but not in control mice. Peyer's patches appeared normal after LPS treatment (arrows).

B. Graphs displays the percentage weight loss 6 hours post-LPS treated Vav-iCre.PDPN$^{fl/fl}$ and the PDPN$^{fl/fl}$ littermate controls, as well as the body weight normalised spleen weight and peritoneal lavage fluid (PLF) haemoglobin quantification. Statistical analysis performed using a two way ANOVA followed by a Bonferroni multiple comparison test for comparison between the untreated and LPS treated groups and a Mann Whitney U test for a two sample group comparison, * = $p<0.05$. Lines above two sample groups indicate a statistical comparison of both groups together with another group.

4.3 Discussion

The results presented in this chapter indicate an important role for platelet CLEC-2 in endotoxin induced peritonitis. Importantly however, there are clear differences in the reactions between the platelet specific CLEC-2 deficient mice and the inducible CLEC-2 deficient mice. These differences suggest that the blood lymphatic mixing caused by lack of platelet CLEC-2 during development results in an increased susceptibility to sepsis.

The similarities between the CLEC-2 deficient mouse models include blood accumulation within the peritoneum sometime in the first 6 hours of immune stimulation. There was also a significant presentation of blood within the small intestine Peyer's patches of both CLEC-2 deficient models. It has been shown that interaction of platelet CLEC-2 with podoplanin expressing FRCs maintains HEV vascular integrity (Herzog et al., 2013). The study showed that spontaneous bleeding in platelet specific CLEC-2 deficient mice or FRC specific podoplanin specific deficient mice only occurred in MAdCAM-1 expressing mucosal lymph nodes. After immune challenge using ovalbumin/complete Freund's adjuvant, MAdCAM-1 becomes upregulated on peripheral lymph nodes and results in blood accumulation within peripheral lymph nodes also. HEVs present in Peyer's patches have been shown to also express high levels of MAdCAM-1 (Ikeda et al., 2003). The peritoneum contains its own HEVs as part of an area of the body known as the greater omentum (Buscher et al., 2016). It has been shown that MAdCAM-1 expressing HEVs are more permeable due to reduced levels of VE-cadherin, an important component of endothelial adherens junctions and barrier function (Herzog et al., 2013). The presence of blood in the peritoneum and Peyer's patches of both CLEC-2 deficient models emphasises the role of platelet

CLEC-2 in maintaining vascular integrity with MAdCAM-1 expressing HEVs seeming to be particularly vulnerable.

It is however more difficult to explain presence of blood in the peritoneum of the haematopoietic lineage specific podoplanin deficient mice and their corresponding lack of blood accumulation within the Peyer's patches of these knockout mice. The study which focused on the role of platelet CLEC-2 and podoplanin FRCs maintaining HEV integrity also revealed that lack of lymphocytes prevented the development of bloody muscosal lymph nodes (Herzog et al., 2013). It may be that podoplanin expression on lymphocytes, such as T cells (Peters et al., 2011), could be involved in maintaining the vascular integrity of peritoneal HEVs along with FRC and is resulting in the blood accumulation seen the Vav-iCre.PDPN$^{fl/fl}$ following LPS immune stimulation. Mass transmigration of lymphocytes therefore would be a key part in the loss of vascular integrity and a longer time period of immune stimulus may result in blood filled Peyer's patches within these mice also.

This hypothesis is supported by the lack of blood seen in the peritoneal lavage fluid in the inducible CLEC-2 knockout mice after 24 hours when it's possible that lymphocyte migration to this area may have reduced. There is also persistence of blood accumulation in the Peyer's patches of the inducible CLEC-2 knockout mice after 24 hours where lymphocytes are likely to still be accumulating in order for the immune system to begin to mount an adaptive response to the stimulus.

The platelet specific CLEC-2 knockout mice presented with other signs of an aggravated immune response that were not present in the inducible CLEC-2 knockout mouse model. An increase in

spleen size through the stimulation of erythropoiesis occurs after *Salmonella* infection and is likely to occur following the injection of the gram negative toxin LPS (Jackson et al., 2010). However, platelet specific knockout mice have a significantly larger spleen than their littermate controls after LPS, without any change in the leukocyte populations. This phenotype can be explained by the presence of splenomegaly within untreated PF4-Cre.CLEC-$2^{fl/fl}$ mice which has been shown to be due to an increase in extramedullary haematopoiesis (Nakamura-Ishizu et al., 2015).

The platelet specific CLEC-2 knockout mice showed a significant increase in a wide range of cytokines and chemokines in the peritoneal lavage fluid. The PF4-Cre.CLEC-$2^{fl/fl}$ mice have been shown to have incomplete separation of the blood and lymphatic systems (Finney et al., 2012). This mixing may be causing an inefficiency in the transport of leukocytes through the body and the large increase in cytokine and chemokine signals may be a compensatory mechanism. This hypothesis is supported by the lack of a significant difference in leukocyte recruitment to the peritoneum, spleen or colon. However, the large increase in cytokines and chemokines meant that the mice showed signs of illness at a much earlier stage than their wildtype littermate controls.

The speculation that the PF4-Cre.CLEC-$2^{fl/fl}$ are compensating for blood lymphatic mixing is also supported by the fact that the inducible CLEC-2 knockout mice, whom do not possess this developmental defect, did not show any significant changes in the cytokine and chemokine levels. Interestingly however, both mouse models possess a trend of lower number of neutrophils and monocytes within their peritoneum. The numbers of leukocytes recruited to the peritoneum is

variable and therefore a greater number of mice would need to be examined to test if it would reach a significant difference.

Interestingly, changes in spleen size, chemokine and cytokines level or leukocyte numbers were not seen in Vav-iCre.PDPN$^{fl/fl}$ mice, which means that any possible differences in early leukocyte recruitment is not likely to be due to an interaction of platelet CLEC-2 with a podoplanin expressing leukocyte population such as inflammatory macrophages.

Also, a difference in leukocyte recruitment may only be possible to find following a longer incubation time of immune stimulation or a model which is most useful to examine the adaptive immune response rather than the innate response. The changes in the vascular integrity to lymph nodes caused by a lack of CLEC-2 may possible disrupt the development of adaptive immune response and would be an interesting area for further research.

The results of this chapter indicate a key role for platelet CLEC-2 in maintaining haemostasis following an inflammatory stimulus. The results also show that lack of platelet CLEC-2 from development leads to an over active immune response in these mice. The causes and consequence of the high levels of cytokines and chemokines remain to be investigated.

Chapter 5

The role of platelet CLEC-2 and podoplanin in mouse models of atherosclerosis and inflammatory bowel disease

5.1 Introduction

The data within this chapter focuses on the role of platelet CLEC-2 and its ligand podoplanin in two mouse models of inflammatory disorders: atherosclerosis and colitis. As such I will introduce the information for these sections separately.

5.1.2 Platelet CLEC-2 and Atherosclerosis

Atherosclerosis is a vascular disease in which the artery-wall thickens due to the accumulation of leukocytes and proliferation of intimal smooth muscle cells (Huo and Ley, 2004). Studies into atherosclerosis were initially done by increasing the fat content in the diet of mice. However the lesions that developed within these mice were restricted to the aortic root (Paigen et al., 1985). This discovery lead to development of genetically engineered mouse models which are more susceptible to the development of atherosclerosis. Mice deficient in apolipoprotein ApoE were first generated in 1992 (Plump et al., 1992) and found to spontaneously develop severe atherosclerosis when on a high fat diet similar to human with an ApoE deficiency (Ohashi et al., 2004). ApoE is an important ligand for the uptake of lipoproteins throughout the body and a deficiency leads to the accumulation of cholesterol ester-enriched particles. The role of platelets in atherosclerosis has been studied for over 30 years. They have been shown to be involved in many stages of the disease from initial plaque growth to eventual plaque rupture which can lead to stroke or myocardial infraction (Huo and Ley, 2004).

In recent years there has been a greater appreciation of atherosclerosis as an inflammation driven disorder. Leukocytes such as macrophages, dendritic cells and lymphocytes have all been shown

to accumulate within atherosclerotic plaque and contribute to the pathology of the disease (Swirski and Nahrendorf, 2013). However, platelets are also believed to contribute to inflammation within blood vessel through activation of the endothelium and release of inflammatory mediators (Nording et al., 2015).

Recent work by Dr. Marie Lordkipandize and Dr. Matthew Harrison in the University of Birmingham showed an important involvement of the platelet receptor CLEC-2 in atherogenesis (unpublished). For this study a double knockout mouse model ($ApoE^{-/-}$ x ER^{T2}-Cre.CLEC-$2^{fl/fl}$) was generated. As previously discussed CLEC-2 expression can be deleted from the ER^{T2} Cre model by treatment with tamoxifen following development. These mice were placed on high fat diet for 6 weeks and the development of atherosclerosis were compared to $ApoE^{-/-}$ littermate control. The results of this study revealed that lack of platelet CLEC-2 leads to an increase in the plaque size. Platelet CLEC-2 is therefore protective against the development of atherosclerosis. The results in this chapter show further investigation into the plaques of the double knockout mice compared to $ApoE^{-/-}$ mouse model, in particular the expression of the CLEC-2 ligand podoplanin.

5.1.2 Inflammatory Bowel Disease

Inflammatory bowel diseases (IBD), which includes Ulcerative Colitis and Crohn's disease are chronic inflammatory disorders of the gastrointestinal tract. Mouse models of colitis have been developed in order to study these complex diseases. The results in this chapter focus on the use of dextran sodium sulphate (DSS) to induce an acute model of colitis.

High platelet counts have long been noted as a feature of IBD and have been shown to correlate with disease severity and levels of serum orosomucoid which is a marker of systemic inflammation (Harries et al., 1983, Shah et al., 1989). Platelets are believed to play several roles in the pathogenesis of colitis. For instance, platelets from IBD patients have shown to express high levels of CD40L which upregulates molecules such as vascular adhesion molecule (VCAM)-1, and intercellular cell adhesion molecule (ICAM)-1 on leukocytes thereby increasing adhesion to the intestine (Danese et al., 2003, Danese et al., 2004).

Increased lymphangiogenesis is a common feature in IBD (Rahier et al., 2011). A recent paper focuses on the influence of platelets on lymphangiogenesis in a colitis model (Sato et al., 2016) . The study demonstrated an increase in lymphatic vessels in colon tissue and that inhibiting lymphangiogenesis results in a worsening of the intestinal inflammation. Furthermore, activated platelets within the intestinal muscosa were shown to inhibit lymphangiogenesis. In line with this platelet depleted mice given DSS experienced a reduction in the degree of inflammation in the colon (Sato et al., 2016).

In this chapter I have investigated the role of platelet CLEC-2 in acute colitis using the DSS model using clinical measurements and evaluation of histology including expression of podoplanin.

5.2 Results Part 1: Role of platelet CLEC-2 and its ligand podoplanin in atherosclerosis

5.2.1 Expression of podoplanin in aortic plaques of atherosclerosis prone mice

ApoE$^{-/-}$ mice spontaneously develop plaques on normal diet, while a high fat western diet accelerates the process (Meir and Leitersdorf, 2004). The aortic sinus section from ApoE$^{-/-}$ x ER^{T2}-Cre.CLEC-2$^{fl/fl}$ (generated by from Dr. Matthew Harrison) are from mice who were placed on tamoxifen diet for 2 weeks, followed by 4 weeks of normal diet before being placed on high fat diet for 6 weeks. The ApoE$^{-/-}$ described in this chapter were aged similarly before being placed on high fat diet for 6 weeks.

Figure 5.1 displays immunofluorescent images of the aortic sinus of atherosclerosis prone (ApoE$^{-/-}$) mice and inducible CLEC-2 deficient atherosclerosis prone mice (ApoE$^{-/-}$ ER^{T2}-Cre.CLEC-2$^{fl/fl}$) mice. Plaque areas in both mice models show the presence of podoplanin expressing cells. However, using quantification of the mean fluorescent intensity of the podoplanin signal within the plaques indicates a higher level of expression in ApoE$^{-/-}$ ER^{T2}-Cre.CLEC-2$^{fl/fl}$ mice. There is also evidence to suggest not only a greater intensity but also an increase in the number of cells expressing podoplanin. This result would suggest that platelet CLEC-2 may be playing a role in supressing podoplanin expressing in atherosclerotic plaques.

Figure 5.1

A

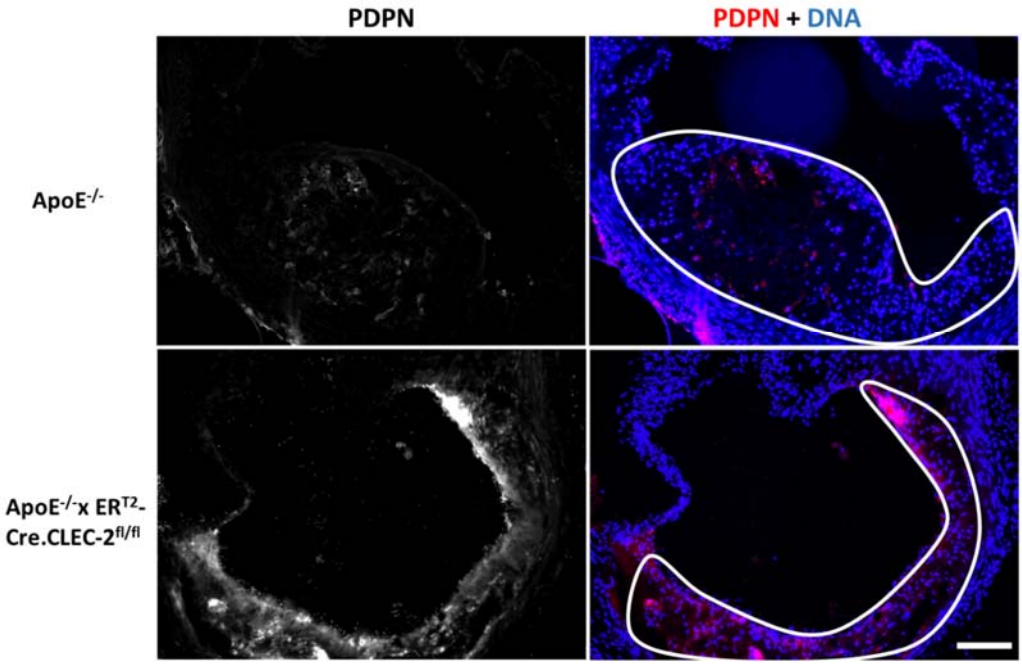

B

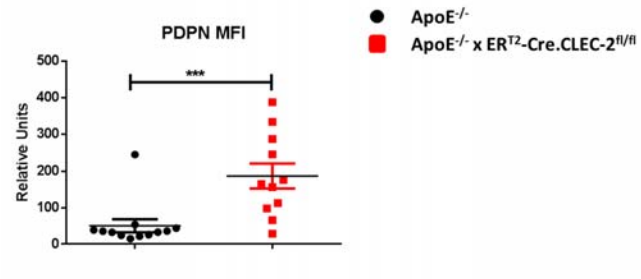

Figure 5.1: Podoplanin expression in the aortic sinus plaques of atherosclerosis prone CLEC-2 sufficient and inducible CLEC-2 deficient mice

A. Representative fluorescent images display podoplanin expression in the aortic sinus plaques of both ApoE$^{-/-}$ and ApoE$^{-/-}$ x ER^{T2}-Cre.CLEC-2$^{fl/fl}$ mice. Outlined white area indicates plaques regions within the image. Representative of 4 mice of each genotype. Scale bar = 100µm.

B. The mean fluorescent intensity of podoplanin within the plaque regions of both ApoE$^{-/-}$ and ApoE$^{-/-}$ x ER^{T2}-Cre.CLEC-2$^{fl/fl}$ mice, calculated using immunofluorescent images. Calculation taken from sections of 4 mice from each genotype. Statistical analysis was preformed using an unpaired t test, ***=p<0.001.

5.2.2 Leukocytes and smooth muscle cells within aortic plaques express podoplanin

Following the discovery of podoplanin within the plaques of both mouse models, we next wanted to investigate what cell types are expressing the CLEC-2 ligand. The aortic plaques of $ApoE^{-/-}$ and $ApoE^{-/-}$ x ER^{T2}-Cre.CLEC-$2^{fl/fl}$ were stained using immunofluorescence with either podoplanin and smooth muscle actin (SMA) or podoplanin and CD45 (Figure 5.2). Smooth muscle actin is a marker for smooth muscle cells and CD45 is a marker for leukocytes (Lai et al., 1998, Hughes and Chan-Ling, 2004). These images show a co-localisation of podoplanin staining with both smooth muscle cells and with leukocytes within the plaques of both mouse models (Figure 5.2B).

Figure 5.2

A

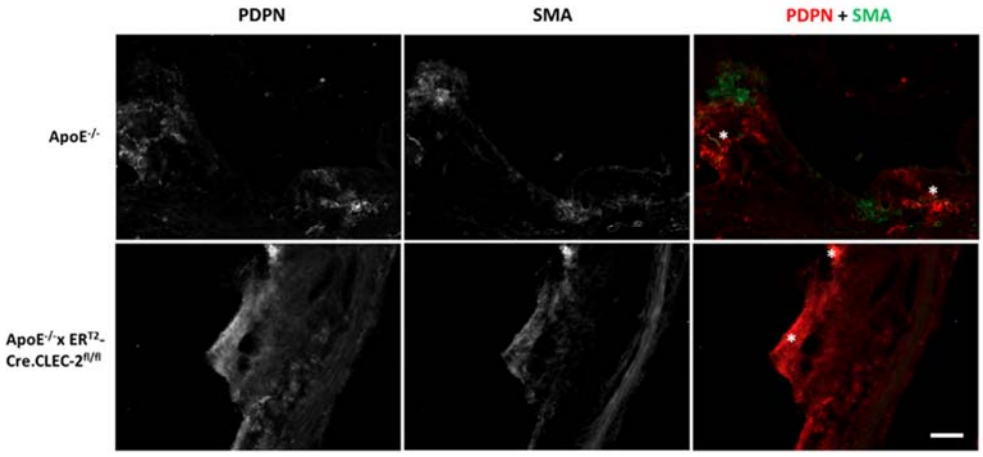

B

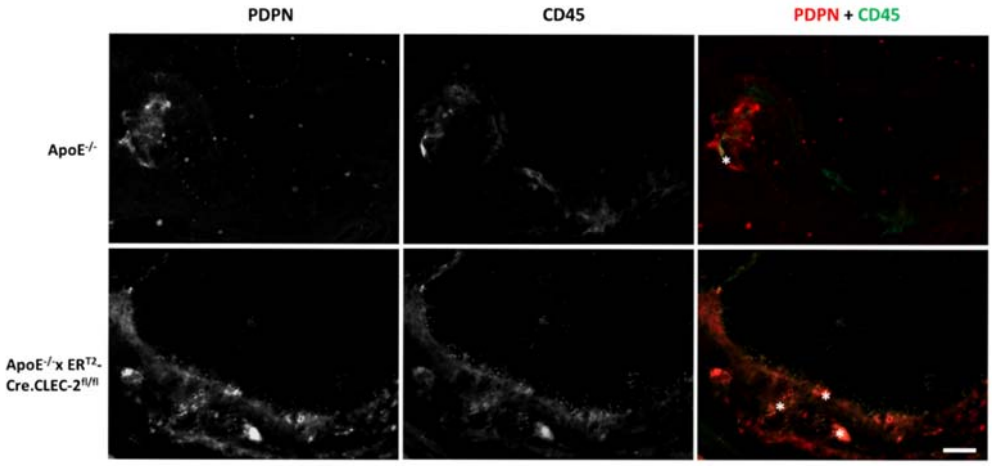

Figure 5.2 Podoplanin co-localisation with smooth muscle cells and leukocytes in aortic sinus plaque regions of atherosclerosis prone mice compared the mice of an inducible CLEC-2 deficient atherosclerosis prone mouse model

A. Representative fluorescent images of podoplanin and smooth muscle actin (SMA) expression within aortic sinus plaques of both ApoE$^{-/-}$ and ApoE$^{-/-}$ x ER^{T2}-Cre.CLEC-2$^{fl/fl}$ mice. White scars indicate areas of co-localisation. Representative of 4 mice of each genotype. Scale bar = 50µm.
B. Representative fluorescent images of podoplanin and CD45 expression within aortic sinus plaques of both ApoE$^{-/-}$ and ApoE$^{-/-}$ x ER^{T2}-Cre.CLEC-2$^{fl/fl}$ mice. White scars indicate areas of co-localisation. Representative of 4 mice of each genotype. Scale bar = 50µm.

5.2.3 No significant difference in podoplanin mRNA levels in the aortic arch of atherosclerosis prone mice, inducible CLEC-2 deficient mice or podoplanin haematopoietic specific deficient mice compared to wild type mice.

Podoplanin mRNA levels were measured in the aortic arches of wildtype mice (C57BL/6) and $ApoE^{-/-}$ mice on a high fat diet. The mRNA levels in an inducible CLEC-2 deficient mice ($ER^{T2}Cre.CLEC\text{-}2^{fl/fl}$) and podoplanin haematopoietic lineage specific deficient mice (Vav-iCre.$PDPN^{fl/fl}$) on normal diet were also measured. The mRNA levels from $ApoE^{-/-}$, $ER^{T2}Cre.CLEC\text{-}2^{fl/fl}$ and Vav-iCre.$PDPN^{fl/fl}$ mice were then normalised to the levels measured in C57BL/6 mice to investigate if there was any significant fold change. No significant difference was found between any of the mouse models tested.

Figure 5.3

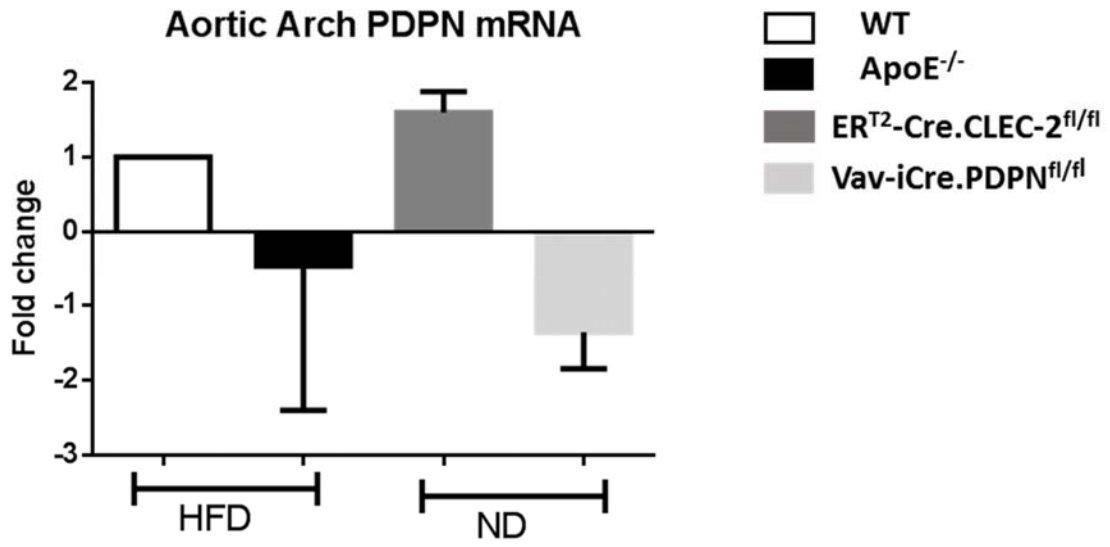

Figure 5.3: Fold changed difference in podoplanin mRNA level within the aortic arch

Graph displays podoplanin mRNA levels in the aortic arch of $ApoE^{-/-}$, ER^{T2}-Cre.CLEC-$2^{fl/fl}$ and Vav-iCre.$PDPN^{fl/fl}$ mice compared to wildtype (C57BL/6) mice. Data representative of 5 WT and $ApoE^{-/-}$ mice and 2 ER^{T2}-Cre.CLEC-$2^{fl/fl}$ and Vav-iCre.$PDPN^{fl/fl}$ mice. HFD= mice given high fat diet for 6 weeks. ND=normal diet. Fold change in podoplanin mRNA levels was calculated using the 2ΔΔCT method detailed in Chapter 2. Statistical analysis was performed using a one way ANOVA followed by a Tukey multiple comparison test.

5.3 Results Part 2: Role of platelet CLEC-2 and its ligand podoplanin in Colitis

5.3.1 DSS treated inducible CLEC-2 deficient mice have a significantly worse clinical score compared to littermate controls.

Dextran sodium sulphate (DSS) induces colitis in mice. The compound has a highly negative charge and is believed to be toxic to the colonic epithelium. Over time it compromises the epithelial barrier integrity in the colon and increases inflammation within the tissue (Chassaing et al., 2014). CLEC-2 inducible knockout mice (ER^{T2}-Cre.CLEC-$2^{fl/fl}$) and their littermate controls (CLEC-$2^{fl/fl}$) both received tamoxifen diet for 2 weeks before being placed on normal diet for 4 week and this was followed by exposure to 6 days of water containing 3% dextran sodium sulphate (DSS). The length and dose of DSS given is known to induce an acute form of colitis (Chassaing et al., 2014).

The clinical signs of colitis of these mice were then monitored daily and scored as described in Figure 5.4A. The weight loss and appearance of the knockout mice did not significantly differ from their littermate controls (not shown). The bleeding score, as measured by a haemocult kit, and stool consistency however was significantly worse in the inducible CLEC-2 knockout mice compared to littermate controls by day 6 (Figure 5.4B). All of the measurements taken together also show a significantly worse difference in in the inducible CLEC-2 knockout mice compared to littermate controls by day 6 indicating that lack of platelet CLEC-2 leads to a worsening of the colitis phenotype in DSS treated mice.

Figure 5.4

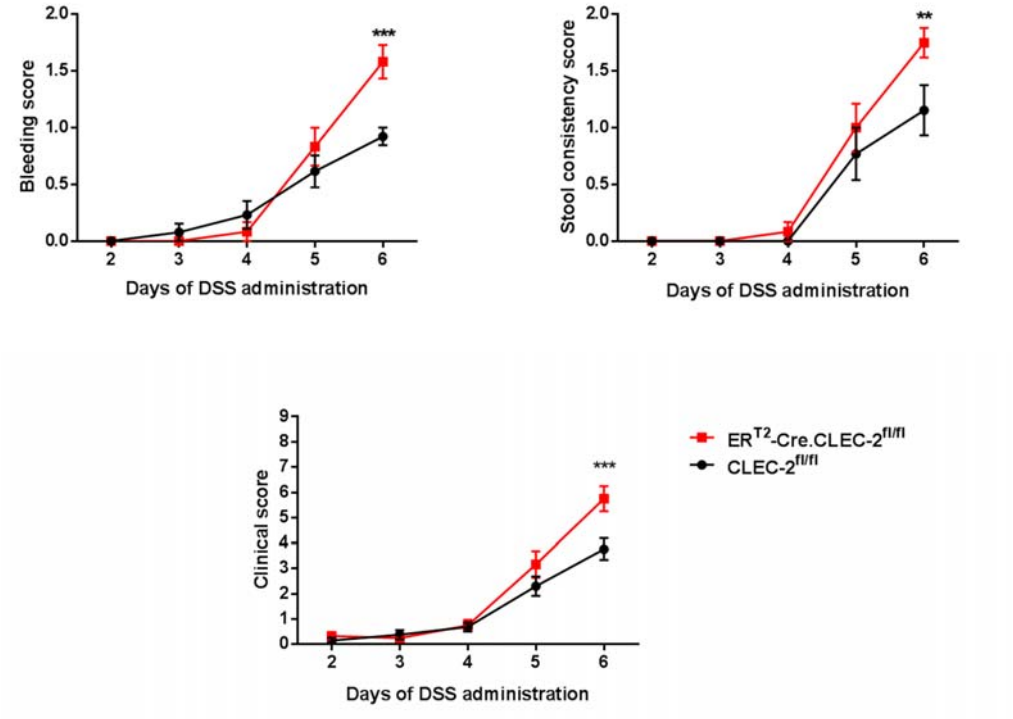

Figure 5.4: Clinical score comparison between an inducible CLEC-2 knockout model and littermate controls over the course of 6 days of DSS administration.

ER^{T2}-Cre.CLEC-2$^{fl/fl}$ and CLEC-2$^{fl/fl}$ littermate controls were exposed to 6 days of water containing 3% dextran sodium sulphate (DSS). Clinical signs of weight loss, appearance, stool consistency and blood loss were monitored. The graphs above display the clinical attributes which showed significant differences in the inducible CLEC-2 knockout mice. Overall clinical score, incorporating all clinical signs measured is also shown. Statistical analysis was performed using a two way ANOVA followed by a Bonferroni multiple comparison test **= $p<0.01$, *** = $p<0.001$, n=8 for each genotype. This work was done by Dr. Siân Lax.

5.3.2 DSS treated inducible CLEC-2 deficient mice have a significantly worse colon histological score compared to littermate controls

The colons from inducible CLEC-2 knockout mice (ER^{T2}-Cre.CLEC-$2^{fl/fl}$) and their littermate controls (CLEC-$2^{fl/fl}$) were sectioned and stained using haemotocylin and eosin (H&E) following 6 days exposure to water containing 3% dextran sodium sulphate (DSS) (Figure 5.5A). These sections were then scored blinding using a method described in Chapter 2 with results shown in Figure 5.5B. Colons from both the knockout mice and the littermate controls display evidence of colitis but the overall histological score was significantly worse in the inducible CLEC-2 deficient mice. Taking the individual soring parameters, there was a significantly worse crypt damage score in the inducible CLEC-2 knockout mice compared to littermate control. This finding correlates with the result seen in the clinical scoring indicating that lack of platelet CLEC-2 leads to a worsening of the colitis phenotype in DSS treated mice (Figure 5.5C).

Figure 5.5

A

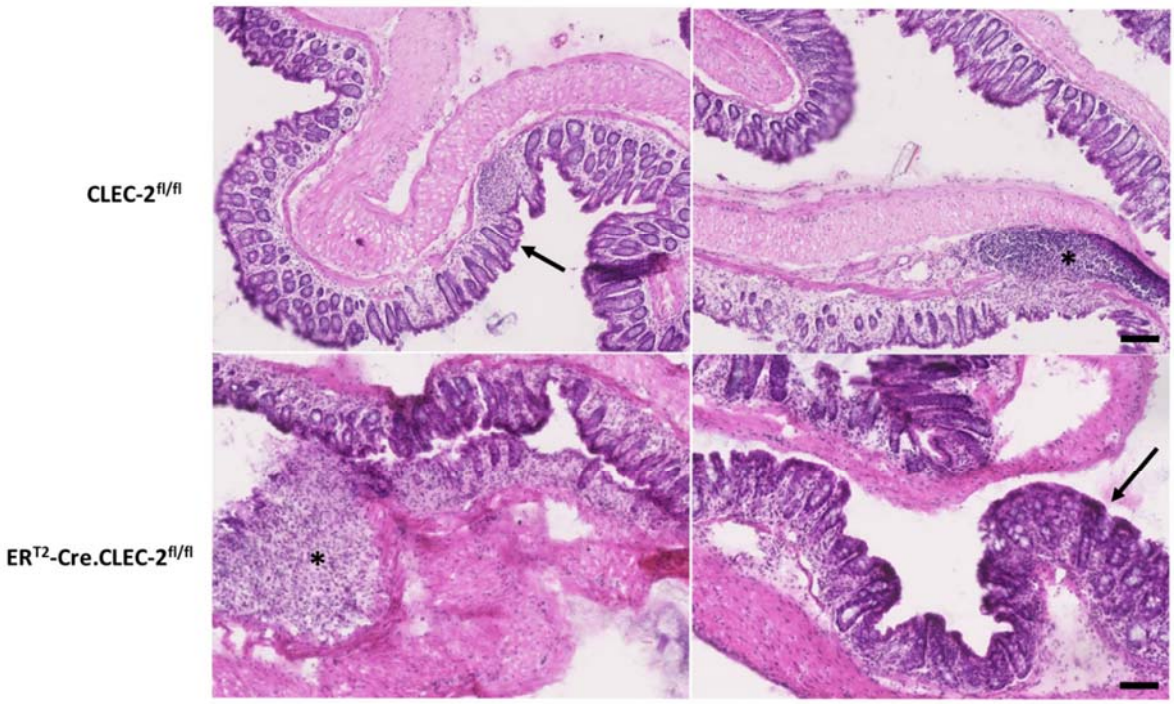
CLEC-2fl/fl
ERT2-Cre.CLEC-2fl/fl

B

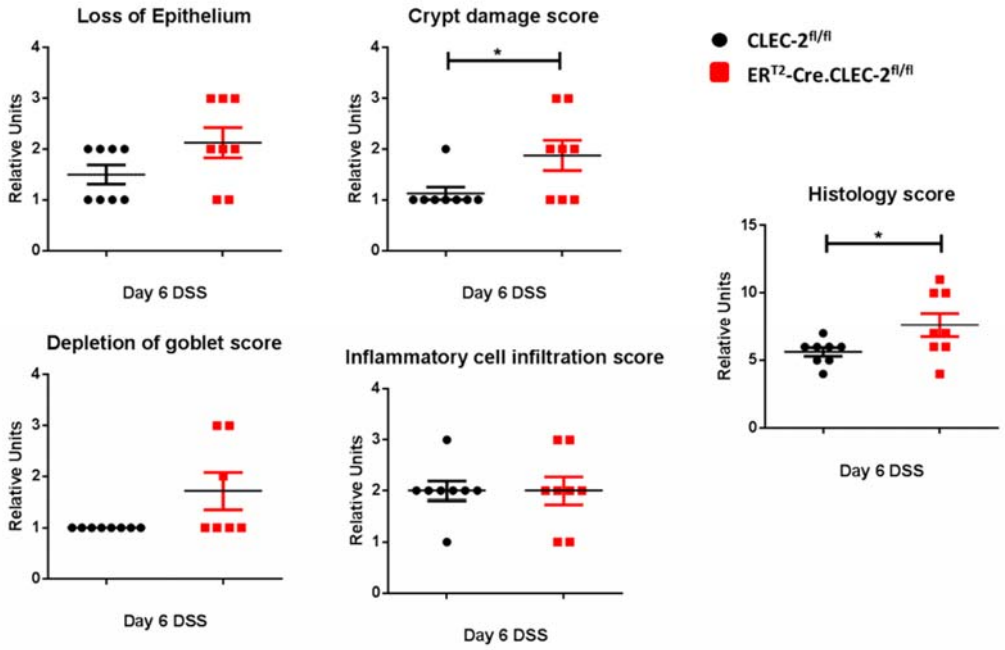
Loss of Epithelium
Crypt damage score
CLEC-2fl/fl
ERT2-Cre.CLEC-2fl/fl
Histology score
Depletion of goblet score
Inflammatory cell infiltration score
Relative Units
Day 6 DSS

Figure 5.5: Histological comparison of the colons of an inducible CLEC-2 knockout model and littermate controls following 6 days of DSS administration.

A. Haematoxylin and Eosin (H+E) images of ER^{T2}-Cre.CLEC-$2^{fl/fl}$ and CLEC-$2^{fl/fl}$ littermate controls following 6 days of DSS administration. Black asterisk points to area of inflammatory cell infiltration and arrows point to goblet depletion and crypt damage.
B. Graphs displays the scoring of H+E images from the colons of these mice (8 mice of each genotype). Statistical analysis was performed using an unpaired t test *= $p<0.05$. Scoring was performed blindly by Dr. Siân Lax.

5.3.3 Podoplanin is expressed in DSS treated colons but not in untreated colons

Colons from untreated and DSS treated inducible CLEC-2 deficient mice (ER^{T2}-Cre.CLEC-$2^{fl/fl}$) and their littermate controls (CLEC-$2^{fl/fl}$) were sectioned and stained for podoplanin expression. Figure 5.2 shows that without DSS treated the colons of both CLEC-2 deficient mice and littermate controls do not show any podoplanin expression. However, following 6 days of DSS treatment both genotypes show a pattern a similar increase and podoplanin expression. This result correlates with previous findings of podoplanin expression within the colon of colitis patients (Geleff et al., 2003).

Figure 5.6

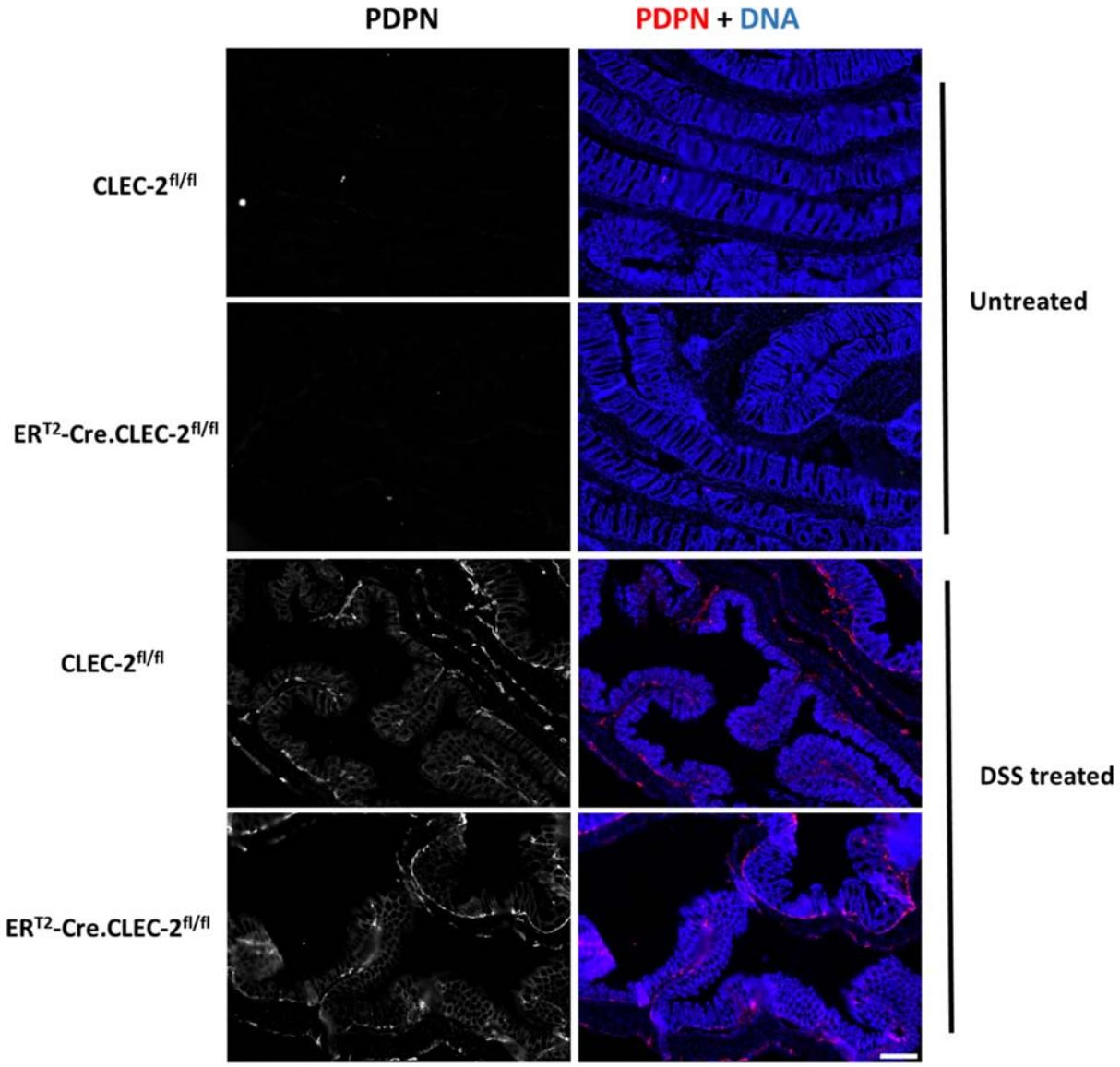

Figure 5.6: Podoplanin expression in the colon of untreated and DSS treated mice comparing inducible CLEC-2 knockout and littermate control mice.

Representative images from the colons of untreated and DSS treated ER^{T2}-Cre.CLEC-$2^{fl/fl}$ and CLEC-$2^{fl/fl}$ littermate controls. Untreated images are representative of 4 mice and DSS images are representative of 8 mice from each genotype. Scale bar = 200µm.

5.3.4 Podoplanin expression on lymphatic vessels and epithelial cells of the colon in DSS treated mice

Following the discovery of podoplanin expression within the colons of DSS treated mice, we wanted to investigate the cell types expressing podoplanin. Figure 5.7A shows immunofluorescent images of podoplanin co-stained with the lymphatic endothelial cell marker lyve-1 (Podgrabinska et al., 2002). The images demonstrate clear co-localisation of podoplanin with lyve-1. Flow cytometry staining also reveals that there is a significant decrease in the median fluorescent intensity of podoplanin on the lymphatic endothelial cells in the colons of DSS treated inducible CLEC-2 knockout mice (ER^{T2}-Cre.CLEC-$2^{fl/fl}$) compared to their littermate controls (CLEC-$2^{fl/fl}$). Podoplanin staining was also found in the untreated colons by flow cytometry but the median fluorescent intensity was low and not significantly different between the inducible CLEC-2 knockout mice and littermate controls. Interestingly there was also a significant decrease in the LEC:BEC ratio of the DSS treated inducible CLEC-2 deficient mice compared to littermate controls highlighting a possible difference in the number of lymphatic vessels in these mice.

Figure 5.8A shows immunofluorescent images of podoplanin co-stained with epithelial cell staining using EpCAM on the colons of DSS treated mice (Trzpis et al., 2007). These images show no apparent co-localisation of podoplanin staining with epithelial cells. However, flow cytometry analysis of the colon revealed that there is weak podoplanin expression on the epithelial cells of DSS treated mice and that there is a significant decrease in the median fluorescent intensity of podoplanin on epithelial cells in the colons of DSS treated inducible CLEC-2 knockout mice (ER^{T2}-Cre.CLEC-$2^{fl/fl}$) compared to littermate control (Figure 5.8B).

Figure 5.7

A

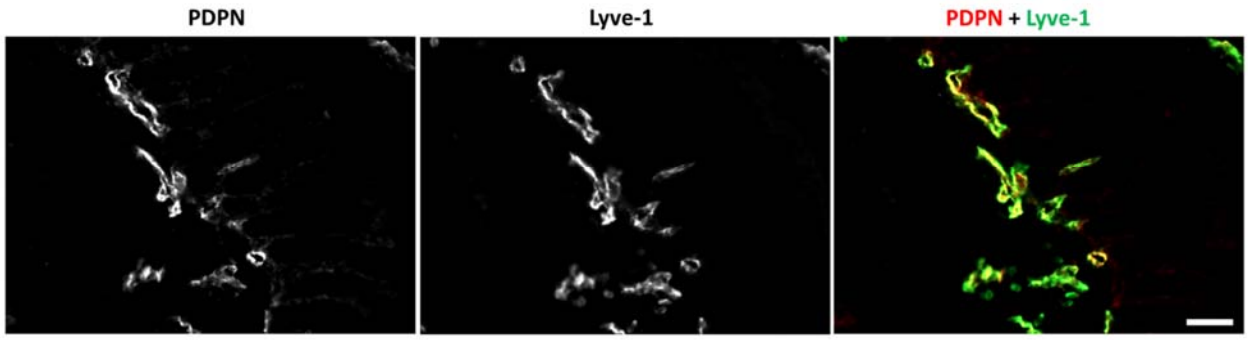

B

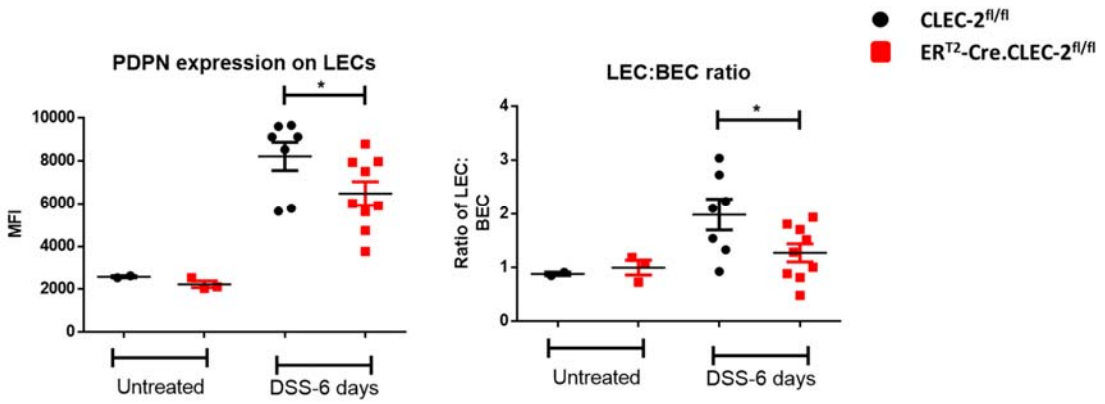

Figure 5.7: Podoplanin expression on lymphatic endothelial cells in the colons of untreated and DSS treated mice of an inducible CLEC-2 knockout mouse model and littermate controls

A. Representative images of podoplanin and lyve-1 co-localisation within the colons of DSS treated mice. Scale bar = 50µm.

B. Podoplanin median fluorescent intensity on lymphatic endothelial cells (LECs) and ratio of LECs to blood endothelial cells (BECs) within the colons treated and untreated ER^{T2}-Cre.CLEC-$2^{fl/fl}$ and CLEC-$2^{fl/fl}$ littermate controls analysed by flow cytometry. Statistical analysis was performed using an unpaired t test *= $p<0.05$. Flow cytometry analysis performed by Dr. Siân Lax.

Figure 5.8

A:

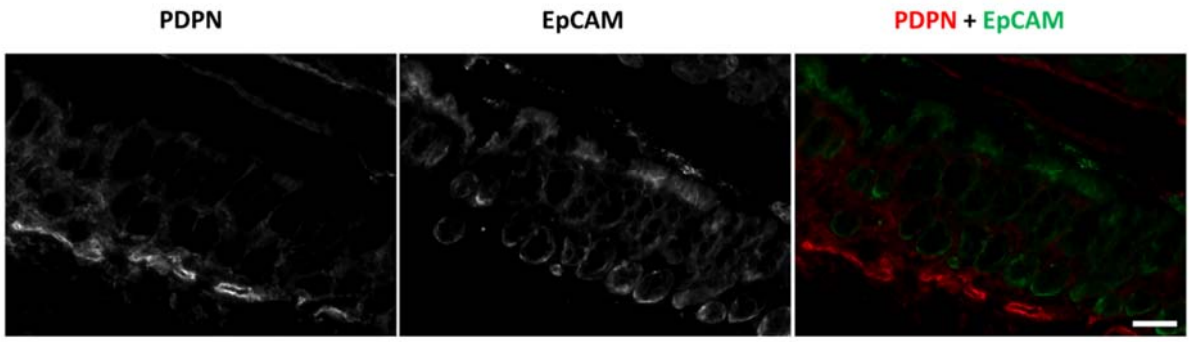

B:

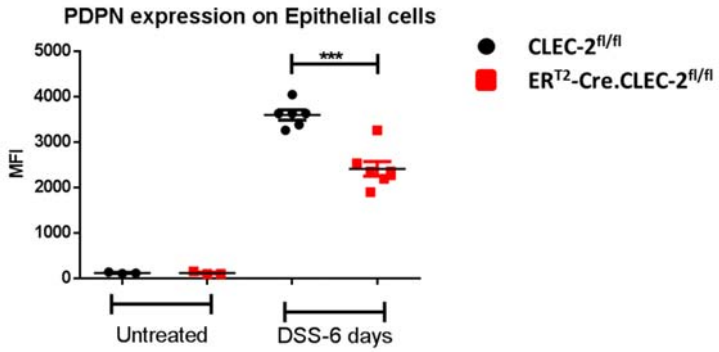

Figure 5.8: Podoplanin expression on epithelial cells in the colons of untreated and DSS treated mice of an inducible CLEC-2 knockout mouse model and littermate controls

A. Representative images of podoplanin and EpCAM within the colons of DSS treated mice. Podoplanin does not appear to co-localise within these images. Scale bar = 50µm.

B. Podoplanin median fluorescent intensity on epithelial cells within the colons treated and untreated ER^{T2}-Cre.CLEC-$2^{fl/fl}$ and CLEC-$2^{fl/fl}$ littermate controls analysed by flow cytometry. Statistical analysis was performed using an unpaired t test *= $p<0.05$. Flow cytometry analysis performed by Dr. Siân Lax.

5.4 Discussion

The results presented in this chapter support a role of platelet CLEC-2 in mouse models of both atherosclerosis and colitis. In both inflammatory models, a lack of platelet CLEC-2 results in a more detrimental phenotype. The inducible CLEC-2 deficient model was used to ensure that any differences seen were not due to the development defects seen in the platelet specific CLEC-2 knockout mouse model. In the case of the atherosclerosis model, a lack of platelet resulted in larger atherosclerotic plaques (Dr. Marie Lordkipanidze and Dr. Matthew Harrison unpublished) and podoplanin expression was increased in aortic plaques of CLEC-2 deficient atherosclerosis prone mice compared to CLEC-2 sufficient atherosclerosis prone mice. In the case of a colitis model, a lack of CLEC-2 results in a worse clinical score in the mice and the histology of the colon was also scored and seen to be significantly worse. Podoplanin expression was increased within the colon tissue of DSS treated mice, but the levels of expression on the lymphatic endothelial cells and epithelial cells of CLEC-2 deficient mice were significantly lower than their wildtype floxed counterparts.

Many research studies have demonstrated the role of platelets in contributing both to the development of atherosclerosis and as the cause of potential mortality through plaque rupture (Nording et al., 2015, Badimon and Vilahur, 2014). However recent unpublished work (Lordkipanidze and Harrison) has demonstrated that platelet CLEC-2 plays a protective role in the development of atherosclerosis in mice. The platelet CLEC-2 ligand podoplanin has been previously reported to be expressed in the plaques localised in the abdominal aorta of human patients (Hatakeyama et al., 2012). This study found that podoplanin was expressed on smooth

muscle cells and leukocytes within the plaques. Podoplanin mRNA levels were the lowest in areas of diffuse intimal thickening (DIT) which characterise the initial stages of atherosclerosis development whereas advanced lesions showed the highest mRNA levels (Hatakeyama et al., 2012).

Podoplanin expression on synovial fibroblasts has been shown to contribute to inflammation in synovial joints through an interaction with platelet CLEC-2 which results in an upregulation of cytokine IL-6 and IL-8 (Del Rey et al., 2014). The high level of podoplanin expression seen in the aortic sinus plaques of CLEC-2 deficient atherosclerosis prone mice, and in advanced atherosclerotic human lesions, leads us to speculate that podoplanin within the plaques also contributes to the inflammatory environment of plaques. Podoplanin is expressed on the plaques of both inducible CLEC-2 deficient and CLEC-2 sufficient atherosclerosis prone mice, where it is found on leukocytes and smooth muscle cells. There are also other cells types within the plaques which are expressing podoplanin which remain to be discovered. Unfortunately, the podoplanin mRNA levels within the aortic arch of inducible CLEC-2 deficient atherosclerosis prone mice could not be tested and no significant differences were found in podoplanin mRNA levels between wildtype or $ApoE^{-/-}$ mice on high fat diet or in the ER^{T2}-Cre.CLEC-$2^{fl/fl}$ and Vav-iCre.$PDPN^{fl/fl}$ mice on a normal diet which were used as negative controls.

Taking these results together, they are suggestive of platelet CLEC-2 playing a protective role in atherosclerosis. The increase of podoplanin expression in mice lacking platelet CLEC-2 suggest raises the possibility that podoplanin may contribute to the growth of atherosclerotic plaques although the basis of this remains to be established. Further investigation into how platelet CLEC-

2 influences podoplanin expression on leukocytes and smooth muscle in plaques and how expression of this glycoprotein leads to more advanced atherosclerosis will be an interesting area of further research.

Platelet CLEC-2 is also shown in this chapter to be protective in an acute model of ulcerative colitis. The model demonstrated that a lack of CLEC-2 leads to a worse clinical outcome, predominantly due to an increase in bleeding in stool samples. This result points to involvement of CLEC-2 in maintaining vascular integrity following an immune stimulus, which has been previously shown (Boulaftali et al., 2013). The histology of the colon of the inducible CLEC-2 deficient mice was also worse than their wildtype littermates. The damage seen to the histology of the colon may be a contributing factor to the higher bleeding score and stool consistency of these mice.

Studying the expression of podoplanin within the colon of DSS treated mice revealed that it is expressed at a high level on LECs. The expression on LECs was also confirmed by flow cytometry which revealed upregulation of podoplanin in both CLEC-$2^{fl/fl}$ and ER^{T2}-Cre.CLEC-$2^{fl/fl}$ mice following treatment with DSS. There was also an increase in LEC:BEC ratio in both mice following treatment with DSS which suggests an increase in lymphangiogenesis. An increase in lymphangiogenesis has been reported previously in mouse models of IBD and evidence of an increase has been found in human samples of IBD (Rahier et al., 2011, D'Alessio et al., 2014). It is thought that the increase in lymphatic vessels aids the resolution of inflammation by providing both bacterial antigens and immune cells a route of exit from the colon tissue (D'Alessio et al., 2014). Interestingly however, both podoplanin expression on LECs and the LEC:BEC ratio in the

inducible CLEC-2 deficient mice is significantly lower than their littermate controls. This results suggests that platelet CLEC-2 is involved in the process of lymphangiogenesis in the colon following the induction of colitis.

A recent paper demonstrated that platelet reduction in mice leads to a less severe DSS initiated colitis phenotype. The study presented evidence that platelets lead to an increase in lymphangiogenesis which can help in the resolution of inflammation in the muscosal layer of the colon as previously discussed (Sato et al., 2016). Work done in our lab by Finney et el demonstrated that migration of LECs and lymphatic vessel formation is reduced in the presence of platelets (Finney et al., 2012). Interestingly, the inhibition of transmigration and lymphatic vessel formation also occurred in the presence of CLEC-2 deficient platelets, albeit to a lesser extent. Our data would suggest that CLEC-2 on platelets acts to reduce lymphangiogenesis, possibly through the interaction with podoplanin expressing LECs, which in turn aggravates the inflammatory phenotype *in vivo* in the colitis mouse model. Human podoplanin expressing monocytes have also been suggested to increase lymphangiogenesis; however there was no significant expression of podoplanin on monocytes in our mouse model (Hur et al., 2014).

Evidence of podoplanin expression was also found on colon epithelial cells by flow cytometry. It is unclear why this was not seen by immunofluorescence but it may be due to levels of podoplanin expression being lower in comparison to lymphatic endothelial cells and therefore difficult to distinguish using this technique. Using the result from flow cytometry the upregulation of podoplanin on epithelial cells within the colons of DSS treated inducible CLEC-2 deficient mice was significantly lower than that in littermate controls. Podoplanin is believed to be involved in

maintaining the shape of glomerular epithelial cells and been shown to change the shape of keratinocytes in which its expressed (Gandarillas et al., 1997, Matsui et al., 1998). The lower level of podoplanin on epithelial cells may be an influencing factor changing the morphology of colon epithelial cells and causing the damage to the colons that is seen in DSS treated inducible CLEC-2 deficient mice. However, this is purely speculative and needs further investigation.

Previous work has also found evidence of CLEC-2 expression in the mucosa of the colon which was shown to suppress tumour progression and invasiveness (Wang et al., 2016). It is possible that CLEC-2 expression on colon epithelial cells is being removed in the inducible CLEC-2 deficient mice after two weeks of tamoxifen diet; however this was not investigated at the time. Podoplanin and CLEC-2 may therefore may be co-expressed on epithelial cells or be interacting with each other on different types of epithelial cells and a lack of CLEC-2 on these cells may be influencing the colitis phenotype. It has been shown that platelet can be activated by DSS specifically through the hemITAM receptor CLEC-2 and the ITAM receptor GPVI (Alshehri et al., 2015). The lack of platelet CLEC-2 may be influencing the level of platelet activation over the course of DSS treatment given to the mice and contributing to the clinical worse phenotype seen in these mice.

In conclusion, evidence from an atherosclerosis and colitis mouse models suggests the involvement of platelet CLEC-2 in both diseases. Lack of platelet CLEC-2 leads to the upregulation of podoplanin within atherosclerotic plaques in comparison to a platelet CLEC-2 expressing counterpart whereas lack of platelet CLEC-2 in a colitis mouse model leads a lesser degree of podoplanin upregulation in colon tissue in comparison to littermate controls. However, in both

cases lack of platelet CLEC-2 results in a worsening in the pathology of the diseases and is likely causing an increase in the inflammatory status. Further investigation into the influence of platelet CLEC-2 into inflammation and how it may be influencing podoplanin expression in different type of inflammatory diseases is an area which needs further investment and research

Chapter 6

General Discussion

6.1 Summary of Results:

I have shown that mouse podoplanin is an adhesion receptor, through its interaction with mouse platelet CLEC-2, under conditions of high shear stress. Using an *in vitro* flow model, I have shown that platelet aggregation occurs at arterial shear rates and that it follows a similar pattern of platelet activation and aggregation as classical haemostasis, involving integrin αIIbβ3, GPIbα and $P2Y_{12}$. The affinity of interaction between mouse podoplanin and CLEC-2 is in the nanomolar range (10-15nM) which is three orders of magnitude greater than between human podoplanin and CLEC-2 and is in the range expected for an adhesion receptor.

Using a mouse model of acute sterile inflammation, I have shown that lack of platelet CLEC-2 from inception results in an enhanced response that leads to increased levels of cytokine and chemokines in the peritoneum of the mice. The increase did not impact immune cell recruitment to the peritoneum, spleen or colon of these mice. The same increase was not found in mice in which CLEC-2 is depleted following development suggesting that it is secondary to the developmental changes rather than loss of CLEC-2 on platelets. A previous study has shown that CLEC-2 is also expressed by a subset of activated dendritic cells and neutrophils and that B cells express exogenously derived CLEC-2 which is lost upon entry into lymph nodes (Lowe et al., 2015b). Leukocytes expressing CLEC-2 may also be contributing to the phenotype seen in the PF4-Cre.CLEC-$2^{fl/fl}$ as studies have shown a fraction of CD45 positive cells undergo recombination in this transgenic mouse model (Pertuy et al., 2015).

Blood accumulation was found in the peritoneum and Peyer's patches of both mouse models, consistent with a role for platelet CLEC-2 in maintaining vascular integrity following an inflammatory reaction as previously shown (Boulaftali et al., 2014, Herzog et al., 2013). Blood accumulation was also found in the peritoneum of haematopoietic specific podoplanin deficient mice suggesting that the role of CLEC-2 in vascular integrity is mediated through its interaction with podoplanin expressing leukocytes. A loss in vascular integrity does not occur in the Peyer's patches of the haematopoietic specific podoplanin deficient mice likely since podoplanin is still expressed by FRCs which is critical in maintaining HEV vascular integrity (Herzog et al., 2013).

I also investigated the influence of platelet CLEC-2 on a non-sterile form of acute inflammation, namely DSS induced colitis. The absence of CLEC-2 results in a more severe clinical phenotype in mice. Following the induction of colitis there is an increase in podoplanin expression in the colons of mice. The increase is seen in both lymphatic endothelial cells (LECs) and epithelial cells. However, there is a significantly lower increase in podoplanin expression in both cells types in the colons of platelet CLEC-2 deficient mice.

In the case of a chronic form of vascular inflammation, namely atherosclerosis, it was previously shown that platelet CLEC-2 caused an increased in plaque size. My work demonstrated that podoplanin is expressed within the plaque of atheroprone mice but there is a significantly greater increase in podoplanin expression in the plaques of platelet CLEC-2 deficient mice. A summary of the results for three mouse models examined can been seen in Figure 6.1.

Figure 6.1: Role of Platelet CLEC-2 in inflammatory disorders

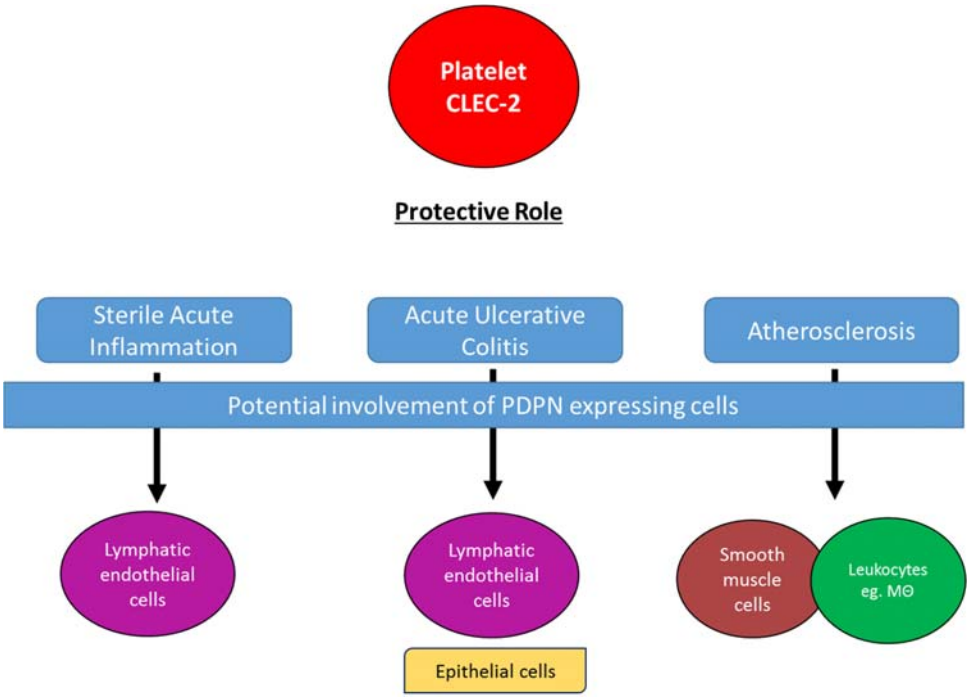

Figure 6.1: Role of Platelet CLEC-2 in inflammatory disorders

The results presented in this thesis demonstrate that platelet CLEC-2 plays a protective biological role in the development of acute and chronic inflammatory disorders. The mechanisms through which it protects the body against inflammatory is not yet clear. There is evidence that podoplanin is involved in the process but the cell expressing the CLEC-2 ligand varies depending on the condition.

6.2 Podoplanin and CLEC-2 interaction in specialised vascular beds

Previous work has shown that a lack of platelet CLEC-2, or podoplanin on the developing neuroepithelium causes the appearance of brain haemorrhages in a developing mouse embryo (Lowe et al., 2015a). It was hypothesised that platelet aggregation through the interaction of CLEC-2 and podoplanin was necessary for the normal development of the cerebral vasculature. Data presented in this thesis demonstrates that mouse podoplanin causes platelet aggregation, dependant interaction with platelet CLEC-2, under arterial rates of shear which are likely to be present in the developing brain (Wang et al., 1992, Rovainen et al., 1992). It is also likely that high shear rates exist in the developing human brain.

The impact that podoplanin has on platelet aggregation under high shear rates may also impact metastasis in podoplanin expressing tumours. Post development podoplanin expression in the brain becomes restricted to the choroid plexus. However it has been shown that podoplanin becomes upregulated in patients with glioblastoma and affects tumour cell migration and therefore development of secondary metastasis (Grau et al., 2015, Peterziel et al., 2012). Patients with primary and metastatic brains tumours are known to be particularly highly predisposed to thromboembolism and many are treated with antiplatelet therapies to prevent this complication from occurring (Gerber et al., 2006). It is possible that these migrating podoplanin expressing tumour cells are effecting the coagulable state of these patients through interaction with platelet CLEC-2 priming the platelets for activation.

Interestingly however this interaction may have more importance in mice than in humans, as the affinity of the interaction is much higher. Previous work using the same *in vitro* flow system described in this thesis revealed that recombinant human podoplanin causes human platelet aggregation solely at venous shear rates. Human lymphatic endothelial cells which express podoplanin also cause platelet aggregation at venous but not arterial shear rates (Navarro-Nunez et al., 2015). This discovery correlates with the binding affinity reported for human CLEC-2 and podoplanin which was found to be 24.5 +/- 3.7 μM (Christou et al., 2008). These results together may indicate that other, as yet undiscovered, CLEC-2 ligands are involved in the platelet aggregation needed during cerebrovasculature development. It could also mean that the mechanisms behind human and mouse cerebrovasculature development differ significantly and it does not rely on platelet aggregation.

The clear difference in the affinity between the mouse forms of CLEC-2 and podoplanin and the human forms of the proteins also has implications for the interpretation of mouse models looking at the involvement of podoplanin and CLEC-2 in homeostasis and disease. As well as cerebrovasculature development, CLEC-2 and podoplanin interaction has an accepted role in mouse lymphatic system development (Finney et al., 2012, Bertozzi et al., 2010, Uhrin et al., 2010, Suzuki-Inoue et al., 2010). However, the difference in the affinity may mean that CLEC-2 and podoplanin does not have the same importance in the development of the human lymphatic system and may involve other CLEC-2 ligands that exist in humans but not mice. Mouse models have also been used to show an involvement of podoplanin and CLEC-2 in diseases such as rheumatoid arthritis and cancer as well as colitis and atherosclerosis discussed in this thesis. In

studying these diseases using mouse models, it is hoped that the results can be extrapolated to human disease and be possible later targets for treatment. However, knowing that the strength of interaction between human CLEC-2 and podoplanin is weaker than in mice bring into question the validity of mouse models in studying the involvement of this receptor-ligand pair in human disease.

6.3 Platelet CLEC-2 and inflammation

It is now widely accepted that platelet function goes far beyond their role in 'haemostatic plug' formation and these anucleate cells have biological roles in areas such as embryonic development and in the functioning of the immune system (Ware et al., 2013). Platelet CLEC-2 has been shown in studies to impact blood-lymphatic development (Finney et al., 2012), brain development (Lowe et al., 2015a), and vascular integrity following an immune stimulus (Bertozzi et al., 2010, Herzog et al., 2013) as well as an involvement in the pathogenesis of inflammatory diseases such as rheumatoid arthritis (Del Rey et al., 2014). The data presented in this thesis suggests that platelet CLEC-2 is intimately involvement in directing platelet activity during both acute and chronic inflammation in particular in colitis and atherosclerosis (Figure 6.1).

Mice lacking platelet CLEC-2 from inception have an over responsive immune reaction in response to a sterile inflammatory stimulus i.e. LPS induced peritonitis. The significantly higher cytokine and chemokine levels may be a compensatory mechanism due to the presence of blood-lymphatic mixing which impedes the transport or effectiveness of cytokines and chemokines released to protect the body against the threat of systemic infection. This result emphasises

importance of platelet CLEC-2 in lymphatic development. The absence of CLEC-2 during development therefore impinges on the functionality of the immune system which heavily relies on a fully separated lymphatic system.

Platelet CLEC-2 is shown in this thesis to be protective in an acute form of colitis. The results in this thesis suggest that platelet CLEC-2 prevents excessive bleeding and helps to maintain healthy colon tissue structure. In contrast, a recent study has found that platelets have been shown to aggravate colitis through the suppression of lymphangiogenesis (Sato et al., 2016). A lack of CLEC-2 resulted in a decrease in lymphangiogenesis, as seen by the lower LEC:BEC ratio in these mice which suggest that platelet CLEC-2 is protective by increasing lymph vessels within the colon. Higher podoplanin expression is often co-insides with an increase in lymphangiogenesis in both colitis and cancer (Geleff et al., 2003, Jankowska-Konsur et al., 2016). The lower levels of podoplanin expressing LECs in CLEC-2 deficient mice therefore agree with the hypothesis that platelet CLEC-2 influences lymph vessel growth. The lack of CLEC-2 is therefore likely resulting in a more severe phenotype due to less lymph vessel growth in the colon necessary to traffic the leukocytes away from the inflamed tissue. Additionally there is increased bleeding in the tissue further perpetuating the severity of the disease.

Platelet CLEC-2 has also been shown to be protective in a mouse model of atherosclerosis (Dr. Marie Lordkipandize and Dr. Matthew Harrison unpublished). The exact mechanism as to how platelet CLEC-2 is protective in atherosclerosis is unclear. Platelets are generally believed to be detrimental in atherogenesis by contributing to the inflammatory environment (Nording et al., 2015), but platelet CLEC-2 seems to have prevent the growth of plaques. A lack of CLEC-2 seem

to result in an increase in podoplanin expression within the plaques of mice. It is possible that platelet CLEC-2, directly or indirectly, prevents an increase in podoplanin expression on leukocytes and other cells which are recruited to a plaque. How exactly podoplanin may be contributing to the growth of plaques is unknown but it could be linked with the shape or movement of the cells in the plaques, as podoplanin is believed to communicate with the cell's cytoskeleton (Martin-Villar et al., 2006).

In both models therefore, platelet CLEC-2 is having the opposite effect in the disease compared to the effect of platelets as a whole. Further investigation into how platelet CLEC-2 is effecting platelet behaviour and the influence of platelets in disease is warranted. In both cases a lack of platelet CLEC-2 has an impact on podoplanin expression within colon tissue and atherosclerotic plaques respectively. The decrease in podoplanin expression in colitis and increase in atherosclerotic may be due to the difference in the time period in of persistence inflammation i.e. DSS given to the mice for 6 days, atheroprone mice on high fat diet for 6 weeks. Looking into how platelet CLEC-2 regulates podoplanin expression, and how this in turn is impacting disease, will be an interesting area of further research.

6.4 Future Work

Further research is needed to understand the mechanism behind the role of platelet CLEC-2 in inflammation. An investigation into the adaptive immune system using the CLEC-2 deficient mouse models could facilitate greater potential understanding of how CLEC-2 is involved in aiding the immune system. CLEC-2 helps prevent blood accumulation within lymph nodes following an immune stimulus. Blood accumulation caused by a lack of CLEC-2 may therefore effect the trafficking and efficacy of adaptive immune cells, eg. B cells and T cells, to lymph nodes and therefore hinder important adaptive response such as the production of antibodies

Secondly, it is not yet clear how CLEC-2 may be influencing podoplanin expression on cells such as lymphatic epithelial cells and leukocytes. The effect may be a direct or indirect influence of platelet CLEC-2. Further investigation of the interaction of platelets and cells expressing podoplanin, rather than the protein alone, could yield interesting results. Using cell culture models would also allow for a comparison between mouse and human cells. Shear flow models or 3D cells matrix models may reveal more physiologically relevant answers

Lastly, similar mouse models of acute and chronic inflammation could be performed using cell type specific podoplanin deficient mice, eg a podoplanin myeloid deficient mouse crossed with an $ApoE^{-/-}$ deficient model and put on high fat diet, or a podoplanin endothelial deficient mouse (Tie2-Cre) treated with DSS. Further investigation into all podoplanin expressing cells which may be involved in a specific model may be necessary before performing these experiments.

6.5 Final Considerations:

The role of platelet CLEC-2 is likely to continue to be heavily researched in the future as more evidence emerges on its involvement in directing the role of platelets beyond that of haemostasis. A greater understanding of the role of podoplanin in health and disease is also needed to better understand its impact on cell behaviour in cells which constitutively express this protein and the growing variety of cells capable of podoplanin expression following an inflammatory stimulus. An important consideration in studies looking into platelet CLEC-2 and podoplanin interaction is the difference in affinity between that of mouse CLEC-2 and podoplanin and human CLEC-2 and podoplanin. This difference impacts the extrapolation of findings in mouse models, particularly in arterial shear rate environments, and its use as a potential clinical target for the treatment of human disease.

References

ABTAHIAN, F., GUERRIERO, A., SEBZDA, E., LU, M. M., ZHOU, R., MOCSAI, A., MYERS, E. E., HUANG, B., JACKSON, D. G., FERRARI, V. A., TYBULEWICZ, V., LOWELL, C. A., LEPORE, J. J., KORETZKY, G. A. & KAHN, M. L. 2003. Regulation of blood and lymphatic vascular separation by signaling proteins SLP-76 and Syk. *Science,* 299**,** 247-51.

ALEXANDER, J. S., CHAITANYA, G. V., GRISHAM, M. B. & BOKTOR, M. 2010. Emerging roles of lymphatics in inflammatory bowel disease. *Ann N Y Acad Sci,* 1207 Suppl 1**,** E75-85.

ALSHEHRI, O. M., MONTAGUE, S., WATSON, S., CARTER, P., SARKER, N., MANNE, B. K., MILLER, J. L., HERR, A. B., POLLITT, A. Y., O'CALLAGHAN, C. A., KUNAPULI, S., ARMAN, M., HUGHES, C. E. & WATSON, S. P. 2015. Activation of glycoprotein VI (GPVI) and C-type lectin-like receptor-2 (CLEC-2) underlies platelet activation by diesel exhaust particles and other charged/hydrophobic ligands. *Biochem J,* 468**,** 459-73.

ASTARITA, J. L., ACTON, S. E. & TURLEY, S. J. 2012. Podoplanin: emerging functions in development, the immune system, and cancer. *Front Immunol,* 3**,** 283.

ASTARITA, J. L., CREMASCO, V., FU, J., DARNELL, M. C., PECK, J. R., NIEVES-BONILLA, J. M., SONG, K., KONDO, Y., WOODRUFF, M. C., GOGINENI, A., ONDER, L., LUDEWIG, B., WEIMER, R. M., CARROLL, M. C., MOONEY, D. J., XIA, L. & TURLEY, S. J. 2015. The CLEC-2-podoplanin axis controls the contractility of fibroblastic reticular cells and lymph node microarchitecture. *Nat Immunol,* 16**,** 75-84.

BADIMON, L. & VILAHUR, G. 2014. Thrombosis formation on atherosclerotic lesions and plaque rupture. *J Intern Med,* 276**,** 618-32.

BENDER, M., MAY, F., LORENZ, V., THIELMANN, I., HAGEDORN, I., FINNEY, B. A., VOGTLE, T., REMER, K., BRAUN, A., BOSL, M., WATSON, S. P. & NIESWANDT, B. 2013. Combined in vivo depletion of glycoprotein VI and C-type lectin-like receptor 2 severely compromises hemostasis and abrogates arterial thrombosis in mice. *Arterioscler Thromb Vasc Biol,* 33**,** 926-34.

BENEZECH, C., NAYAR, S., FINNEY, B. A., WITHERS, D. R., LOWE, K., DESANTI, G. E., MARRIOTT, C. L., WATSON, S. P., CAAMANO, J. H., BUCKLEY, C. D. & BARONE, F. 2014. CLEC-2 is required for development and maintenance of lymph nodes. *Blood,* 123**,** 3200-7.

BERGMEIER, W., BOUVARD, D., EBLE, J. A., MOKHTARI-NEJAD, R., SCHULTE, V., ZIRNGIBL, H., BRAKEBUSCH, C., FASSLER, R. & NIESWANDT, B. 2001. Rhodocytin (aggretin) activates platelets lacking alpha(2)beta(1) integrin, glycoprotein VI, and the ligand-binding domain of glycoprotein Ibalpha. *J Biol Chem,* 276**,** 25121-6.

BERTOZZI, C. C., SCHMAIER, A. A., MERICKO, P., HESS, P. R., ZOU, Z., CHEN, M., CHEN, C. Y., XU, B., LU, M. M., ZHOU, D., SEBZDA, E., SANTORE, M. T., MERIANOS, D. J., STADTFELD, M., FLAKE, A. W., GRAF, T., SKODA, R., MALTZMAN, J. S., KORETZKY, G. A. & KAHN, M. L. 2010. Platelets regulate lymphatic vascular development through CLEC-2-SLP-76 signaling. *Blood,* 116**,** 661-70.

BONO, P., WASENIUS, V. M., HEIKKILA, P., LUNDIN, J., JACKSON, D. G. & JOENSUU, H. 2004. High LYVE-1-positive lymphatic vessel numbers are associated with poor outcome in breast cancer. *Clin Cancer Res,* 10**,** 7144-9.

BORGOGNONE, A., NAVARRO-NUNEZ, L., CORREIA, J. N., POLLITT, A. Y., THOMAS, S. G., EBLE, J. A., PULCINELLI, F. M., MADHANI, M. & WATSON, S. P. 2014. CLEC-2-dependent activation of mouse platelets is weakly inhibited by cAMP but not by cGMP. *J Thromb Haemost,* 12**,** 550-9.

BOULAFTALI, Y., HESS, P. R., GETZ, T. M., CHOLKA, A., STOLLA, M., MACKMAN, N., OWENS, A. P., 3RD, WARE, J., KAHN, M. L. & BERGMEIER, W. 2013. Platelet ITAM signaling is critical for vascular integrity in inflammation. *J Clin Invest,* 123**,** 908-16.

BOULAFTALI, Y., HESS, P. R., KAHN, M. L. & BERGMEIER, W. 2014. Platelet Immunoreceptor Tyrosine-Based Activation Motif (ITAM) Signaling and Vascular Integrity. *Circ Res,* 114**,** 1174-84.

BREITENEDER-GELEFF, S., MATSUI, K., SOLEIMAN, A., MERANER, P., POCZEWSKI, H., KALT, R., SCHAFFNER, G. & KERJASCHKI, D. 1997. Podoplanin, novel 43-kd membrane protein of glomerular epithelial cells, is down-regulated in puromycin nephrosis. *Am J Pathol,* 151**,** 1141-52.

BRENNAN, M. P., LOUGHMAN, A., DEVOCELLE, M., ARASU, S., CHUBB, A. J., FOSTER, T. J. & COX, D. 2009. Elucidating the role of Staphylococcus epidermidis serine-aspartate repeat protein G in platelet activation. *J Thromb Haemost,* 7**,** 1364-72.

BRINKMANN, V., REICHARD, U., GOOSMANN, C., FAULER, B., UHLEMANN, Y., WEISS, D. S., WEINRAUCH, Y. & ZYCHLINSKY, A. 2004. Neutrophil extracellular traps kill bacteria. *Science,* 303**,** 1532-5.

BUSCHER, K., WANG, H., ZHANG, X., STRIEWSKI, P., WIRTH, B., SAGGU, G., LUTKE-ENKING, S., MAYADAS, T. N., LEY, K., SOROKIN, L. & SONG, J. 2016. Protection from septic peritonitis by rapid neutrophil recruitment through omental high endothelial venules. *Nat Commun,* 7**,** 10828.

CHAIPAN, C., SOILLEUX, E. J., SIMPSON, P., HOFMANN, H., GRAMBERG, T., MARZI, A., GEIER, M., STEWART, E. A., EISEMANN, J., STEINKASSERER, A., SUZUKI-INOUE, K., FULLER, G. L., PEARCE, A. C., WATSON, S. P., HOXIE, J. A., BARIBAUD, F. & POHLMANN, S. 2006. DC-SIGN and CLEC-2 mediate human immunodeficiency virus type 1 capture by platelets. *J Virol,* 80**,** 8951-60.

CHAPMAN, L. M., AGGREY, A. A., FIELD, D. J., SRIVASTAVA, K., TURE, S., YUI, K., TOPHAM, D. J., BALDWIN, W. M., 3RD & MORRELL, C. N. 2012. Platelets present antigen in the context of MHC class I. *J Immunol,* 189**,** 916-23.

CHASSAING, B., AITKEN, J. D., MALLESHAPPA, M. & VIJAY-KUMAR, M. 2014. Dextran sulfate sodium (DSS)-induced colitis in mice. *Curr Protoc Immunol,* 104**,** Unit 15 25.

CHENG, A. M., ROWLEY, B., PAO, W., HAYDAY, A., BOLEN, J. B. & PAWSON, T. 1995. Syk tyrosine kinase required for mouse viability and B-cell development. *Nature,* 378**,** 303-6.

CHRISTOU, C. M., PEARCE, A. C., WATSON, A. A., MISTRY, A. R., POLLITT, A. Y., FENTON-MAY, A. E., JOHNSON, L. A., JACKSON, D. G., WATSON, S. P. & O'CALLAGHAN, C. A. 2008. Renal cells activate the platelet receptor CLEC-2 through podoplanin. *Biochem J,* 411**,** 133-40.

CLARK, S. R., MA, A. C., TAVENER, S. A., MCDONALD, B., GOODARZI, Z., KELLY, M. M., PATEL, K. D., CHAKRABARTI, S., MCAVOY, E., SINCLAIR, G. D., KEYS, E. M., ALLEN-VERCOE, E., DEVINNEY, R., DOIG, C. J., GREEN, F. H. & KUBES, P. 2007. Platelet TLR4 activates neutrophil extracellular traps to ensnare bacteria in septic blood. *Nat Med,* 13**,** 463-9.

CLEMENTS, J. L., LEE, J. R., GROSS, B., YANG, B., OLSON, J. D., SANDRA, A., WATSON, S. P., LENTZ, S. R. & KORETZKY, G. A. 1999. Fetal hemorrhage and platelet dysfunction in SLP-76-deficient mice. *J Clin Invest,* 103**,** 19-25.

CLEMENTS, J. L., YANG, B., ROSS-BARTA, S. E., ELIASON, S. L., HRSTKA, R. F., WILLIAMSON, R. A. & KORETZKY, G. A. 1998. Requirement for the leukocyte-specific adapter protein SLP-76 for normal T cell development. *Science,* 281**,** 416-9.

COLLER, B. S. & SHATTIL, S. J. 2008. The GPIIb/IIIa (integrin alphaIIbbeta3) odyssey: a technology-driven saga of a receptor with twists, turns, and even a bend. *Blood,* 112**,** 3011-25.

COLONNA, M., SAMARIDIS, J. & ANGMAN, L. 2000. Molecular characterization of two novel C-type lectin-like receptors, one of which is selectively expressed in human dendritic cells. *Eur J Immunol,* 30**,** 697-704.

COPELAND, S., WARREN, H. S., LOWRY, S. F., CALVANO, S. E., REMICK, D., INFLAMMATION & THE HOST RESPONSE TO INJURY, I. 2005. Acute inflammatory response to endotoxin in mice and humans. *Clin Diagn Lab Immunol,* 12**,** 60-7.

COPPINGER, J. A., O'CONNOR, R., WYNNE, K., FLANAGAN, M., SULLIVAN, M., MAGUIRE, P. B., FITZGERALD, D. J. & CAGNEY, G. 2007. Moderation of the platelet releasate response by aspirin. *Blood,* 109**,** 4786-92.

CORKEN, A., RUSSELL, S., DENT, J., POST, S. R. & WARE, J. 2014. Platelet glycoprotein Ib-IX as a regulator of systemic inflammation. *Arterioscler Thromb Vasc Biol,* 34**,** 996-1001.

CUENI, L. N. & DETMAR, M. 2009. Galectin-8 interacts with podoplanin and modulates lymphatic endothelial cell functions. *Exp Cell Res,* 315**,** 1715-23.

D'ALESSIO, S., CORREALE, C., TACCONI, C., GANDELLI, A., PIETROGRANDE, G., VETRANO, S., GENUA, M., ARENA, V., SPINELLI, A., PEYRIN-BIROULET, L., FIOCCHI, C. & DANESE, S. 2014. VEGF-C-dependent stimulation of lymphatic function ameliorates experimental inflammatory bowel disease. *J Clin Invest,* 124**,** 3863-78.

DANESE, S., DE LA MOTTE, C., STURM, A., VOGEL, J. D., WEST, G. A., STRONG, S. A., KATZ, J. A. & FIOCCHI, C. 2003. Platelets trigger a CD40-dependent inflammatory response in the microvasculature of inflammatory bowel disease patients. *Gastroenterology,* 124**,** 1249-64.

DANESE, S., MOTTE CD CDE, L. & FIOCCHI, C. 2004. Platelets in inflammatory bowel disease: clinical, pathogenic, and therapeutic implications. *Am J Gastroenterol,* 99**,** 938-45.

DEL REY, M. J., FARE, R., IZQUIERDO, E., USATEGUI, A., RODRIGUEZ-FERNANDEZ, J. L., SUAREZ-FUEYO, A., CANETE, J. D. & PABLOS, J. L. 2014. Clinicopathological correlations of podoplanin (gp38) expression in rheumatoid synovium and its potential contribution to fibroblast platelet crosstalk. *PLoS One,* 9**,** e99607.

DEPPERMANN, C. & KUBES, P. 2016. Platelets and infection. *Semin Immunol*.

DU, X. 2007. Signaling and regulation of the platelet glycoprotein Ib-IX-V complex. *Curr Opin Hematol,* 14**,** 262-9.

DUMONT, D. J., JUSSILA, L., TAIPALE, J., LYMBOUSSAKI, A., MUSTONEN, T., PAJUSOLA, K., BREITMAN, M. & ALITALO, K. 1998. Cardiovascular failure in mouse embryos deficient in VEGF receptor-3. *Science,* 282**,** 946-9.

FARR, A. G., BERRY, M. L., KIM, A., NELSON, A. J., WELCH, M. P. & ARUFFO, A. 1992. Characterization and cloning of a novel glycoprotein expressed by stromal cells in T-dependent areas of peripheral lymphoid tissues. *J Exp Med,* 176**,** 1477-82.

FASNACHT, N., HUANG, H. Y., KOCH, U., FAVRE, S., AUDERSET, F., CHAI, Q., ONDER, L., KALLERT, S., PINSCHEWER, D. D., MACDONALD, H. R., TACCHINI-COTTIER, F., LUDEWIG, B., LUTHER, S. A. & RADTKE, F. 2014. Specific fibroblastic niches in secondary lymphoid organs orchestrate distinct Notch-regulated immune responses. *J Exp Med,* 211**,** 2265-79.

FATTOUH, R., GUO, C. H., LAM, G. Y., GAREAU, M. G., NGAN, B. Y., GLOGAUER, M., MUISE, A. M. & BRUMELL, J. H. 2013. Rac2-deficiency leads to exacerbated and protracted colitis in response to Citrobacter rodentium infection. *PLoS One,* 8**,** e61629.

FEHON, R. G., MCCLATCHEY, A. I. & BRETSCHER, A. 2010. Organizing the cell cortex: the role of ERM proteins. *Nat Rev Mol Cell Biol,* 11**,** 276-87.

FERRER-MARIN, F., STANWORTH, S., JOSEPHSON, C. & SOLA-VISNER, M. 2013. Distinct differences in platelet production and function between neonates and adults: implications for platelet transfusion practice. *Transfusion,* 53**,** 2814-21; quiz 2813.

FINNEY, B. A., SCHWEIGHOFFER, E., NAVARRO-NUNEZ, L., BENEZECH, C., BARONE, F., HUGHES, C. E., LANGAN, S. A., LOWE, K. L., POLLITT, A. Y., MOURAO-SA, D., SHEARDOWN, S., NASH, G. B.,

SMITHERS, N., REIS E SOUSA, C., TYBULEWICZ, V. L. & WATSON, S. P. 2012. CLEC-2 and Syk in the megakaryocytic/platelet lineage are essential for development. *Blood,* 119**,** 1747-56.

FRANCOIS, M., CAPRINI, A., HOSKING, B., ORSENIGO, F., WILHELM, D., BROWNE, C., PAAVONEN, K., KARNEZIS, T., SHAYAN, R., DOWNES, M., DAVIDSON, T., TUTT, D., CHEAH, K. S., STACKER, S. A., MUSCAT, G. E., ACHEN, M. G., DEJANA, E. & KOOPMAN, P. 2008. Sox18 induces development of the lymphatic vasculature in mice. *Nature,* 456**,** 643-7.

FU, J., GERHARDT, H., MCDANIEL, J. M., XIA, B., LIU, X., IVANCIU, L., NY, A., HERMANS, K., SILASI-MANSAT, R., MCGEE, S., NYE, E., JU, T., RAMIREZ, M. I., CARMELIET, P., CUMMINGS, R. D., LUPU, F. & XIA, L. 2008. Endothelial cell O-glycan deficiency causes blood/lymphatic misconnections and consequent fatty liver disease in mice. *J Clin Invest,* 118**,** 3725-37.

GANDARILLAS, A., SCHOLL, F. G., BENITO, N., GAMALLO, C. & QUINTANILLA, M. 1997. Induction of PA2.26, a cell-surface antigen expressed by active fibroblasts, in mouse epidermal keratinocytes during carcinogenesis. *Mol Carcinog,* 20**,** 10-8.

GELEFF, S., SCHOPPMANN, S. F. & OBERHUBER, G. 2003. Increase in podoplanin-expressing intestinal lymphatic vessels in inflammatory bowel disease. *Virchows Arch,* 442**,** 231-7.

GERBER, D. E., GROSSMAN, S. A. & STREIFF, M. B. 2006. Management of venous thromboembolism in patients with primary and metastatic brain tumors. *J Clin Oncol,* 24**,** 1310-8.

GHOSHAL, K. & BHATTACHARYYA, M. 2014. Overview of Platelet Physiology: Its Hemostatic and Nonhemostatic Role in Disease Pathogenesis. *ScientificWorldJournal,* 2014**,** 781857.

GIRARD, J. P., MOUSSION, C. & FORSTER, R. 2012. HEVs, lymphatics and homeostatic immune cell trafficking in lymph nodes. *Nat Rev Immunol,* 12**,** 762-73.

GITTENBERGER-DE GROOT, A. C., MAHTAB, E. A., HAHURIJ, N. D., WISSE, L. J., DERUITER, M. C., WIJFFELS, M. C. & POELMANN, R. E. 2007. Nkx2.5-negative myocardium of the posterior heart field and its correlation with podoplanin expression in cells from the developing cardiac pacemaking and conduction system. *Anat Rec (Hoboken),* 290**,** 115-22.

GITZ, E., POLLITT, A. Y., GITZ-FRANCOIS, J. J., ALSHEHRI, O., MORI, J., MONTAGUE, S., NASH, G. B., DOUGLAS, M. R., GARDINER, E. E., ANDREWS, R. K., BUCKLEY, C. D., HARRISON, P. & WATSON, S. P. 2014. CLEC-2 expression is maintained on activated platelets and on platelet microparticles. *Blood,* 124**,** 2262-70.

GOERGE, T., HO-TIN-NOE, B., CARBO, C., BENARAFA, C., REMOLD-O'DONNELL, E., ZHAO, B. Q., CIFUNI, S. M. & WAGNER, D. D. 2008. Inflammation induces hemorrhage in thrombocytopenia. *Blood,* 111**,** 4958-64.

GRAU, S. J., TRILLSCH, F., TONN, J. C., GOLDBRUNNER, R. H., NOESSNER, E., NELSON, P. J. & VON LUETTICHAU, I. 2015. Podoplanin increases migration and angiogenesis in malignant glioma. *Int J Clin Exp Pathol,* 8**,** 8663-70.

GROS, A., SYVANNARATH, V., LAMRANI, L., OLLIVIER, V., LOYAU, S., GOERGE, T., NIESWANDT, B., JANDROT-PERRUS, M. & HO-TIN-NOE, B. 2015. Single platelets seal neutrophil-induced vascular breaches via GPVI during immune-complex-mediated inflammation in mice. *Blood,* 126**,** 1017-26.

HABTEZION, A., NGUYEN, L. P., HADEIBA, H. & BUTCHER, E. C. 2016. Leukocyte Trafficking to the Small Intestine and Colon. *Gastroenterology,* 150**,** 340-54.

HAGERLING, R., POLLMANN, C., ANDREAS, M., SCHMIDT, C., NURMI, H., ADAMS, R. H., ALITALO, K., ANDRESEN, V., SCHULTE-MERKER, S. & KIEFER, F. 2013. A novel multistep mechanism for initial lymphangiogenesis in mouse embryos based on ultramicroscopy. *EMBO J,* 32**,** 629-44.

HANSSON, G. K. & HERMANSSON, A. 2011. The immune system in atherosclerosis. *Nat Immunol,* 12**,** 204-12.

HARRIES, A. D., FITZSIMONS, E., FIFIELD, R., DEW, M. J. & RHOADES, J. 1983. Platelet count: a simple measure of activity in Crohn's disease. *Br Med J (Clin Res Ed),* 286**,** 1476.

HATA, M., AMANO, I., TSURUGA, E., KOJIMA, H. & SAWA, Y. 2010. Immunoelectron microscopic study of podoplanin localization in mouse salivary gland myoepithelium. *Acta Histochem Cytochem,* 43**,** 77-82.

HATAKEYAMA, K., KANEKO, M. K., KATO, Y., ISHIKAWA, T., NISHIHIRA, K., TSUJIMOTO, Y., SHIBATA, Y., OZAKI, Y. & ASADA, Y. 2012. Podoplanin expression in advanced atherosclerotic lesions of human aortas. *Thromb Res,* 129**,** e70-6.

HERZOG, B. H., FU, J., WILSON, S. J., HESS, P. R., SEN, A., MCDANIEL, J. M., PAN, Y., SHENG, M., YAGO, T., SILASI-MANSAT, R., MCGEE, S., MAY, F., NIESWANDT, B., MORRIS, A. J., LUPU, F., COUGHLIN, S. R., MCEVER, R. P., CHEN, H., KAHN, M. L. & XIA, L. 2013. Podoplanin maintains high endothelial venule integrity by interacting with platelet CLEC-2. *Nature,* 502**,** 105-9.

HESS, P. R., RAWNSLEY, D. R., JAKUS, Z., YANG, Y., SWEET, D. T., FU, J., HERZOG, B., LU, M., NIESWANDT, B., OLIVER, G., MAKINEN, T., XIA, L. & KAHN, M. L. 2014. Platelets mediate lymphovenous hemostasis to maintain blood-lymphatic separation throughout life. *J Clin Invest,* 124**,** 273-84.

HICKEY, M. J. & KUBES, P. 2009. Intravascular immunity: the host-pathogen encounter in blood vessels. *Nat Rev Immunol,* 9**,** 364-75.

HITCHCOCK, J. R., COOK, C. N., BOBAT, S., ROSS, E. A., FLORES-LANGARICA, A., LOWE, K. L., KHAN, M., DOMINGUEZ-MEDINA, C. C., LAX, S., CARVALHO-GASPAR, M., HUBSCHER, S., RAINGER, G. E., COBBOLD, M., BUCKLEY, C. D., MITCHELL, T. J., MITCHELL, A., JONES, N. D., VAN ROOIJEN, N., KIRCHHOFER, D., HENDERSON, I. R., ADAMS, D. H., WATSON, S. P. & CUNNINGHAM, A. F. 2015. Inflammation drives thrombosis after Salmonella infection via CLEC-2 on platelets. *J Clin Invest,* 125**,** 4429-46.

HO-TIN-NOE, B., DEMERS, M. & WAGNER, D. D. 2011. How platelets safeguard vascular integrity. *J Thromb Haemost,* 9 Suppl 1**,** 56-65.

HORBAR, J. D., BADGER, G. J., CARPENTER, J. H., FANAROFF, A. A., KILPATRICK, S., LACORTE, M., PHIBBS, R., SOLL, R. F. & MEMBERS OF THE VERMONT OXFORD, N. 2002. Trends in mortality and morbidity for very low birth weight infants, 1991-1999. *Pediatrics,* 110**,** 143-51.

HOU, T. Z., BYSTROM, J., SHERLOCK, J. P., QURESHI, O., PARNELL, S. M., ANDERSON, G., GILROY, D. W. & BUCKLEY, C. D. 2010. A distinct subset of podoplanin (gp38) expressing F4/80+ macrophages mediate phagocytosis and are induced following zymosan peritonitis. *FEBS Lett,* 584**,** 3955-61.

HUANG, T. F., LIU, C. Z. & YANG, S. H. 1995. Aggretin, a novel platelet-aggregation inducer from snake (Calloselasma rhodostoma) venom, activates phospholipase C by acting as a glycoprotein Ia/IIa agonist. *Biochem J,* 309 (Pt 3)**,** 1021-7.

HUGHES, C. E., POLLITT, A. Y., MORI, J., EBLE, J. A., TOMLINSON, M. G., HARTWIG, J. H., O'CALLAGHAN, C. A., FUTTERER, K. & WATSON, S. P. 2010. CLEC-2 activates Syk through dimerization. *Blood,* 115**,** 2947-55.

HUGHES, S. & CHAN-LING, T. 2004. Characterization of smooth muscle cell and pericyte differentiation in the rat retina in vivo. *Invest Ophthalmol Vis Sci,* 45**,** 2795-806.

HUO, Y. & LEY, K. F. 2004. Role of platelets in the development of atherosclerosis. *Trends Cardiovasc Med,* 14**,** 18-22.

HUR, J., JANG, J. H., OH, I. Y., CHOI, J. I., YUN, J. Y., KIM, J., CHOI, Y. E., KO, S. B., KANG, J. A., KANG, J., LEE, S. E., LEE, H., PARK, Y. B. & KIM, H. S. 2014. Human podoplanin-positive monocytes and platelets enhance lymphangiogenesis through the activation of the podoplanin/CLEC-2 axis. *Mol Ther*.

ICHISE, H., ICHISE, T., OHTANI, O. & YOSHIDA, N. 2009. Phospholipase Cgamma2 is necessary for separation of blood and lymphatic vasculature in mice. *Development,* 136**,** 191-5.

IKEDA, S., KUDSK, K. A., FUKATSU, K., JOHNSON, C. D., LE, T., REESE, S. & ZARZAUR, B. L. 2003. Enteral feeding preserves mucosal immunity despite in vivo MAdCAM-1 blockade of lymphocyte homing. *Ann Surg,* 237**,** 677-85; discussion 685.

INOUE, K., OZAKI, Y., SATOH, K., WU, Y., YATOMI, Y., SHIN, Y. & MORITA, T. 1999. Signal transduction pathways mediated by glycoprotein Ia/IIa in human platelets: comparison with those of glycoprotein VI. *Biochem Biophys Res Commun,* 256**,** 114-20.

JACKSON, A., NANTON, M. R., O'DONNELL, H., AKUE, A. D. & MCSORLEY, S. J. 2010. Innate immune activation during Salmonella infection initiates extramedullary erythropoiesis and splenomegaly. *J Immunol,* 185**,** 6198-204.

JANEWAY, C. A., JR. & MEDZHITOV, R. 2002. Innate immune recognition. *Annu Rev Immunol,* 20**,** 197-216.

JANKOWSKA-KONSUR, A., KOBIERZYCKI, C., GRZEGRZOLKA, J., PIOTROWSKA, A., GOMULKIEWICZ, A., GLATZEL-PLUCINSKA, N., REICH, A., PODHORSKA-OKOLOW, M., DZIEGIEL, P. & SZEPIETOWSKI, J. C. 2016. Podoplanin Expression Correlates with Disease Progression in Mycosis Fungoides. *Acta Derm Venereol*.

JUNG, C., HUGOT, J. P. & BARREAU, F. 2010. Peyer's Patches: The Immune Sensors of the Intestine. *Int J Inflam,* 2010**,** 823710.

KANEKO, M. K., KATO, Y., KITANO, T. & OSAWA, M. 2006. Conservation of a platelet activating domain of Aggrus/podoplanin as a platelet aggregation-inducing factor. *Gene,* 378**,** 52-7.

KARKKAINEN, M. J., HAIKO, P., SAINIO, K., PARTANEN, J., TAIPALE, J., PETROVA, T. V., JELTSCH, M., JACKSON, D. G., TALIKKA, M., RAUVALA, H., BETSHOLTZ, C. & ALITALO, K. 2004. Vascular endothelial growth factor C is required for sprouting of the first lymphatic vessels from embryonic veins. *Nat Immunol,* 5**,** 74-80.

KATO, Y., FUJITA, N., KUNITA, A., SATO, S., KANEKO, M., OSAWA, M. & TSURUO, T. 2003. Molecular identification of Aggrus/T1alpha as a platelet aggregation-inducing factor expressed in colorectal tumors. *J Biol Chem,* 278**,** 51599-605.

KATO, Y., KANEKO, M., SATA, M., FUJITA, N., TSURUO, T. & OSAWA, M. 2005. Enhanced expression of Aggrus (T1alpha/podoplanin), a platelet-aggregation-inducing factor in lung squamous cell carcinoma. *Tumour Biol,* 26**,** 195-200.

KATO, Y., KANEKO, M. K., KUNITA, A., ITO, H., KAMEYAMA, A., OGASAWARA, S., MATSUURA, N., HASEGAWA, Y., SUZUKI-INOUE, K., INOUE, O., OZAKI, Y. & NARIMATSU, H. 2008. Molecular analysis of the pathophysiological binding of the platelet aggregation-inducing factor podoplanin to the C-type lectin-like receptor CLEC-2. *Cancer Sci,* 99**,** 54-61.

KERJASCHKI, D., REGELE, H. M., MOOSBERGER, I., NAGY-BOJARSKI, K., WATSCHINGER, B., SOLEIMAN, A., BIRNER, P., KRIEGER, S., HOVORKA, A., SILBERHUMER, G., LAAKKONEN, P., PETROVA, T., LANGER, B. & RAAB, I. 2004. Lymphatic neoangiogenesis in human kidney transplants is associated with immunologically active lymphocytic infiltrates. *J Am Soc Nephrol,* 15**,** 603-12.

KERRIGAN, A. M., DENNEHY, K. M., MOURAO-SA, D., FARO-TRINDADE, I., WILLMENT, J. A., TAYLOR, P. R., EBLE, J. A., REIS E SOUSA, C. & BROWN, G. D. 2009. CLEC-2 is a phagocytic activation receptor expressed on murine peripheral blood neutrophils. *J Immunol,* 182**,** 4150-7.

KERRIGAN, A. M., NAVARRO-NUNEZ, L., PYZ, E., FINNEY, B. A., WILLMENT, J. A., WATSON, S. P. & BROWN, G. D. 2012. Podoplanin-expressing inflammatory macrophages activate murine platelets via CLEC-2. *J Thromb Haemost,* 10**,** 484-6.

KONDO, M., WAGERS, A. J., MANZ, M. G., PROHASKA, S. S., SCHERER, D. C., BEILHACK, G. F., SHIZURU, J. A. & WEISSMAN, I. L. 2003. Biology of hematopoietic stem cells and progenitors: implications for clinical application. *Annu Rev Immunol,* 21**,** 759-806.

LAI, L., ALAVERDI, N., MALTAIS, L. & MORSE, H. C., 3RD 1998. Mouse cell surface antigens: nomenclature and immunophenotyping. *J Immunol,* 160**,** 3861-8.

LAVETI, D., KUMAR, M., HEMALATHA, R., SISTLA, R., NAIDU, V. G., TALLA, V., VERMA, V., KAUR, N. & NAGPAL, R. 2013. Anti-inflammatory treatments for chronic diseases: a review. *Inflamm Allergy Drug Targets,* 12**,** 349-61.

LI, Z., YANG, F., DUNN, S., GROSS, A. K. & SMYTH, S. S. 2011. Platelets as immune mediators: their role in host defense responses and sepsis. *Thromb Res,* 127**,** 184-8.

LIEVENS, D. & VON HUNDELSHAUSEN, P. 2011. Platelets in atherosclerosis. *Thromb Haemost,* 106**,** 827-38.

LOPEZ, J. A. & DONG, J. F. 1997. Structure and function of the glycoprotein Ib-IX-V complex. *Curr Opin Hematol,* 4**,** 323-9.

LOWE, K. L., FINNEY, B. A., DEPPERMANN, C., HAGERLING, R., GAZIT, S. L., FRAMPTON, J., BUCKLEY, C., CAMERER, E., NIESWANDT, B., KIEFER, F. & WATSON, S. P. 2015a. Podoplanin and CLEC-2 drive cerebrovascular patterning and integrity during development. *Blood,* 125**,** 3769-77.

LOWE, K. L., NAVARRO-NUNEZ, L., BENEZECH, C., NAYAR, S., KINGSTON, B. L., NIESWANDT, B., BARONE, F., WATSON, S. P., BUCKLEY, C. D. & DESANTI, G. E. 2015b. The expression of mouse CLEC-2 on leucocyte subsets varies according to their anatomical location and inflammatory state. *Eur J Immunol,* 45**,** 2484-93.

LOWE, K. L., NAVARRO-NUNEZ, L. & WATSON, S. P. 2012. Platelet CLEC-2 and podoplanin in cancer metastasis. *Thromb Res,* 129 Suppl 1**,** S30-7.

MACHLUS, K. R. & ITALIANO, J. E., JR. 2013. The incredible journey: From megakaryocyte development to platelet formation. *J Cell Biol,* 201**,** 785-96.

MAHTAB, E. A., WIJFFELS, M. C., VAN DEN AKKER, N. M., HAHURIJ, N. D., LIE-VENEMA, H., WISSE, L. J., DERUITER, M. C., UHRIN, P., ZAUJEC, J., BINDER, B. R., SCHALIJ, M. J., POELMANN, R. E. & GITTENBERGER-DE GROOT, A. C. 2008. Cardiac malformations and myocardial abnormalities in podoplanin knockout mouse embryos: Correlation with abnormal epicardial development. *Dev Dyn,* 237**,** 847-57.

MALAVIYA, R., IKEDA, T., ROSS, E. & ABRAHAM, S. N. 1996. Mast cell modulation of neutrophil influx and bacterial clearance at sites of infection through TNF-alpha. *Nature,* 381**,** 77-80.

MANTOVANI, A. & GARLANDA, C. 2013. Platelet-macrophage partnership in innate immunity and inflammation. *Nat Immunol,* 14**,** 768-70.

MARTIN-VILLAR, E., FERNANDEZ-MUNOZ, B., PARSONS, M., YURRITA, M. M., MEGIAS, D., PEREZ-GOMEZ, E., JONES, G. E. & QUINTANILLA, M. 2010. Podoplanin associates with CD44 to promote directional cell migration. *Mol Biol Cell,* 21**,** 4387-99.

MARTIN-VILLAR, E., MEGIAS, D., CASTEL, S., YURRITA, M. M., VILARO, S. & QUINTANILLA, M. 2006. Podoplanin binds ERM proteins to activate RhoA and promote epithelial-mesenchymal transition. *J Cell Sci,* 119**,** 4541-53.

MARTIN-VILLAR, E., SCHOLL, F. G., GAMALLO, C., YURRITA, M. M., MUNOZ-GUERRA, M., CRUCES, J. & QUINTANILLA, M. 2005. Characterization of human PA2.26 antigen (T1alpha-2, podoplanin), a small membrane mucin induced in oral squamous cell carcinomas. *Int J Cancer,* 113**,** 899-910.

MARTINEZ-CORRAL, I., ULVMAR, M. H., STANCZUK, L., TATIN, F., KIZHATIL, K., JOHN, S. W., ALITALO, K., ORTEGA, S. & MAKINEN, T. 2015. Nonvenous origin of dermal lymphatic vasculature. *Circ Res,* 116**,** 1649-54.

MATSUI, K., BREITENEDER-GELEFF, S. & KERJASCHKI, D. 1998. Epitope-specific antibodies to the 43-kD glomerular membrane protein podoplanin cause proteinuria and rapid flattening of podocytes. *J Am Soc Nephrol,* 9**,** 2013-26.

MAUSE, S. F., VON HUNDELSHAUSEN, P., ZERNECKE, A., KOENEN, R. R. & WEBER, C. 2005. Platelet microparticles: a transcellular delivery system for RANTES promoting monocyte recruitment on endothelium. *Arterioscler Thromb Vasc Biol,* 25**,** 1512-8.

MCNICOL, A. & ISRAELS, S. J. 2008. Beyond hemostasis: the role of platelets in inflammation, malignancy and infection. *Cardiovasc Hematol Disord Drug Targets,* 8**,** 99-117.

MEBIUS, R. E. & KRAAL, G. 2005. Structure and function of the spleen. *Nat Rev Immunol,* 5**,** 606-16.

MEIR, K. S. & LEITERSDORF, E. 2004. Atherosclerosis in the apolipoprotein-E-deficient mouse: a decade of progress. *Arterioscler Thromb Vasc Biol,* 24**,** 1006-14.

MORRELL, C. N., AGGREY, A. A., CHAPMAN, L. M. & MODJESKI, K. L. 2014. Emerging roles for platelets as immune and inflammatory cells. *Blood,* 123**,** 2759-67.

NAGAE, M., MORITA-MATSUMOTO, K., KATO, M., KANEKO, M. K., KATO, Y. & YAMAGUCHI, Y. 2014. A platform of C-type lectin-like receptor CLEC-2 for binding O-glycosylated podoplanin and nonglycosylated rhodocytin. *Structure,* 22**,** 1711-21.

NAKAMURA-ISHIZU, A., TAKUBO, K., KOBAYASHI, H., SUZUKI-INOUE, K. & SUDA, T. 2015. CLEC-2 in megakaryocytes is critical for maintenance of hematopoietic stem cells in the bone marrow. *J Exp Med,* 212**,** 2133-46.

NAKAZAWA, Y., SATO, S., NAITO, M., KATO, Y., MISHIMA, K., ARAI, H., TSURUO, T. & FUJITA, N. 2008. Tetraspanin family member CD9 inhibits Aggrus/podoplanin-induced platelet aggregation and suppresses pulmonary metastasis. *Blood,* 112**,** 1730-9.

NAVARRO-NUNEZ, L., POLLITT, A. Y., LOWE, K., LATIF, A., NASH, G. B. & WATSON, S. P. 2015. Platelet adhesion to podoplanin under flow is mediated by the receptor CLEC-2 and stabilised by Src/Syk-dependent platelet signalling. *Thromb Haemost,* 113**,** 1109-20.

NAVARRO, A., PEREZ, R. E., REZAIEKHALIGH, M. H., MABRY, S. M. & EKEKEZIE, II 2011. Polarized migration of lymphatic endothelial cells is critically dependent on podoplanin regulation of Cdc42. *Am J Physiol Lung Cell Mol Physiol,* 300**,** L32-42.

NAVDAEV, A., CLEMETSON, J. M., POLGAR, J., KEHREL, B. E., GLAUNER, M., MAGNENAT, E., WELLS, T. N. & CLEMETSON, K. J. 2001. Aggretin, a heterodimeric C-type lectin from Calloselasma rhodostoma (Malayan pit viper), stimulates platelets by binding to alpha2beta1 integrin and glycoprotein Ib, activating Syk and phospholipase Cgamma 2, but does not involve the glycoprotein VI/Fc receptor gamma chain collagen receptor. *J Biol Chem,* 276**,** 20882-9.

NEURATH, M. F. 2014. Cytokines in inflammatory bowel disease. *Nat Rev Immunol,* 14**,** 329-42.

NI, H. & FREEDMAN, J. 2003. Platelets in hemostasis and thrombosis: role of integrins and their ligands. *Transfus Apher Sci,* 28**,** 257-64.

NODA, Y., AMANO, I., HATA, M., KOJIMA, H. & SAWA, Y. 2010. Immunohistochemical examination on the distribution of cells expressed lymphatic endothelial marker podoplanin and LYVE-1 in the mouse tongue tissue. *Acta Histochem Cytochem,* 43**,** 61-8.

NORDING, H. M., SEIZER, P. & LANGER, H. F. 2015. Platelets in inflammation and atherogenesis. *Front Immunol,* 6**,** 98.

NOSE, K., SAITO, H. & KUROKI, T. 1990. Isolation of a gene sequence induced later by tumor-promoting 12-O-tetradecanoylphorbol-13-acetate in mouse osteoblastic cells (MC3T3-E1) and expressed constitutively in ras-transformed cells. *Cell Growth Differ,* 1**,** 511-8.

OGURA, H., KAWASAKI, T., TANAKA, H., KOH, T., TANAKA, R., OZEKI, Y., HOSOTSUBO, H., KUWAGATA, Y., SHIMAZU, T. & SUGIMOTO, H. 2001. Activated platelets enhance microparticle formation and platelet-leukocyte interaction in severe trauma and sepsis. *J Trauma,* 50**,** 801-9.

OHASHI, R., MU, H., YAO, Q. & CHEN, C. 2004. Cellular and molecular mechanisms of atherosclerosis with mouse models. *Trends Cardiovasc Med,* 14**,** 187-90.

PAIGEN, B., MORROW, A., BRANDON, C., MITCHELL, D. & HOLMES, P. 1985. Variation in susceptibility to atherosclerosis among inbred strains of mice. *Atherosclerosis,* 57**,** 65-73.

PERTUY, F., AGUILAR, A., STRASSEL, C., ECKLY, A., FREUND, J. N., DULUC, I., GACHET, C., LANZA, F. & LEON, C. 2015. Broader expression of the mouse platelet factor 4-cre transgene beyond the megakaryocyte lineage. *J Thromb Haemost,* 13**,** 115-25.

PETERS, A., BURKETT, P. R., SOBEL, R. A., BUCKLEY, C. D., WATSON, S. P., BETTELLI, E. & KUCHROO, V. K. 2015. Podoplanin negatively regulates CD4+ effector T cell responses. *J Clin Invest,* 125**,** 129-40.

PETERS, A., PITCHER, L. A., SULLIVAN, J. M., MITSDOERFFER, M., ACTON, S. E., FRANZ, B., WUCHERPFENNIG, K., TURLEY, S., CARROLL, M. C., SOBEL, R. A., BETTELLI, E. & KUCHROO, V. K. 2011. Th17 cells induce ectopic lymphoid follicles in central nervous system tissue inflammation. *Immunity,* 35**,** 986-96.

PETERSEN, T. N., BRUNAK, S., VON HEIJNE, G. & NIELSEN, H. 2011. SignalP 4.0: discriminating signal peptides from transmembrane regions. *Nat Methods,* 8**,** 785-6.

PETERZIEL, H., MULLER, J., DANNER, A., BARBUS, S., LIU, H. K., RADLWIMMER, B., PIETSCH, T., LICHTER, P., SCHUTZ, G., HESS, J. & ANGEL, P. 2012. Expression of podoplanin in human astrocytic brain tumors is controlled by the PI3K-AKT-AP-1 signaling pathway and promoter methylation. *Neuro Oncol,* 14**,** 426-39.

PLUMP, A. S., SMITH, J. D., HAYEK, T., AALTO-SETALA, K., WALSH, A., VERSTUYFT, J. G., RUBIN, E. M. & BRESLOW, J. L. 1992. Severe hypercholesterolemia and atherosclerosis in apolipoprotein E-deficient mice created by homologous recombination in ES cells. *Cell,* 71**,** 343-53.

PODGRABINSKA, S., BRAUN, P., VELASCO, P., KLOOS, B., PEPPER, M. S. & SKOBE, M. 2002. Molecular characterization of lymphatic endothelial cells. *Proc Natl Acad Sci U S A,* 99**,** 16069-74.

POLLITT, A. Y., GRYGIELSKA, B., LEBLOND, B., DESIRE, L., EBLE, J. A. & WATSON, S. P. 2010. Phosphorylation of CLEC-2 is dependent on lipid rafts, actin polymerization, secondary mediators, and Rac. *Blood,* 115**,** 2938-46.

POLLITT, A. Y., POULTER, N. S., GITZ, E., NAVARRO-NUNEZ, L., WANG, Y. J., HUGHES, C. E., THOMAS, S. G., NIESWANDT, B., DOUGLAS, M. R., OWEN, D. M., JACKSON, D. G., DUSTIN, M. L. & WATSON, S. P. 2014. Syk and Src family kinases regulate C-type lectin receptor 2 (CLEC-2)-mediated clustering of podoplanin and platelet adhesion to lymphatic endothelial cells. *J Biol Chem,* 289**,** 35695-710.

RAHIER, J. F., DE BEAUCE, S., DUBUQUOY, L., ERDUAL, E., COLOMBEL, J. F., JOURET-MOURIN, A., GEBOES, K. & DESREUMAUX, P. 2011. Increased lymphatic vessel density and lymphangiogenesis in inflammatory bowel disease. *Aliment Pharmacol Ther,* 34**,** 533-43.

REED, G. L., FITZGERALD, M. L. & POLGAR, J. 2000. Molecular mechanisms of platelet exocytosis: insights into the "secrete" life of thrombocytes. *Blood,* 96**,** 3334-42.

REN, Q., YE, S. & WHITEHEART, S. W. 2008. The platelet release reaction: just when you thought platelet secretion was simple. *Curr Opin Hematol,* 15**,** 537-41.

RIEDEMANN, N. C., GUO, R. F. & WARD, P. A. 2003. Novel strategies for the treatment of sepsis. *Nat Med,* 9**,** 517-24.

RIVERA, A., SIRACUSA, M. C., YAP, G. S. & GAUSE, W. C. 2016. Innate cell communication kick-starts pathogen-specific immunity. *Nat Immunol,* 17**,** 356-63.

ROVAINEN, C. M., WANG, D. B. & WOOLSEY, T. A. 1992. Strobe epi-illumination of fluorescent beads indicates similar velocities and wall shear rates in brain arterioles of newborn and adult mice. *Microvasc Res,* 43**,** 235-9.

SACHS, U. J. & NIESWANDT, B. 2007. In vivo thrombus formation in murine models. *Circ Res,* 100**,** 979-91.

SATO, H., HIGASHIYAMA, M., HOZUMI, H., SATO, S., FURUHASHI, H., TAKAJO, T., MARUTA, K., YASUTAKE, Y., NARIMATSU, K., YOSHIKAWA, K., KURIHARA, C., OKADA, Y., WATANABE, C., KOMOTO, S.,

TOMITA, K., NAGAO, S., MIURA, S. & HOKARI, R. 2016. Platelet interaction with lymphatics aggravates intestinal inflammation by suppressing lymphangiogenesis. *Am J Physiol Gastrointest Liver Physiol,* 311**,** G276-85.

SAVAGE, B., ALMUS-JACOBS, F. & RUGGERI, Z. M. 1998. Specific synergy of multiple substrate-receptor interactions in platelet thrombus formation under flow. *Cell,* 94**,** 657-66.

SAVAGE, B., SALDIVAR, E. & RUGGERI, Z. M. 1996. Initiation of platelet adhesion by arrest onto fibrinogen or translocation on von Willebrand factor. *Cell,* 84**,** 289-97.

SCHACHT, V., RAMIREZ, M. I., HONG, Y. K., HIRAKAWA, S., FENG, D., HARVEY, N., WILLIAMS, M., DVORAK, A. M., DVORAK, H. F., OLIVER, G. & DETMAR, M. 2003. T1alpha/podoplanin deficiency disrupts normal lymphatic vasculature formation and causes lymphedema. *EMBO J,* 22**,** 3546-56.

SCHIWON, M., WEISHEIT, C., FRANKEN, L., GUTWEILER, S., DIXIT, A., MEYER-SCHWESINGER, C., POHL, J. M., MAURICE, N. J., THIEBES, S., LORENZ, K., QUAST, T., FUHRMANN, M., BAUMGARTEN, G., LOHSE, M. J., OPDENAKKER, G., BERNHAGEN, J., BUCALA, R., PANZER, U., KOLANUS, W., GRONE, H. J., GARBI, N., KASTENMULLER, W., KNOLLE, P. A., KURTS, C. & ENGEL, D. R. 2014. Crosstalk between sentinel and helper macrophages permits neutrophil migration into infected uroepithelium. *Cell,* 156**,** 456-68.

SCHOLL, F. G., GAMALLO, C., VILARO, S. & QUINTANILLA, M. 1999. Identification of PA2.26 antigen as a novel cell-surface mucin-type glycoprotein that induces plasma membrane extensions and increased motility in keratinocytes. *J Cell Sci,* 112 (Pt 24)**,** 4601-13.

SCHOUTEN, M., WIERSINGA, W. J., LEVI, M. & VAN DER POLL, T. 2008. Inflammation, endothelium, and coagulation in sepsis. *J Leukoc Biol,* 83**,** 536-45.

SCHULTE-MERKER, S., SABINE, A. & PETROVA, T. V. 2011. Lymphatic vascular morphogenesis in development, physiology, and disease. *J Cell Biol,* 193**,** 607-18.

SEMPLE, J. W., ITALIANO, J. E., JR. & FREEDMAN, J. 2011. Platelets and the immune continuum. *Nat Rev Immunol,* 11**,** 264-74.

SENIS, Y. A., TOMLINSON, M. G., GARCIA, A., DUMON, S., HEATH, V. L., HERBERT, J., COBBOLD, S. P., SPALTON, J. C., AYMAN, S., ANTROBUS, R., ZITZMANN, N., BICKNELL, R., FRAMPTON, J., AUTHI, K. S., MARTIN, A., WAKELAM, M. J. & WATSON, S. P. 2007. A comprehensive proteomics and genomics analysis reveals novel transmembrane proteins in human platelets and mouse megakaryocytes including G6b-B, a novel immunoreceptor tyrosine-based inhibitory motif protein. *Mol Cell Proteomics,* 6**,** 548-64.

SEVERIN, S., POLLITT, A. Y., NAVARRO-NUNEZ, L., NASH, C. A., MOURAO-SA, D., EBLE, J. A., SENIS, Y. A. & WATSON, S. P. 2011. Syk-dependent phosphorylation of CLEC-2: a novel mechanism of hem-immunoreceptor tyrosine-based activation motif signaling. *J Biol Chem,* 286**,** 4107-16.

SEYMOUR, R. S., BOSIOCIC, V. & SNELLING, E. P. 2016. Fossil skulls reveal that blood flow rate to the brain increased faster than brain volume during human evolution. *Royal Society Open Science,* 3**,** 160305.

SHAH, A., MORGAN, G., ROSE, J. D., FIFIELD, R. & RHODES, J. 1989. Platelet number and size in relation to serum orosomucoid concentration in Crohn's disease. *Med Lab Sci,* 46**,** 79-80.

SHATTIL, S. J., KIM, C. & GINSBERG, M. H. 2010. The final steps of integrin activation: the end game. *Nat Rev Mol Cell Biol,* 11**,** 288-300.

SIEGEMUND, S., SHEPHERD, J., XIAO, C. & SAUER, K. 2015. hCD2-iCre and Vav-iCre mediated gene recombination patterns in murine hematopoietic cells. *PLoS One,* 10**,** e0124661.

SMYTH, S. S., MCEVER, R. P., WEYRICH, A. S., MORRELL, C. N., HOFFMAN, M. R., AREPALLY, G. M., FRENCH, P. A., DAUERMAN, H. L., BECKER, R. C. & PLATELET COLLOQUIUM, P. 2009. Platelet functions beyond hemostasis. *J Thromb Haemost,* 7**,** 1759-66.

SRINIVASAN, R. S., DILLARD, M. E., LAGUTIN, O. V., LIN, F. J., TSAI, S., TSAI, M. J., SAMOKHVALOV, I. M. & OLIVER, G. 2007. Lineage tracing demonstrates the venous origin of the mammalian lymphatic vasculature. *Genes Dev,* 21**,** 2422-32.

STANWORTH, S. J. 2012. Thrombocytopenia, bleeding, and use of platelet transfusions in sick neonates. *Hematology Am Soc Hematol Educ Program,* 2012**,** 512-6.

SUURONEN, T., NUUTINEN, T., HUUSKONEN, J., OJALA, J., THORNELL, A. & SALMINEN, A. 2005. Anti-inflammatory effect of selective estrogen receptor modulators (SERMs) in microglial cells. *Inflamm Res,* 54**,** 194-203.

SUZUKI-INOUE, K., FULLER, G. L., GARCIA, A., EBLE, J. A., POHLMANN, S., INOUE, O., GARTNER, T. K., HUGHAN, S. C., PEARCE, A. C., LAING, G. D., THEAKSTON, R. D., SCHWEIGHOFFER, E., ZITZMANN, N., MORITA, T., TYBULEWICZ, V. L., OZAKI, Y. & WATSON, S. P. 2006. A novel Syk-dependent mechanism of platelet activation by the C-type lectin receptor CLEC-2. *Blood,* 107**,** 542-9.

SUZUKI-INOUE, K., INOUE, O., DING, G., NISHIMURA, S., HOKAMURA, K., ETO, K., KASHIWAGI, H., TOMIYAMA, Y., YATOMI, Y., UMEMURA, K., SHIN, Y., HIRASHIMA, M. & OZAKI, Y. 2010. Essential in vivo roles of the C-type lectin receptor CLEC-2: embryonic/neonatal lethality of CLEC-2-deficient mice by blood/lymphatic misconnections and impaired thrombus formation of CLEC-2-deficient platelets. *J Biol Chem,* 285**,** 24494-507.

SUZUKI-INOUE, K., KATO, Y., INOUE, O., KANEKO, M. K., MISHIMA, K., YATOMI, Y., YAMAZAKI, Y., NARIMATSU, H. & OZAKI, Y. 2007. Involvement of the snake toxin receptor CLEC-2, in podoplanin-mediated platelet activation, by cancer cells. *J Biol Chem,* 282**,** 25993-6001.

SWIRSKI, F. K. & NAHRENDORF, M. 2013. Leukocyte behavior in atherosclerosis, myocardial infarction, and heart failure. *Science,* 339**,** 161-6.

TAKAGI, S., SATO, S., OH-HARA, T., TAKAMI, M., KOIKE, S., MISHIMA, Y., HATAKE, K. & FUJITA, N. 2013. Platelets promote tumor growth and metastasis via direct interaction between Aggrus/podoplanin and CLEC-2. *PLoS One,* 8**,** e73609.

TAKEUCHI, O. & AKIRA, S. 2010. Pattern recognition receptors and inflammation. *Cell,* 140**,** 805-20.

TAMMELA, T. & ALITALO, K. 2010. Lymphangiogenesis: Molecular mechanisms and future promise. *Cell,* 140**,** 460-76.

TANG, T., LI, L., TANG, J., LI, Y., LIN, W. Y., MARTIN, F., GRANT, D., SOLLOWAY, M., PARKER, L., YE, W., FORREST, W., GHILARDI, N., ORAVECZ, T., PLATT, K. A., RICE, D. S., HANSEN, G. M., ABUIN, A., EBERHART, D. E., GODOWSKI, P., HOLT, K. H., PETERSON, A., ZAMBROWICZ, B. P. & DE SAUVAGE, F. J. 2010. A mouse knockout library for secreted and transmembrane proteins. *Nat Biotechnol,* 28**,** 749-55.

TAPIA-GONZALEZ, S., CARRERO, P., PERNIA, O., GARCIA-SEGURA, L. M. & DIZ-CHAVES, Y. 2008. Selective oestrogen receptor (ER) modulators reduce microglia reactivity in vivo after peripheral inflammation: potential role of microglial ERs. *J Endocrinol,* 198**,** 219-30.

TIEDT, R., SCHOMBER, T., HAO-SHEN, H. & SKODA, R. C. 2007. Pf4-Cre transgenic mice allow the generation of lineage-restricted gene knockouts for studying megakaryocyte and platelet function in vivo. *Blood,* 109**,** 1503-6.

TISONCIK, J. R., KORTH, M. J., SIMMONS, C. P., FARRAR, J., MARTIN, T. R. & KATZE, M. G. 2012. Into the eye of the cytokine storm. *Microbiol Mol Biol Rev,* 76**,** 16-32.

TRZPIS, M., MCLAUGHLIN, P. M., DE LEIJ, L. M. & HARMSEN, M. C. 2007. Epithelial cell adhesion molecule: more than a carcinoma marker and adhesion molecule. *Am J Pathol,* 171**,** 386-95.

TURNER, M., MEE, P. J., COSTELLO, P. S., WILLIAMS, O., PRICE, A. A., DUDDY, L. P., FURLONG, M. T., GEAHLEN, R. L. & TYBULEWICZ, V. L. 1995. Perinatal lethality and blocked B-cell development in mice lacking the tyrosine kinase Syk. *Nature,* 378**,** 298-302.

TURNER, M. D., NEDJAI, B., HURST, T. & PENNINGTON, D. J. 2014. Cytokines and chemokines: At the crossroads of cell signalling and inflammatory disease. *Biochim Biophys Acta,* 1843**,** 2563-2582.

UHRIN, P., ZAUJEC, J., BREUSS, J. M., OLCAYDU, D., CHRENEK, P., STOCKINGER, H., FUERTBAUER, E., MOSER, M., HAIKO, P., FASSLER, R., ALITALO, K., BINDER, B. R. & KERJASCHKI, D. 2010. Novel function for blood platelets and podoplanin in developmental separation of blood and lymphatic circulation. *Blood,* 115**,** 3997-4005.

VARGA-SZABO, D., PLEINES, I. & NIESWANDT, B. 2008. Cell adhesion mechanisms in platelets. *Arterioscler Thromb Vasc Biol,* 28**,** 403-12.

VENKATA, C., KASHYAP, R., FARMER, J. C. & AFESSA, B. 2013. Thrombocytopenia in adult patients with sepsis: incidence, risk factors, and its association with clinical outcome. *J Intensive Care,* 1**,** 9.

WANG, D., FENG, J., WEN, R., MARINE, J. C., SANGSTER, M. Y., PARGANAS, E., HOFFMEYER, A., JACKSON, C. W., CLEVELAND, J. L., MURRAY, P. J. & IHLE, J. N. 2000. Phospholipase Cgamma2 is essential in the functions of B cell and several Fc receptors. *Immunity,* 13**,** 25-35.

WANG, D. B., BLOCHER, N. C., SPENCE, M. E., ROVAINEN, C. M. & WOOLSEY, T. A. 1992. Development and remodeling of cerebral blood vessels and their flow in postnatal mice observed with in vivo videomicroscopy. *J Cereb Blood Flow Metab,* 12**,** 935-46.

WANG, L., YIN, J., WANG, X., SHAO, M., DUAN, F., WU, W., PENG, P., JIN, J., TANG, Y., RUAN, Y., SUN, Y. & GU, J. 2016. C-Type Lectin-Like Receptor 2 Suppresses AKT Signaling and Invasive Activities of Gastric Cancer Cells by Blocking Expression of Phosphoinositide 3-Kinase Subunits. *Gastroenterology,* 150**,** 1183-1195 e16.

WANG, Y. & THORLACIUS, H. 2005. Mast cell-derived tumour necrosis factor-alpha mediates macrophage inflammatory protein-2-induced recruitment of neutrophils in mice. *Br J Pharmacol,* 145**,** 1062-8.

WARE, J., CORKEN, A. & KHETPAL, R. 2013. Platelet function beyond hemostasis and thrombosis. *Curr Opin Hematol,* 20**,** 451-6.

WATSON, A. A., BROWN, J., HARLOS, K., EBLE, J. A., WALTER, T. S. & O'CALLAGHAN, C. A. 2007. The crystal structure and mutational binding analysis of the extracellular domain of the platelet-activating receptor CLEC-2. *J Biol Chem,* 282**,** 3165-72.

WEBER, C. 2005. Platelets and chemokines in atherosclerosis: partners in crime. *Circ Res,* 96**,** 612-6.

WETTERWALD, A., HOFFSTETTER, W., CECCHINI, M. G., LANSKE, B., WAGNER, C., FLEISCH, H. & ATKINSON, M. 1996. Characterization and cloning of the E11 antigen, a marker expressed by rat osteoblasts and osteocytes. *Bone,* 18**,** 125-32.

WICKI, A., LEHEMBRE, F., WICK, N., HANTUSCH, B., KERJASCHKI, D. & CHRISTOFORI, G. 2006. Tumor invasion in the absence of epithelial-mesenchymal transition: podoplanin-mediated remodeling of the actin cytoskeleton. *Cancer Cell,* 9**,** 261-72.

WIGLE, J. T., HARVEY, N., DETMAR, M., LAGUTINA, I., GROSVELD, G., GUNN, M. D., JACKSON, D. G. & OLIVER, G. 2002. An essential role for Prox1 in the induction of the lymphatic endothelial cell phenotype. *EMBO J,* 21**,** 1505-13.

WILLIAMS, M. C., CAO, Y., HINDS, A., RISHI, A. K. & WETTERWALD, A. 1996. T1 alpha protein is developmentally regulated and expressed by alveolar type I cells, choroid plexus, and ciliary epithelia of adult rats. *Am J Respir Cell Mol Biol,* 14**,** 577-85.

XIA, L., JU, T., WESTMUCKETT, A., AN, G., IVANCIU, L., MCDANIEL, J. M., LUPU, F., CUMMINGS, R. D. & MCEVER, R. P. 2004. Defective angiogenesis and fatal embryonic hemorrhage in mice lacking core 1-derived O-glycans. *J Cell Biol,* 164**,** 451-9.

XU, Y., YUAN, L., MAK, J., PARDANAUD, L., CAUNT, M., KASMAN, I., LARRIVEE, B., DEL TORO, R., SUCHTING, S., MEDVINSKY, A., SILVA, J., YANG, J., THOMAS, J. L., KOCH, A. W., ALITALO, K., EICHMANN, A. &

BAGRI, A. 2010. Neuropilin-2 mediates VEGF-C-induced lymphatic sprouting together with VEGFR3. *J Cell Biol,* 188**,** 115-30.

YANG, Y., GARCIA-VERDUGO, J. M., SORIANO-NAVARRO, M., SRINIVASAN, R. S., SCALLAN, J. P., SINGH, M. K., EPSTEIN, J. A. & OLIVER, G. 2012. Lymphatic endothelial progenitors bud from the cardinal vein and intersomitic vessels in mammalian embryos. *Blood,* 120**,** 2340-8.

ZUCKER-FRANKLIN, D., SEREMETIS, S. & ZHENG, Z. Y. 1990. Internalization of human immunodeficiency virus type I and other retroviruses by megakaryocytes and platelets. *Blood,* 75**,** 1920-3.